

AD 737687



TECHNICAL REPORT NO. 3-783

AN ANALYTICAL MODEL FOR PREDICTING CROSS-COUNTRY VEHICLE PERFORMANCE

APPENDIX C: VEHICLE PERFORMANCE IN VERTICAL OBSTACLES (SURFACE GEOMETRY)

by

C. A. Blackmon, N. R. Murphy, Jr.



DDC
RECEIVED
MAR 8 1972
RECEIVED

Reproduced by
NATIONAL TECHNICAL
INFORMATION SERVICE
Springfield, Va 22151

February 1972

Sponsored by Advanced Research Projects Agency and Directorate of Research,
Development and Engineering, U. S. Army Materiel Command

Service Agency U. S. Army Materiel Command

Conducted by U. S. Army Engineer Waterways Experiment Station, Vicksburg, Mississippi

APPROVED FOR PUBLIC RELEASE; DISTRIBUTION UNLIMITED

102
100

DISCLAIMER NOTICE

THIS DOCUMENT IS THE BEST
QUALITY AVAILABLE.

COPY FURNISHED CONTAINED
A SIGNIFICANT NUMBER OF
PAGES WHICH DO NOT
REPRODUCE LEGIBLY.

ACCESSION for	
CFSTI	WHITE SECTION <input checked="" type="checkbox"/>
DDC	DIFF SECTION <input type="checkbox"/>
ENAH. CED.	<input type="checkbox"/>
JUSTIFICATION.....	
.....	
BY.....	
DISTRIBUTION/AVAILABILITY CODES	
DIST.	AVAIL. and/or SPECIAL
A	

Destroy this report when no longer needed. Do not return it to the originator.

The findings in this report are not to be construed as an official Department of the Army position unless so designated by other authorized documents.



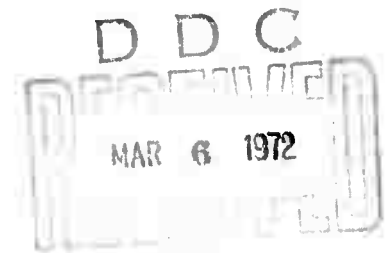
TECHNICAL REPORT NO. 3-783

AN ANALYTICAL MODEL FOR PREDICTING CROSS-COUNTRY VEHICLE PERFORMANCE

APPENDIX C: VEHICLE PERFORMANCE IN VERTICAL OBSTACLES (SURFACE GEOMETRY)

by

C. A. Blackmon, N. R. Murphy, Jr.



February 1972

**Sponsored by Advanced Research Projects Agency and Directorate of Research,
Development and Engineering, U. S. Army Materiel Command**

Service Agency U. S. Army Materiel Command

Project Nos. I-T-0-62112-A-131 and I-T-0-62103-A-046-02

Conducted by U. S. Army Engineer Waterways Experiment Station, Vicksburg, Mississippi

ARMY-MRC VICKSBURG, MISS

APPROVED FOR PUBLIC RELEASE; DISTRIBUTION UNLIMITED

DOCUMENT CONTROL DATA - R & D

(Security classification of title, body of abstract and indexing annotation must be entered when the overall report is classified)

1. ORIGINATING ACTIVITY (Corporate author)

U. S. Army Engineer Waterways Experiment Station
Vicksburg, Mississippi

2a. REPORT SECURITY CLASSIFICATION

Unclassified

2b. GROUP

3. REPORT TITLE

AN ANALYTICAL MODEL FOR PREDICTING CROSS-COUNTRY VEHICLE PERFORMANCE; APPENDIX C:
VEHICLE PERFORMANCE IN VERTICAL OBSTACLES (SURFACE GEOMETRY)

4. DESCRIPTIVE NOTES (Type of report and inclusive dates)

Appendix C to a final report not yet published

5. AUTHOR(S) (First name, middle initial, last name)

Claude A. Blackmon
Newell R. Murphy, Jr.

6. REPORT DATE

February 1972

7a. TOTAL NO. OF PAGES

102

7b. NO. OF REFS

26

8a. CONTRACT OR GRANT NO.

ARPA Order No. 400

8b. PROJECT NO.

c. 1-T-0-62112-A-131 and

d. 1-T-0-62103-A-046-02

9a. ORIGINATOR'S REPORT NUMBER(S)

Technical Report No. 3-783, Appendix C

9b. OTHER REPORT NO(S) (Any other numbers that may be assigned this report)

10. DISTRIBUTION STATEMENT

Approved for public release; distribution unlimited.

11. SUPPLEMENTARY NOTES

12. SPONSORING MILITARY ACTIVITY

Advanced Research Projects Agency and
Directorate of Research, Development and
Engineering, U. S. Army Materiel Command

13. ABSTRACT

This appendix presents a brief history of vehicle dynamics modeling, a recapitulation of the U. S. Army Engineer Waterways Experiment Station approach to the problem of predicting vehicle performance in terrain containing discrete vertical obstacles, and descriptions of dynamic response prediction models for the M60A1 tank and M37 truck, and compares measured and predicted vehicle performance in terms of peak vertical and longitudinal accelerations for 78 rigid obstacle tests with the two vehicles. Major conclusions from the tests were that performances of the M60A1 tank and M37 truck in terms of peak vertical and peak longitudinal accelerations experienced at the driver's seat when traversing discrete, rigid obstacles can be correlated with impact speed, that the mathematical techniques described yield reasonably accurate predictions of the speed at which the M60A1 tank can contact a rigid obstacle without exceeding specified tolerance limits, and that refinement is needed in the dynamic response prediction model for the M37 truck.

14.	KEY WORDS	LINK A		LINK B		LINK C	
		ROLE	WT	ROLE	WT	ROLE	WT
	Cross-country models						
	Mathematical models						
	Military vehicles						
	Obstacles						
	Off-road vehicles						
	Surface geometry						
	Vehicle dynamics						

THE CONTENTS OF THIS REPORT ARE NOT TO BE
USED FOR ADVERTISING, PUBLICATION, OR
PROMOTIONAL PURPOSES. CITATION OF TRADE
NAMES DOES NOT CONSTITUTE AN OFFICIAL EN-
DORSEMENT OR APPROVAL OF THE USE OF SUCH
COMMERCIAL PRODUCTS.

FOREWORD

The study reported herein was performed by the U. S. Army Engineer Waterways Experiment Station (WES) for the Office, Secretary of Defense (OSD), Advanced Research Projects Agency (ARPA), and is a portion of one task of the overall Mobility Environmental Research Study (MERS) sponsored by OSD/ARPA for which the WES was the prime contractor and the U. S. Army Materiel Command (AMC) was the service agent. The broad mission of Project MERS was to determine the effects of the various features of the physical environment on the performance of cross-country ground contact vehicles and to provide therefrom data that can be used to improve both the design and employment of such vehicles. A condition of the project was that the data be interpretable in terms of vehicle requirements for Southeast Asia. The funds employed for this study were allocated to WES through AMC under ARPA Order No. 400. Some funds for preparation and publication of this report were provided by the Research, Development and Engineering Directorate, AMC, under Department of the Army Project 1-T-O-62112-A-131, "Environmental Constraints on Materiel," and Project 1-T-O-62103-A-046-02, "Surface Mobility."

This appendix is one of seven to a report entitled An Analytical Model for Predicting Cross-Country Vehicle Performance (in preparation). These appendixes are:

- A. Instrumentation of Test Vehicles (July 1967)
- B. Vehicle Performance in Lateral and Longitudinal Obstacles (Vegetation)
 - Volume I: Lateral Obstacles (December 1968)
 - Volume II: Longitudinal Obstacles (July 1968)

- C. Vehicle Performance in Vertical Obstacles (Surface Geometry) (February 1972)
- D. Performance of Amphibious Vehicles in the Water-Land Interface (Hydrologic Geometry) (February 1970)
- E. Quantification of the Screening Effects of Vegetation on Driver's Vision and Vehicle Speed (April 1971)
- F. Soil-Vehicle Relations on Soft Clay Soils (Surface Composition) (August 1970)
- G. Application of Analytical Model to United States and Thailand Terrains (in preparation)

This study was conducted by personnel of the Mobility and Environmental (M&E) Division, under the general supervision of Mr. W. J. Turnbull, Technical Assistant for Soils and Engineering (retired); Mr. W. G. Shockley and Mr. S. J. Knight, Chief and Assistant Chief, respectively, M&E Division; and under the direct supervision of Mr. A. A. Rula, Chief, Vehicle Studies Branch (VSB).

The field tests reported herein were conducted during the period January-June 1968 by Mr. J. L. Gargaro, VSB, and G. Switzer, Mobility Research Branch (MRB); the mathematical models of the M60A1 tank and M37 truck used to make the performance predictions were formulated and described by Mr. N. R. Murphy, Jr., MRB, and the analysis of the data presented was performed by Mr. C. A. Blackmon, VSB. This report was prepared by Messrs. Blackmon and Murphy.

Acknowledgment is made to Mr. W. A. Gross, Jr., and Mr. P. R. Gula, Development and Proof Services, Aberdeen Proving Ground (APG), for their support and assistance during the conduct of the field tank tests reported herein.

Directors of the WES during this study and the preparation of this report were COL Alex G. Sutton, Jr., CE, COL John R. Oswalt, Jr., CE, COL Levi A. Brown, CE, and COL Ernest D. Peixotto, CE. Technical Directors were Messrs. J. B. Tiffany and F. R. Brown.

CONTENTS

	<u>Page</u>
FOREWORD	v
CONVERSION FACTORS, BRITISH TO METRIC UNITS OF MEASUREMENT . . .	ix
SUMMARY.	xi
PART I: INTRODUCTION.	C1
Background	C1
Purpose and Scope	C2
A History of Vehicle Dynamics Modeling	C3
PART II: THE WES APPROACH	C9
Obstacle-Vehicle Interaction Categories	C9
Dynamic Response Prediction Model for M60A1 Tank	C10
Dynamic Response Prediction Model for M37 Truck	C20
PART III: TEST PROGRAMS	C27
Test Vehicles	C27
Test Areas	C27
Tests Conducted	C30
Data Collected	C31
Prediction Data Obtained	C31
PART IV: ANALYSIS OF DATA	C32
Method of Analysis and Evaluation of Predictions	C32
Peak Vertical Acceleration-Obstacle Height-Speed Relations.	C33
Peak Longitudinal Acceleration-Obstacle Height-Speed Relations.	C37
Notes and Observations	C40
PART V: CONCLUSIONS AND RECOMMENDATIONS	C42
Conclusions.	C42
Recommendations.	C42
LITERATURE CITED	C44
TABLES C1-C8	
PLATES C1-C13	

CONTENTS

	<u>Page</u>
COMPUTER PROGRAM FOR SIMULATING DYNAMIC RESPONSE OF M60A1 TANK, AND DICTIONARY OF PROGRAM VARIABLES	
COMPUTER PROGRAM FOR SIMULATING DYNAMIC RESPONSE OF M37 TRUCK, AND DICTIONARY OF PROGRAM VARIABLES	

CONVERSION FACTORS, BRITISH TO METRIC UNITS OF MEASUREMENT

British units of measurement used in this report can be converted to metric units as follows:

<u>Multiply</u>	<u>By</u>	<u>To Obtain</u>
inches	2.54	centimeters
feet	0.3048	meters
square inches	6.4516	square centimeters
cubic feet	0.0283168	cubic meters
pounds	0.45359237	kilograms
kip	453.59237	kilograms
short tons (2000 lb)	907.185	kilograms
pounds per square inch	0.070307	kilograms per square centimeter
foot-pounds	0.138255	meter-kilograms
miles per hour	1.609344	kilometers per hour

SUMMARY

This appendix presents a brief history of vehicle dynamics modeling, a recapitulation of the U. S. Army Engineer Waterways Experiment Station approach to the problem of predicting vehicle performance in terrain containing discrete vertical obstacles, and descriptions of dynamic response prediction models for the M60A1 tank and M37 truck, and compares measured and predicted vehicle performance in terms of peak vertical and longitudinal accelerations for 78 rigid obstacle tests with the two vehicles. Major conclusions from the tests were that performances of the M60A1 tank and M37 truck in terms of peak vertical and peak longitudinal accelerations experienced at the driver's seat when traversing discrete, rigid obstacles can be correlated with impact speed, that the mathematical techniques described yield reasonably accurate predictions of the speed at which the M60A1 tank can contact a rigid obstacle without exceeding specified tolerance limits, and that refinement is needed in the dynamic response prediction model for the M37 truck.

AN ANALYTICAL MODEL FOR PREDICTING
CROSS-COUNTRY VEHICLE PERFORMANCE

APPENDIX C: VEHICLE PERFORMANCE IN VERTICAL
OBSTACLES (SURFACE GEOMETRY)

PART I: INTRODUCTION

Background

1. The main text of this report (not yet published) describes the development of an analytical model for predicting the cross-country performance of a vehicle. The model was based on an energy concept within the framework of classical mechanics which requires that cause-and-effect relations be established between discrete terrain factors and vehicle response. This appendix deals with the effects of a single terrain factor--vertical obstacles. The term "obstacle" in general refers to all features of the terrain, except soil, that are inhibitory to vehicle mobility. The obstacle-effects spectrum of vehicle mobility ranges from complete immobilization to minor speed reduction. For the purpose of the overall study, obstacles were categorized according to the direction of motion forced upon a vehicle negotiating the obstacle, i.e. vertical, lateral, or longitudinal.

2. Perhaps the most universal single terrain feature that produces an inhibiting effect on vehicle ground mobility is small-scale surface geometry. Surface geometry features occur in a bewildering array of sizes and configurations, and produce effects on vehicles that range from "vibration" to "shock" to "immobilization," depending on the speed and size of the vehicle in relation to the size and spacing of obstacles.

3. Vibration-producing features are those surface irregularities of heights that can be measured in inches* rather than feet, and of

* A table of factors for converting British units of measurement to metric units is presented on page ix.

distance between features that can be measured in feet rather than tens of feet. The dominant interaction for vibration-producing features is dynamic and is concentrated in the action of the vehicle suspension as the vehicle passes over the features at a speed in excess of creep speed, say 5 mph or more, with the vehicle speed limited by considerations of driver and/or cargo safety.

4. Shock-inducing features occur as discrete "bumps" and produce a dynamic interaction that also is concentrated in the vehicle suspension system. The dynamic action associated with these features is of a high-amplitude, low-frequency nature. The vehicle speed is ultimately limited by considerations of driver and/or cargo safety.

5. Features that are likely to produce immobilizations occur as discrete obstacles, as do the shock-inducing features; however, the former are of such size and shape that their negotiation can be considered in terms of static phenomena since an attempt to traverse them must be made at creep speed. The controlling factors of obstacle-vehicle interaction for these features are the geometry of the feature, the geometry of the vehicle body and running gear, and the ability of the vehicle to exert sufficient tractive effort to lift itself over the feature.

6. Early testing did little more than outline the problem. It was apparent that nothing less than an elaborate computer program would suffice, hence the major effort of this study was directed toward examination of current mathematical modeling techniques and the refinement thereof.

Purpose and Scope

7. This appendix presents a brief history of vehicle dynamics modeling, a discussion of the U. S. Army Engineer Waterways Experiment Station (WES) approach to the problem of predicting vehicle performance when traversing discrete vertical obstacles, a description of the dynamics submodels used, and a comparison of measured and predicted vehicle performance.

8. Seventy-eight obstacle-vehicle tests were run with two vehicles at several speeds over a range of obstacle heights. Dynamic response predictions in terms of peak vertical acceleration and peak longitudinal acceleration were made for 34 combinations of obstacle height and vehicle speed. The tests and predictions were limited to the vehicles crossing a rigid, nondeformable obstacle on a uniformly hard surface.

A History of Vehicle Dynamics Modeling

In retrospect

9. Since the advent of the automobile (especially since the 1920's), research by government and industry has been conducted on a continuing basis in various countries with regard to highway design and construction and also vehicle design, with particular emphasis on steering control, power train, and suspension--the principal contributors to the safety, efficiency, and riding comfort of on-road vehicles.

10. The speed at which a driver of a vehicle will traverse obstacles or continuous irregular terrain is controlled primarily by the level of vibration activity that does not exceed his particular ride comfort level. Vehicle vibration or ride is sensed by a driver or passenger through sight, touch, and hearing in response to external stimuli, such as motions, forces, and sounds. Whenever this sensation becomes too severe, the driver will alter the vehicle's speed until the sensation reaches an acceptable level. This sensation, therefore, is a significant factor in determining the speed of a vehicle over a given terrain. The irregular terrain-vehicle problem is essentially one of dynamics, and its solution must include the combined effects of the surface being traversed, the vehicle, and the driver. Because of the complexity of the problem and the desire to produce better riding vehicles, considerable effort has been expended on modeling dynamic vehicle response.

11. Because of the lack of mathematical techniques required in modeling suspension systems, much of the early work consisted of

cut-and-try methods. The first significant contributions to an analytical treatment of vehicle dynamics were performed by Rowell,¹ Guest,² and Olley³ in the early 1920's and 30's.

12. In 1941, a mechanical differential analyzer was built by Schilling and Fuchs⁴ specifically for suspension analysis, and although it was suited to only a single-degree-of-freedom system, it did permit the inclusion of the nonlinear characteristic of shock absorbers. The analyzer was used in the continuous determination of transient motions and in the portrayal of the effect on motion by changes in the characteristics of the shock absorber. This differential analyzer was the forerunner of today's analog computer, and its development led to rapid advances in suspension analysis and design. By the 1950's, it was widely exploited by the automotive industry.

13. In 1953, Jeska⁵ developed a four-degree-of-freedom model that included pitch and bounce of the body and vertical motions of the front and rear wheels. The forcing function was an actual road wave measured by a photographic technique. In 1955, Bodeau, Bollinger, and Lipkin⁶ of Ford Motor Company developed a detailed ride analysis in which a nine-degree-of-freedom model was used to describe a passenger car. In 1960, Kohr⁷ of General Motors Corporation developed a mathematical simulation of automobile ride. In his simulation, a measured road profile was recorded on magnetic tape, and the tape was fed through an analog computer model of the vehicle to predict the vehicle motions, i.e. pitch, bounce, and roll. The resulting motions were used to drive a vibration simulator, which was used as a laboratory means of assessing the effect of the vibration on humans.

14. Until about 1960, the analysis of ride had been concerned primarily with the suspension system and means of improving the ride quality. Although considerable work was done in the area of human tolerance to vibration, a means for quantifying human tolerance to vibrations had not been developed. Van Deusen⁸ has shown that very little of the research done actually pertains to the off-road environment. Most experiments have been devised to assess human response to sinusoidal motion in only one direction, while the more complex ride comfort

problems involve random vibrations in various directions. The most frequently used criteria have been those of Dieckman⁹ and Janeway,¹⁰ who developed simple formulas for relating comfort limits to amplitude and frequency of vibration. There have been several studies of "on-the-road" measurements of ride comfort. For example, Von Eldik Thieme¹¹ examined the Dieckman-Janeway criteria in the actual vehicle environment, but he met with little success. Van Deusen^{12,13} and Versace¹⁴ used a technique, referred to as cross modality, in which subjects received noise signals through earphones and adjusted and matched the signal's level to the sensation level of ride vibration. A statistical analysis showed favorable correlations of the measured accelerations with ride sensation, and at least indicated that correlations between ride sensation and vibration were possible.

15. In the late 1950's the Department of Defense began to recognize the significance of vehicle vibration on off-road mobility and weapon efficiency. An extensive effort was begun to quantify the vehicle vibration problem and to correlate it with human response and terrain characteristics. Interest was shifted from deterministic to stochastic techniques. The latter technique consists of classifying terrain profiles by certain pertinent statistics and analyzing the response statistically. The groundwork for this type of analysis was begun in 1959 by Bogdanoff and Kozin,¹⁵ who described in detail the statistical analysis of the responses of simple linear systems to random terrain inputs. Although the vehicle models were simple and idealized, the analyses provided a starting point and yielded much useful information regarding fundamental relations between pertinent vehicle parameters and statistical terrain quantities. This study preceded studies of Bieniek¹⁶ (1960), Van Deusen¹⁷ (1962), and Bussman¹⁸ (1964), who followed essentially the same approach as that described by Bogdanoff and Kozin. The one notable exception was Van Deusen's introduction of a nonlinear vehicle system into his statistical analysis.

16. Organized discrete obstacle-vehicle research in the Western world was given special attention as the result of World War II experiences. Early U. S. military efforts were concerned with designing

military vehicles that would reduce immobilizations caused by obstacle interference. Obstacle test courses were constructed at Aberdeen Proving Ground (APG), and tests on these courses have become part of the overall vehicle engineering evaluation test program. Results of these studies led to the recent development of articulated vehicles. Discrete obstacle-vehicle research studies in the United States gained more emphasis about the mid-1950's when terrain factors other than soils were introduced as deterrents to off-road vehicle travel, and more attention was given to obstacle geometry interference and the effects of dynamic response on vehicle performance. By the early 1960's these studies produced several static and quasi-dynamic models which related, by simple two-dimensional static mechanics, slope and obstacle geometry to go-no go performance.

17. In 1963, the U. S. Army Tank-Automotive Command (TACOM) began basic research on the effects of vehicle vibration on human response. This work was based on the results of past studies and so was oriented toward quantifying the effects of random vibration on vehicle-driver performance. Two performance parameters were developed to describe human response--acceleration density and absorbed power. Of the two performance parameters, absorbed power is preferred in quantifying human response to vibration since it is a descriptor of the flow of energy from the vibrating vehicle to the driver. This led to the TACOM V-ride concept in which ride limiting speed is determined as that speed at which the driver's absorbed power reaches 6 watts. During the 1960's the Department of Defense sponsored several studies in the development and application of ad hoc comprehensive cross-country models in which V-ride was incorporated as a submodel.

18. In the early 1960's the scope of WES mobility research was expanded, and static and dynamic surface configuration, vehicle, driver interaction studies were initiated. In 1965, FMC Corporation conducted a study¹⁹ for WES to determine the feasibility of using a digital computer to simulate the dynamic response of ground vehicles traveling over unyielding irregular terrain segments. This study resulted in the development of a generalized mathematical model of an n-axle vehicle

which, within limits, is suitable for both wheeled and tracked vehicles.

Current approaches

19. Today's practice in modeling the effects of surface configuration on vehicle performance consists essentially of two types of analysis which are separated on the basis of the kind of vehicle and/or driver interaction anticipated. Regardless of the analysis performed, the terrain profile and associated discrete obstacles generally are considered rigid. This consideration represents the worst conditions that might be encountered from the standpoint of the vehicle's vibrational behavior. If a terrain unit contains an irregular surface that can be easily overridden by a vehicle without inducing frequent shock, vehicle performance is predicted by a dynamic model. In this case, the problem is commonly identified as surface roughness, and the profile used is a statistically uniform surface profile. If a terrain unit contains discrete obstacles larger than those included in the rough terrain analysis and which are likely to produce immobilizations, it is assumed that traversing or circumventing the obstacles will be accomplished at a creep speed and the interactions are treated as static phenomena. The models used in such terrain situations are thus static models. The controlling factors in the relation of a static model are the geometry of the obstacle and vehicle configuration. If the discrete obstacles that the vehicle must pass over occur at wide spacings (e.g. dikes), and they can be overridden at speeds greater than creep speeds, a dynamic model is used to determine the maximum override speed.

20. Current vehicle dynamic models simulate mathematically the dynamic response of selected points within a vehicle (usually at the driver's seat or in the cargo compartment) as it traverses discrete obstacles or rough terrain. Performance is generally expressed in terms of relations between speed and such response quantities as absorbed power, root-mean-square acceleration, or peak acceleration, and then referenced to established tolerances for horizontal and vertical accelerations and power limits. Most dynamic models predict only vertical motions; however, they can readily be modified to include horizontal and, if necessary, lateral motions. The mathematical techniques

involved in the formulation of dynamic models are common to all models, but differences occur in the details of representing the terrain, vehicle, and driver limits, and in the size of the computer required.

21. Mathematical descriptions of vehicle behavior in surmounting obstacles are a combination of dynamic and static models. Discrete obstacles such as rocks, boulders, mounds, scarps, ditches, etc., are usually first examined to determine whether or not there will be spatial interference between the obstacles and the nonpropelling vehicle structure. This examination may proceed in either two or three dimensions: with or without compliance of the vehicle running gear, suspension, or structure; with or without compliance of the obstacle itself; or by spatial matching of the vehicle and the obstacle, either of which may be described more or less completely. In some instances, the vehicle underside is modeled to scale, usually in two dimensions. In others, the vehicle shape is idealized to the quantitative description and location of salient features, and matching is done through the application of complex but ordinary trigonometry and geometry. The latter procedure is, of course, more suitable for computer use. Where the number of obstacle configurations assumed in an area is relatively small, however, the scale-model experiments can be conducted once and for all, and the results stored for subsequent computer consultation as needed. In addition to static examination regarding obstacle-vehicle geometry interference aspects, it is necessary also to describe the dynamic response of the vehicle when traversing a given obstacle at a given speed. It is this problem upon which this report is focused.

PART II: THE WES APPROACH

Obstacle-Vehicle Interaction Categories

22. Early efforts at WES were directed toward developing instrumentation²⁰ and test procedures to measure and record vehicle response. It was apparent that a model for predicting the effects of vertical obstacles must consider at least three broad categories of obstacle-vehicle interactions.

Obstacle geometry interference

23. This model was designed to answer such questions as: Is it possible for the vehicle to cross the obstacle without hanging up? Is the obstacle of such size and configuration that the vehicle might be in danger of up-ending? Is there sufficient traction? Initially, a two-dimensional scale model of the vehicle and of the obstacle was used to answer the first two questions and to determine a maximum attitude angle which was compared with the maximum negotiable slope to determine a simple go-no go. A procedure for determining maximum slope negotiable is given in Appendix D²¹ of this report. Subsequently, a computer program was written that mathematically determined the same performance parameters.

Speed limited by maneuvering

24. A method for determining whether or not the vehicle can circumvent the obstacle on the basis of a theoretical parameter, "area denied," and empirical relations of area denied and speed made good were developed to answer such questions as: Is it possible for the vehicle to circumvent the obstacles? What reduction in speed is brought about if the vehicle does circumvent the obstacles? This method is described in Appendix B, Volume I,²² of this report. A computer program was written that utilized a somewhat refined procedure for computing area denied and the effect of area denied on vehicle speed.

Speed limited by dynamic response

25. If the vehicle can traverse the obstacle, the maximum safe

speed at which it can cross the obstacle must be determined. To do this, the performance parameters and conditions that limit speed must be known. A system for predicting vehicle dynamic response was being developed concurrently with the conduct of the MERS vehicle field test programs, but the input and output requirements of the prediction system were not known at the time the test programs were conducted. Consequently, the response data taken during the MERS test programs did not entirely satisfy the requirements of the prediction system to the extent that they could be used for comparison with predicted values. However, the test results did tend to confirm previous cross-country studies,²³ which show that the maximum peak vertical acceleration tolerated by the driver while trying to maintain a maximum safe speed was approximately 2.5 g's. An additional tolerance limit of 2.0-g peak longitudinal acceleration was established on the basis of competent experience and judgment. Other tests²⁴ confirmed that peak vertical acceleration and peak longitudinal acceleration could be adequately measured in vehicle tests. Computer models for mathematically simulating vehicle dynamic response were developed to predict peak vertical acceleration and peak longitudinal acceleration for rigid-frame wheeled and tracked vehicles crossing discrete obstacles. Descriptions of the models are discussed in subsequent paragraphs.

Dynamic Response Prediction Model for M60A1 Tank

26. A mathematical model of the M60A1 tank was developed to simulate the dynamic response of the tank while crossing rigid obstacles perpendicular to the path of travel. The intent of this model was to portray as nearly as possible the significant features of the motions of interest, namely, those in the vicinity of the driver, and to predict obstacle limiting speeds based on some preselected tolerance criterion at a minimum cost. The model thus does not contain the detail that might be required, for example, in designing a vehicle suspension system.

27. A schematic diagram of the system that was modeled is shown

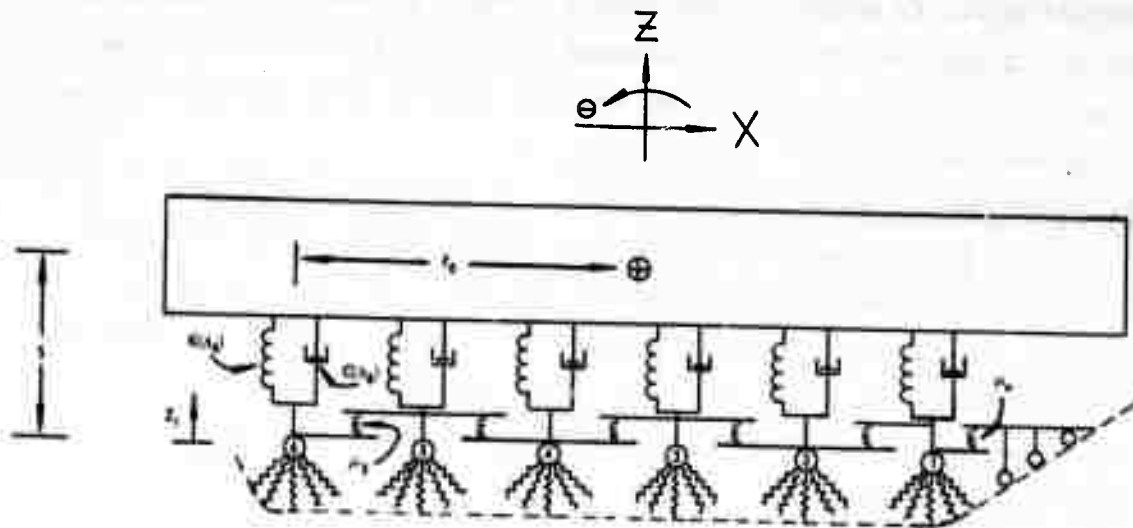


Fig. C1. Schematic of M60A1 tank

in fig. C1. This model consists of nine degrees of freedom that include the bounce, pitch, and surge of the center of gravity of the main frame and the vertical motions of each of the six bogie wheels. Motion in this context includes displacement, velocity, and acceleration. In addition, the motions in the vicinity of the driver are computed.* The geometry effects of the bogies are represented by radially projecting stiff springs and the track compliance by interconnecting springs between the bogies and three "feelers" appropriately positioned in front of the first bogie and connected to it by a spring.

28. The longitudinal motion (X in reference axis, fig. C1) is accounted for only in the acceleration determined from the horizontal forces resulting from deflections of the bogie spring segments. The horizontal components of the segment forces are summed for each bogie, and the horizontal acceleration is obtained by dividing this summation by the mass of the tank. This method of accounting for horizontal

* Because of certain geometric interferences, it is not possible to locate an accelerometer at the driver position. An accelerometer intended to measure the accelerations in the vicinity of the driver can be conveniently located at a position 1 ft to the right and 2 ft behind the center of the driver's seat.

accelerations is somewhat analogous to towing a vehicle across an obstacle, always maintaining a constant velocity, and determining the increased towing force required to tow the vehicle over the obstacle at the given velocity.

Equations of motion

29. The differential equations describing the motion of this system were developed by first establishing an appropriate set of coordinates and sign convention and then placing the system in a displaced configuration such that each coordinate was affected. The relative displacements of the masses produce forces on each mass as shown by the free body diagram in fig. C2. The vehicle characteristics used in

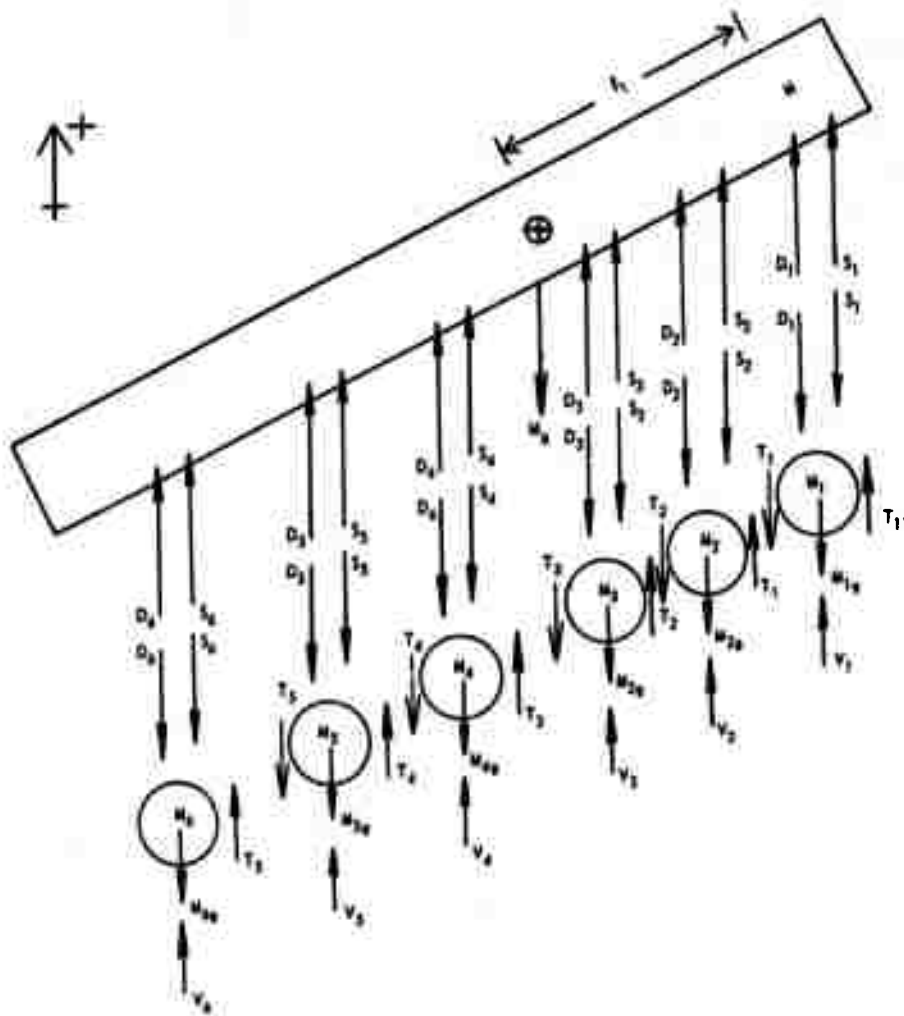


Fig. C2. Vertical forces acting on M60A1 tank free body

predicting vehicle dynamic response are given in table C1. Using Newton's second law of motion and summing the forces on the main frame and on each bogie led to the series of equations listed below.

Forces on the main frame (sprung mass):

$$\begin{aligned}
 M\ddot{z} &= - \left[\sum_{i=1}^6 k(\Delta_i)\Delta_i + \sum_{i=1}^6 c(\dot{\Delta}_i)\dot{\Delta}_i + Mg \right] \\
 I\ddot{\theta} &= - \left[\sum_{i=1}^3 k(\Delta_i)\Delta_i l_i \cos \theta + \sum_{i=1}^3 c(\dot{\Delta}_i)\dot{\Delta}_i l_i \cos \theta \right. \\
 &\quad \left. - \sum_{i=3}^6 k(\Delta_i)\Delta_i l_i \cos \theta - \sum_{i=3}^6 c(\dot{\Delta}_i)\dot{\Delta}_i l_i \cos \theta + Q \right] \\
 M\ddot{x} &= \sum_{i=1}^6 H_i
 \end{aligned}$$

Vertical forces on the bogies (unsprung mass):

$$\begin{aligned}
 M_1\ddot{z}_1 &= k(\Delta_1)\Delta_1 + c(\dot{\Delta}_1)\dot{\Delta}_1 + \mu_1\delta_1 - \mu_0\delta_0 - M_1g + V_1 \\
 M_2\ddot{z}_2 &= k(\Delta_2)\Delta_2 + c(\dot{\Delta}_2)\dot{\Delta}_2 - \mu_1\delta_1 + \mu_2\delta_2 - M_2g + V_2 \\
 M_3\ddot{z}_3 &= k(\Delta_3)\Delta_3 + c(\dot{\Delta}_3)\dot{\Delta}_3 - \mu_2\delta_2 + \mu_3\delta_3 - M_3g + V_3 \\
 M_4\ddot{z}_4 &= k(\Delta_4)\Delta_4 + c(\dot{\Delta}_4)\dot{\Delta}_4 - \mu_3\delta_3 + \mu_4\delta_4 - M_4g + V_4 \\
 M_5\ddot{z}_5 &= k(\Delta_5)\Delta_5 + c(\dot{\Delta}_5)\dot{\Delta}_5 - \mu_4\delta_4 + \mu_5\delta_5 - M_5g + V_5 \\
 M_6\ddot{z}_6 &= k(\Delta_6)\Delta_6 + c(\dot{\Delta}_6)\dot{\Delta}_6 - \mu_5\delta_5 - M_6g + V_6
 \end{aligned}$$

where

$$\begin{aligned}
 \text{for } 1 \leq i \leq 3 \quad \Delta_i &= z + l_i \sin \theta - z_i, \quad \dot{\Delta}_i = \dot{z} + l_i \dot{\theta} \cos \theta - \dot{z}_i \\
 4 \leq i \leq 6 \quad \Delta_i &= z - l_i \sin \theta - z_i, \quad \dot{\Delta}_i = \dot{z} - l_i \dot{\theta} \cos \theta - \dot{z}_i
 \end{aligned}$$

and

Q = moment about the center of gravity of the main frame produced by horizontal forces, $Q = \sum_{i=1}^6 (H_i)(S + \Delta_i)$

l_i = distance from center of gravity of main frame to contact point of i^{th} bogie

$k(\Delta_i)$ = force-deflection relation for i^{th} bogie suspension (fig. C3)

$c(\Delta_i)$ = force-velocity relation for i^{th} bogie suspension (fig. C4)

V_i = resultant vertical force of spring segments of i^{th} bogie

H_i = resultant horizontal force of spring segments of i^{th} bogie

$\delta_i = z_{i+1} - z_i$ = relative displacement between adjacent bogies

μ_i = spring constant for i^{th} track spring; in this study, for $1 \leq i \leq 5$ $\mu_i = 375 \text{ lb/in.}$, $\mu_0 = 600 \text{ lb/in.}$

30. Observation of photographs of the tank crossing the highest obstacle (18 in.) revealed that the greatest pitch angle expected would be on the order of 9 deg or less. It is seen that if

$$\theta = 9 \text{ deg}$$

then

$$\cos \theta = \cos 9 \text{ deg} = 0.988 \approx 1$$

and

$$9 \text{ deg} = \frac{\pi}{20} = 0.157 \text{ radian}$$

Since

$$\sin 9 \text{ deg} = 0.156 \approx 0.157$$

the small angle assumption, i.e. $\cos \theta = 1$, $\sin \theta = \theta$, is valid. For this reason, and to simplify the calculations, the small angle concept was used in the equations above.

31. Once the motions at the center of gravity of the main frame have been determined, the motions in the vicinity of the driver can be

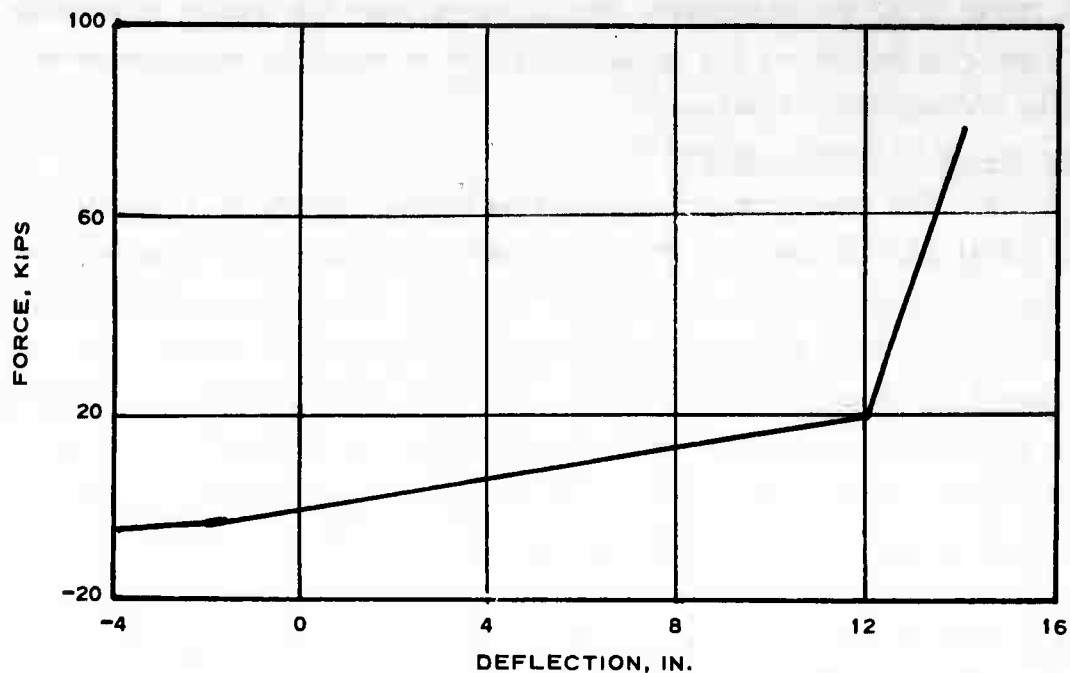


Fig. C3. M60A1 suspension spring force versus deflection

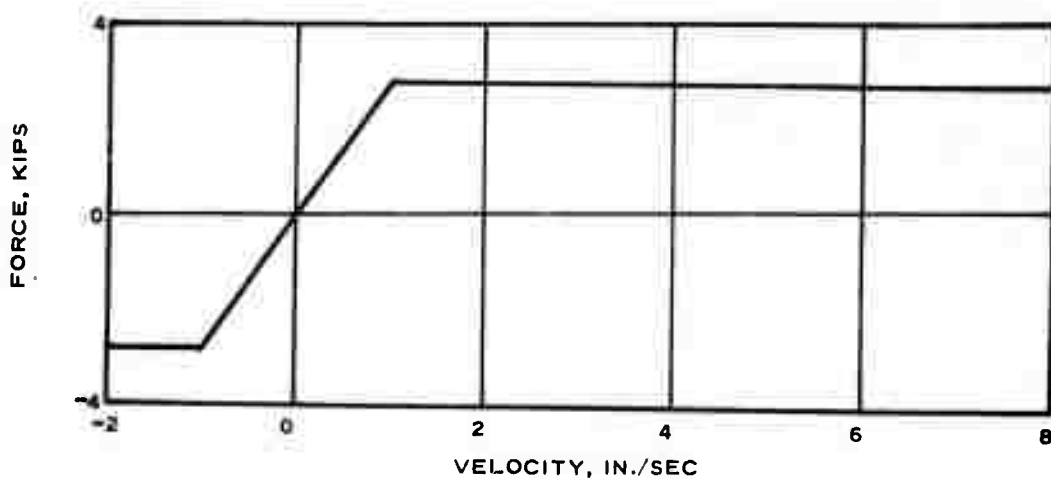


Fig. C4. M60A1 suspension damping force versus velocity

determined by combining the translatory and rotational motions to yield the equation:

$$\ddot{Z}_{DR} = \ddot{Z}_{CG} + 35\ddot{\theta}$$

The value of 35 in. represents the distance from the center of gravity to a point 2 ft behind the driver, a point at which an accelerometer can be conveniently located.

Computation of track forces

32. The track compliance is represented chiefly by interconnecting linear springs between the bogies and three "feelers" that are connected to the front bogie by a stiff spring. The spring constants used in this study were determined by observing photographs of the tank in different positions on an obstacle. From these photographs, estimates were made of the influence on the displacement of adjacent bogies of displacing a particular bogie. Knowing the approximate mass of each bogie assembly, an appropriate spring constant could be determined. Close observation further revealed that upon approaching an obstacle larger than about 6 in. high the initial track-obstacle contact tended to lift the front bogie and guide it over the obstacle. This lifting has a significant effect on the longitudinal motion. To simulate this effect, three feelers were positioned in front of the first bogie, each at a different threshold height, to conform with the geometry of the leading portion of the track. The influence of the feelers in lifting the front bogie depends on the height and shape of the encountering obstacle. Since no information was available to enable the determination of an effective spring constant, an arbitrary value of 600 lb/in. was chosen. Although this value was estimated, it shows that with a proper determination of a spring constant these longitudinal accelerations can be adequately simulated.

Bogie spring segments

33. The segmented wheel concept²⁵ was used in the model to (a) enable predictions of longitudinal accelerations, (b) include important geometry effects of the bogies, and (c) incorporate a means for describing the composite compliance of the real bogie-track-obstacle system. This composite compliance of the real system includes such phenomena as the effects of the small terrain and obstacle deformations, track deformations, and envelopment characteristics among others that otherwise in the model would be represented as infinitely rigid.

34. Each bogie was divided into twelve 10-deg segments, six on each side of the vertical position as shown in fig. C5. To account for

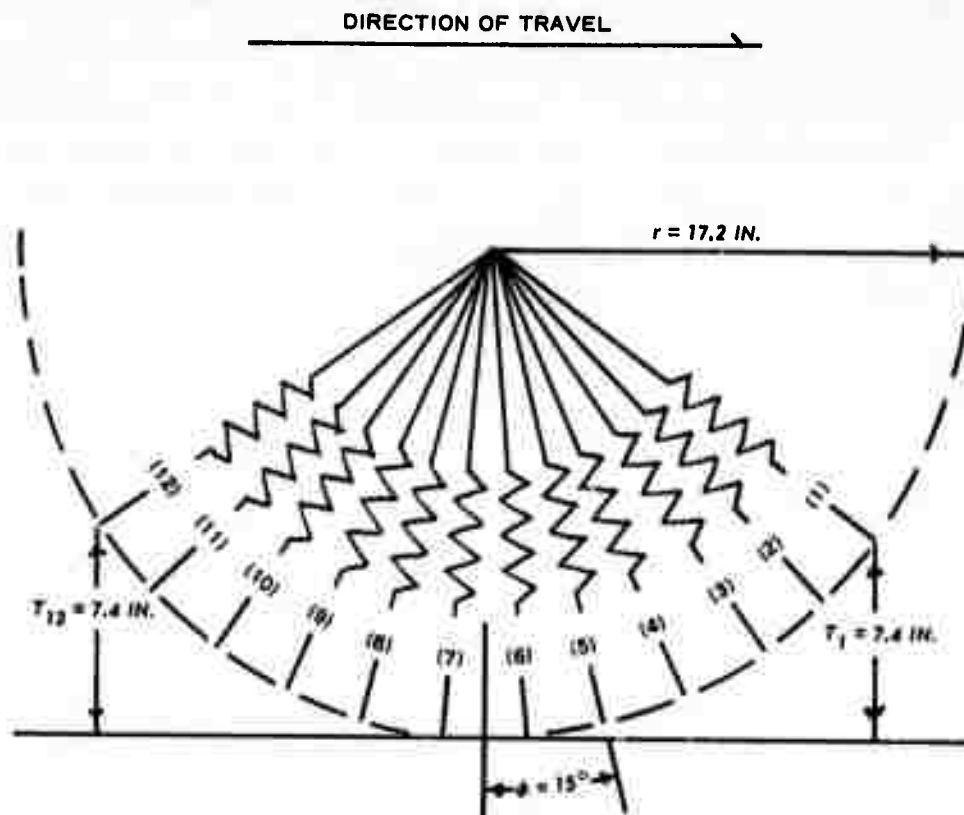


Fig. C5. Schematic showing bogie spring segment configuration

the track thickness, an effective bogie radius of 17.2 in. was used. At these conditions, an average horizontal spacing of 2.357 in. coincided closely with each spring position.

Determination of threshold heights

35. To compute the deflections of each spring segment, the segment threshold heights, T_1 , were first computed. These heights are simply the heights to each spring of the undeflected wheel (see fig. C5). The segment deflection, ξ_1 , is then computed by the equation:

$$\xi_i = \begin{cases} Y_i - T_i - z_i, & Y_i - T_i - z_i \geq 0 \\ 0, & Y_i - T_i - z_i < 0 \end{cases}$$

where

Y_i = vertical obstacle height beneath the i^{th} segment

z_i = vertical axle displacement of i^{th} bogie

36. The segment deflections are permitted to have positive values only; negative values are replaced by zero. The reference from which vertical displacements are measured is the point that locates the bogie axle when the bogie is imagined to be rigid and in static equilibrium. Static deviations from this reference correspond to static wheel deflections, and superposed on these static deflections are the dynamic obstacle-induced deflections.

Computation of vertical and horizontal forces

37. The resultant vertical and horizontal forces on the first bogie axle due to the spring segment deflections are given by equations:

$$V_1 = \sum_{i=1}^{12} (k_v \cos \phi_i) \xi_i$$
$$H_1 = \sum_{i=1}^{12} (k_h \sin \phi_i) \xi_i$$

where

k_v and k_h = segment spring constants for the vertical and horizontal modes, respectively

ϕ_i = angle of the i^{th} segment from the vertical

ξ_i = vertical deflection of the i^{th} segment

38. Generally, k_v and k_h would have the same value. However, the increased stiffness noted in the horizontal mode warranted a higher spring constant in the horizontal mode. These values, k_v and k_h , were determined by examining oscillograph records for several tests over a 10-in.-high obstacle. These k values were adjusted until the model outputs adequately portrayed the gross features of the acceleration-time histories from the oscillographs. The choice of the 10-in. obstacle was quite arbitrary; it was chosen solely because it was close to the median obstacle height that the M60A1 tank would be expected to traverse. Ideally, such k values would be determined by

appropriately instrumenting the bogies and performing a series of systematic tests that would lead to the determination of a proper set of values.

39. Defining $\gamma_i = k_v \cos \phi_i$ and $\sigma_i = k_h \sin \phi_i$, a γ -array and a σ -array are established in the same manner as the array of threshold heights, thus simplifying the computations of the resultant vertical and horizontal forces.

Computation of moment produced by horizontal forces

40. An important contribution to the moments about the center of gravity of the main frame is the horizontal forces acting on the bogies. A schematic diagram, showing only the front and rear suspensions, is given in fig. C6 to illustrate the manner in which the horizontal forces contribute to the moment. Using the small angle assumption and the established sign convention that the suspension deflection, Δ , is negative in the equilibrium position, the following equation is used to compute the moment, Q , due to horizontal forces.

$$Q = - \sum_{i=1}^3 (H_i) [(S + \Delta_i) - (\ell_i)\theta] - \sum_{i=4}^6 (H_i) [(S + \Delta_i) + (\ell_i)\theta]$$

where

the quantities in brackets represent the moment arm from the center of gravity to the i^{th} bogie

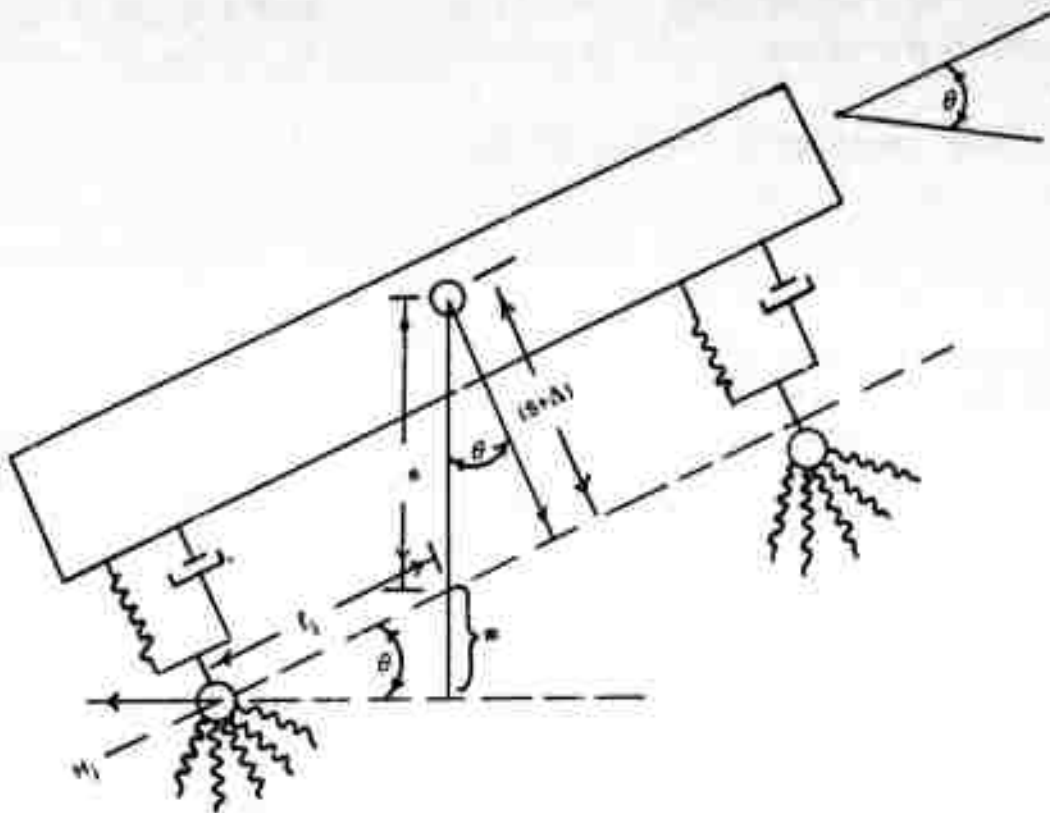
S = vertical distance from the center of gravity to the bogie axles in the undeflected state

H_i = resultant horizontal force of the i^{th} bogie

ℓ_i = longitudinal distance from the center of gravity to the i^{th} bogie

Computer program

41. A complete listing of the digital computer program and a dictionary of the computer variables used are given at the end of this appendix. This is a FORTRAN IV program written for a GE-430 time-sharing system. Mixed mode operations, which are acceptable in this system, were used on occasion where it proved advantageous in reducing



MOMENT AT CENTER OF GRAVITY OF FORCE, $H_i = H_i(m + n)$

WHERE

$$n = \frac{s + \Delta}{\cos \theta} = s + \Delta$$

$$m = l_i \sin \theta = l_i \theta$$

$$Q_i = H_i[(s + \Delta) + l_i \theta]$$

Fig. C6. Schematic showing moment of horizontal forces

the logic or the number of required statements. The file entitled "Fimake" serves as a convenient method to build and input the obstacles.

Dynamic Response Prediction Model for M37 Truck

42. The development of the mathematical model of the M37 truck to simulate the dynamic response of the truck while crossing rigid obstacles followed the same reasoning as that given in paragraph 26 for the M60A1 tank.

43. A schematic diagram of the system that was modeled is given in fig. C7. This model consists of four degrees of freedom that

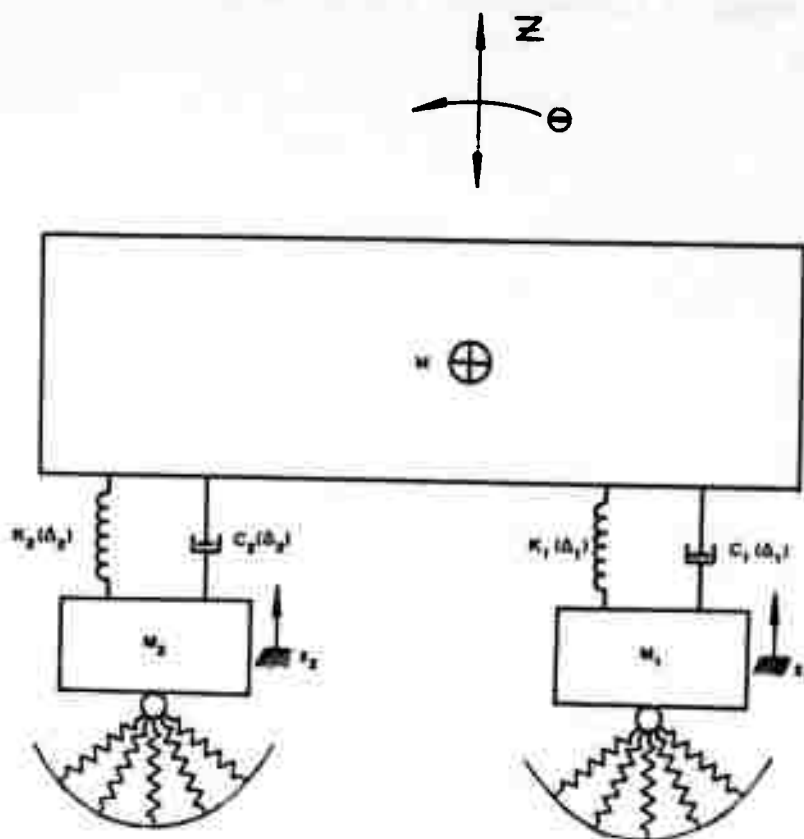


Fig. C7. Schematic of truck model

include bounce and pitch of the center of gravity of the main frame and the vertical motions of both axles. A significant difference in the two mathematical models is that longitudinal motion is not taken into account in the M37 truck model. The motions in the vicinity of the driver* are computed from the predicted motions at the center of gravity. The frame of the truck was considered rigid, and only the pneumatic tires and suspensions were considered to contribute to the sprung motion of the frame. The model includes all pertinent nonlinearities in the suspension. Vehicle characteristics used are given in table C2.

* Accelerometers can be conveniently located underneath the center of the driver's seat.

Equations of motion

44. The differential equations describing the motions of this system were developed in a manner analogous to that described in paragraph 29. Again, using Newton's second law of motion and summing the forces on the body and on each axle led to the series of equations listed below.

Forces on body (sprung mass):

$$\begin{aligned} M\ddot{z} &= K_1(\Delta_1)(z_1 - z - a \sin \theta) + C_1(\dot{\Delta}_1)(\dot{z}_1 - \dot{z} - a\dot{\theta} \cos \theta) \\ &\quad + K_2(\Delta_2)(z_2 - z + b \sin \theta) + C_2(\dot{\Delta}_2)(\dot{z}_2 - \dot{z} + b\dot{\theta} \cos \theta) - Mg \\ I\ddot{\theta} &= K_1(\Delta_1)a(z_1 - z - a \sin \theta) + C_1(\dot{\Delta}_1)a(\dot{z}_1 - \dot{z} - a\dot{\theta} \cos \theta) \\ &\quad - K_2(\Delta_2)b(z_2 - z + b \sin \theta) - C_2(\dot{\Delta}_2)b(\dot{z}_2 - \dot{z} + b\dot{\theta} \cos \theta) \end{aligned}$$

Forces on front axle (unsprung mass):

$$\begin{aligned} M_1\ddot{z}_1 &= -K_1(\Delta_1)(z_1 - z - a \sin \theta) - C_1(\dot{\Delta}_1)(\dot{z}_1 - \dot{z} - a\dot{\theta} \cos \theta) \\ &\quad + \sum_{i=1}^{10} \gamma_{i1}(p_{i1} - z_1) - M_1g \end{aligned}$$

Forces on rear axle (unsprung mass):

$$\begin{aligned} M_2\ddot{z}_2 &= -K_2(\Delta_2)(z_2 - z + b \sin \theta) - C_2(\dot{\Delta}_2)(\dot{z}_2 - \dot{z} + b\dot{\theta} \cos \theta) \\ &\quad + \sum_{i=1}^{10} \gamma_{i2}(p_{i2} - z_2) - M_2g \end{aligned}$$

where

$$\begin{aligned} \Delta_1 &= z_1 - z - a \sin \theta, \quad \dot{\Delta}_1 = \dot{z}_1 - \dot{z} - a\dot{\theta} \cos \theta \\ \Delta_2 &= z_2 - z + b \sin \theta, \quad \dot{\Delta}_2 = \dot{z}_2 - \dot{z} + b\dot{\theta} \cos \theta \end{aligned}$$

For this study, the suspension spring coefficients were represented by third-order polynomials, as shown in fig. C8. These polynomials were obtained by curve-fitting the actual force-deflection relations, and are reasonable approximations. The suspension damping is as follows:

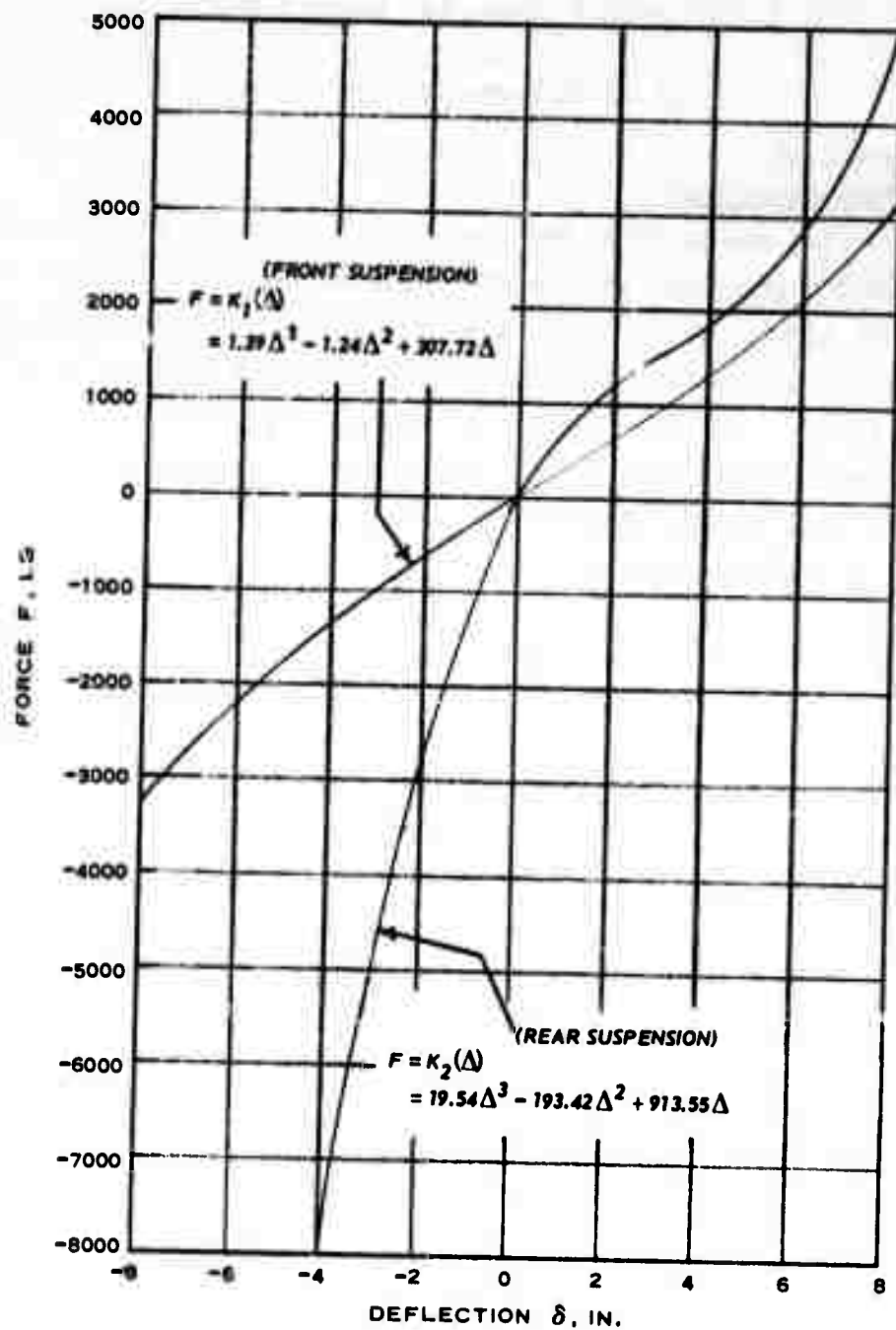


Fig. C8. Force versus deflection for front and rear suspensions of M37 truck model

$$C_1(\dot{\Delta}_1) = 11.8 \text{ lb-sec/in. (compression)}$$

$$= 22.8 \text{ lb-sec/in. (extension)}$$

$$C_2(\dot{\Delta}_2) = 12.0 \text{ lb-sec/in. (compression)}$$

$$= 49.0 \text{ lb-sec/in. (extension)}$$

Determination of
tire-terrain compliance

45. Each wheel, which represented a 9.00x16, 8-PR tire at 45-psi* inflation pressure, was divided into ten segments, five on each side of the tire's center line, as shown in fig. C9. The measured load-deflection relation (fig. C10) for the 9.00x16 tire at 45-psi inflation pressure was such that a center-line deflection of 1.5 in. required a load of 2860 lb. At this deflection, four spring segments are influenced, two on each side of the center line (fig. C9). The spring constant K can be determined from the statics equation:

$$F = \sum_{i=1}^{10} K \cos \phi_i \Delta_i$$

where

$$\Delta_i = \begin{cases} Y_i - \text{THRESH}(i) - Z, & Y_i - \text{THRESH}(i) - Z \geq 0 \\ 0, & Y_i - \text{THRESH}(i) - Z < 0 \end{cases}$$

Y_i = vertical height of terrain profile beneath i^{th} segment

Z = vertical displacement of axle

$\text{THRESH}(i)$ = height from the zero reference to the i^{th} spring of the undeflected wheel (see fig. C9)

For this case and due to the symmetry of the segments about the center line the equation reduces to

* The difference in the load-deflection relation between 40 psi (at which subsequent tests were conducted) and 45 psi was deemed negligible.

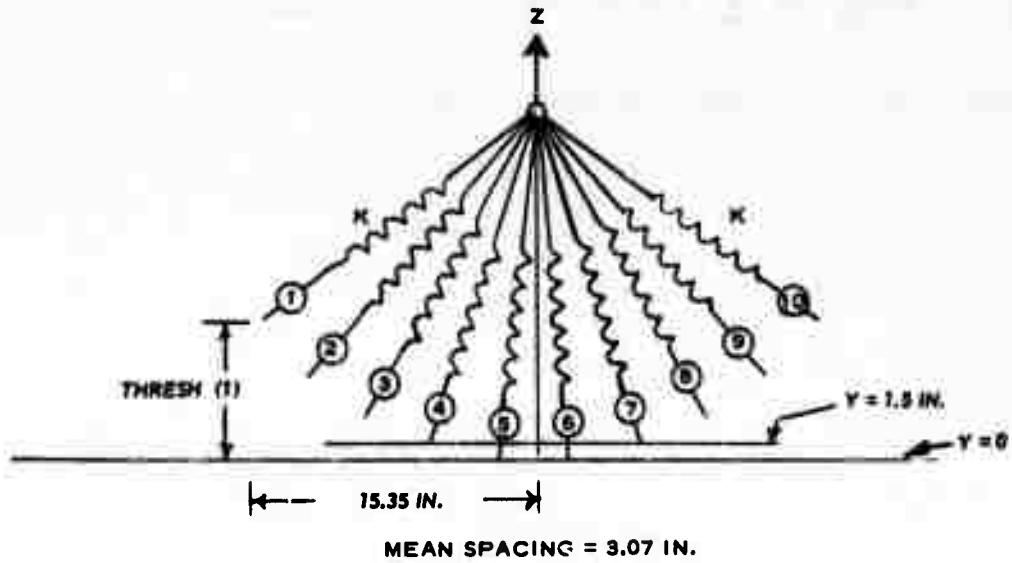


Fig. C9. Schematic of segmented wheel

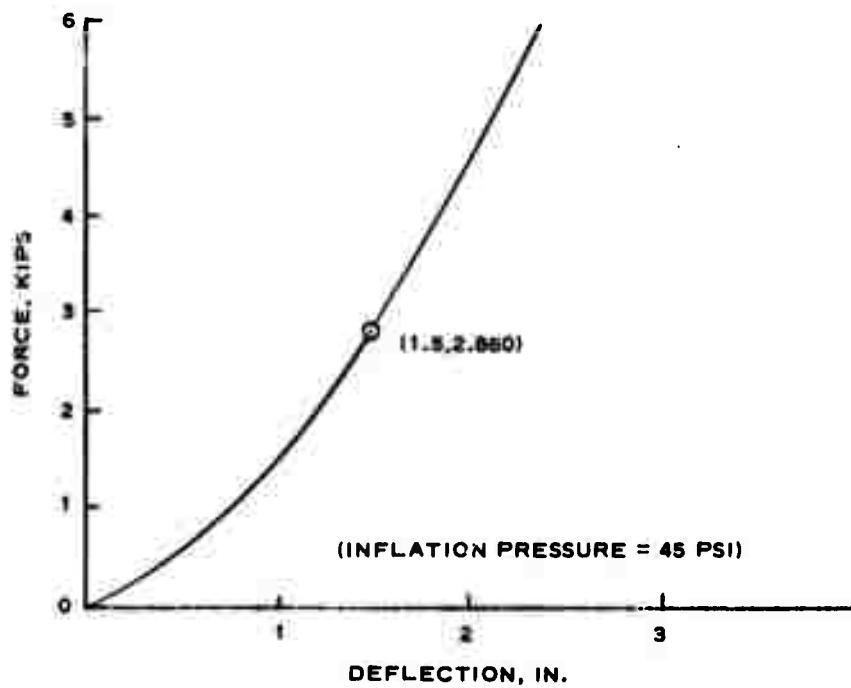


Fig. C10. Force versus deflection for the 9.00x16, 8-PR tire

$$2860 = 2K \sum_{i=1}^2 1.4 \cos \frac{11.7^\circ}{2} + 0.7 \cos 11.7^\circ + \frac{11.7^\circ}{2}$$

where the effective radial deflections are:

$$\Delta_5 = \Delta_6 = 1.4 \text{ in.}$$

$$\Delta_4 = \Delta_7 = 0.7 \text{ in.}$$

Solving for K yields

$$K = 675 \text{ lb/in.}$$

Defining $\text{GAMMA} = K \cos \phi_i = 675 \cos \phi_i$ yields the following relations for the segments of the front and back wheels:

$$\text{GAMMA}(1) = \text{GAMMA}(10) = \text{GAMMA}(11) = \text{GAMMA}(20) = 411.75$$

$$\text{GAMMA}(2) = \text{GAMMA}(9) = \text{GAMMA}(12) = \text{GAMMA}(19) = 506.25$$

$$\text{GAMMA}(3) = \text{GAMMA}(8) = \text{GAMMA}(13) = \text{GAMMA}(18) = 587.25$$

$$\text{GAMMA}(4) = \text{GAMMA}(7) = \text{GAMMA}(14) = \text{GAMMA}(17) = 648.00$$

$$\text{GAMMA}(5) = \text{GAMMA}(6) = \text{GAMMA}(15) = \text{GAMMA}(16) = 668.25$$

A similar relation is derived for the threshold heights of each segment $\text{THRESH}(i)$.

46. A mean spacing of 3.07 in. was determined to be adequate for portraying the projected spacing of the springs. As a result, all profile points were spaced 3.07 in. apart, and no interpolation scheme was employed to estimate elevation between adjacent points.

47. No damping was incorporated in the tire compliance since in actual vehicles this damping is negligible compared with that of the suspensions. This truck model was forced to traverse each obstacle at a constant speed, and the outputs consisted of motions of the main frame and axles in terms of displacement-, velocity-, and acceleration-time histories.

Computer program

48. A complete listing of the digital computer program and a dictionary of the computer variables used are given at the end of this appendix. This is a FORTRAN IV program written for a GE-430 time-sharing system.

PART III: TEST PROGRAMS

49. Although several series of obstacle-vehicle tests were conducted in efforts to establish testing procedures and criteria for dynamic response, the first test program that yielded data acceptable for verification of the WES vehicle dynamics model was conducted at Aberdeen Proving Ground (APG) with an M60A1 tank. These tests were conducted during the period 6-9 May 1968. Subsequently, an obstacle test course was constructed at WES, and tests with an M37 truck were conducted intermittently thereon during 1968 and 1969 for another study.²⁶

Test Vehicles

50. Pertinent physical characteristics for the M60A1 tank and the M37 truck are given in tables C3 and C4, respectively. Photographs of the vehicles are included in fig. C11. The test vehicles were equipped with electronic systems* to measure and record time, distance traveled, and vertical and longitudinal accelerations.

Test Areas

APG

51. The test area at APG was a nearly level asphalt strip (fig. C12). Six different sized obstacles were constructed of hardwood and fastened to the strip with steel rods. These obstacles were 12 ft in length and ranged from 6 to 18 in. in height. A sketch of the obstacle configurations with dimensions indicated is shown in fig. C13.

WES

52. A 200-ft-long test course (fig. C14) constructed of concrete, asphalt, and steel was used for the tests at WES. This course was designed to accommodate either single or multiple obstacles, both rigid and deformable. The obstacles can be arranged to excite primarily the

* This instrumentation is described in detail in reference 20.



a. M60A1 tank

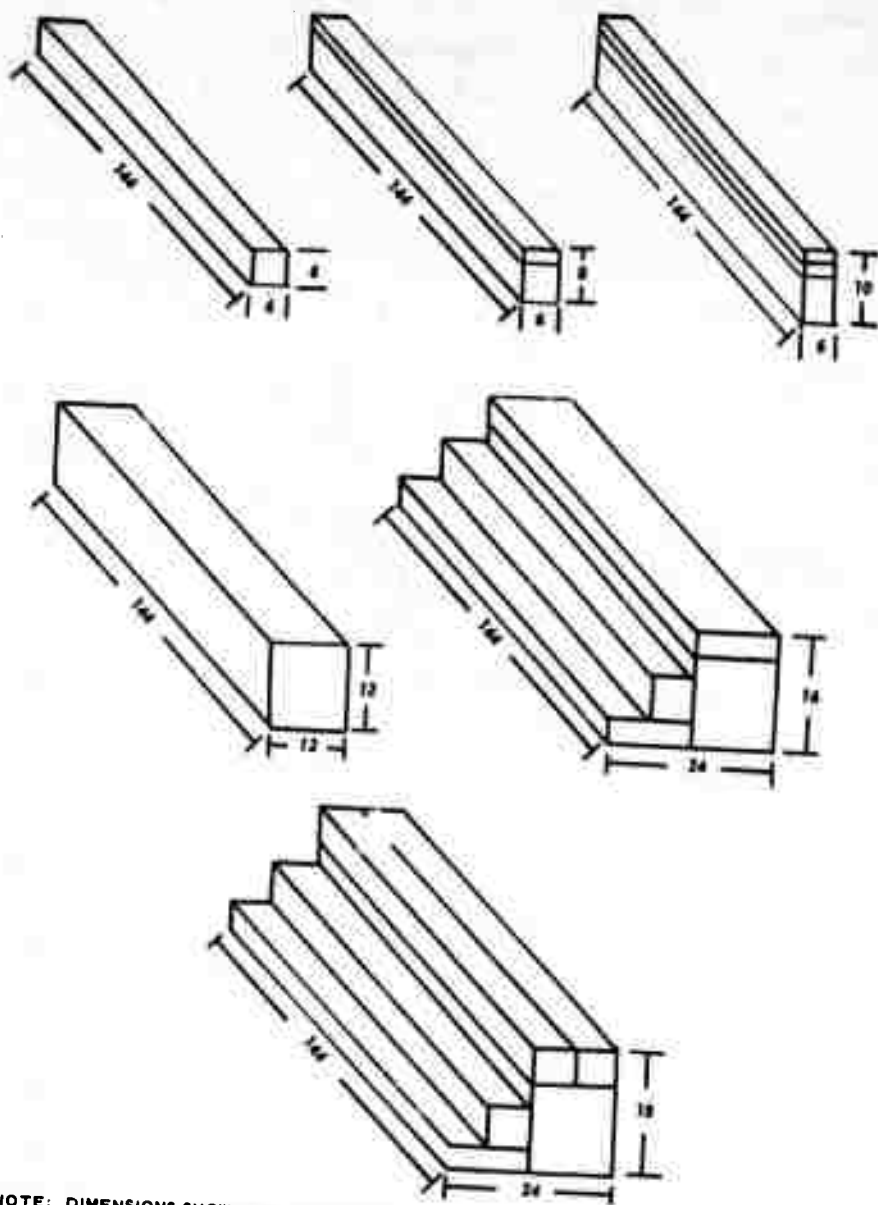


b. M37 truck, cargo, 3/4-ton, 4x4

Fig. C11. Test vehicles



Fig. C12. Test course layout, APG



NOTE: DIMENSIONS SHOWN ARE IN INCHES.

Fig. C13. Obstacle configurations



Fig. C14. Obstacle course at WES

pitch and bounce motions of the vehicle (as was done for the tests reported herein) or to excite all components of motion, i.e. pitch, roll, bounce, and yaw, in the direction of and perpendicular to the direction of travel. Only single obstacles were used in this study. The obstacles were half-round in configuration and were welded directly to steel rods embedded in the test course. Obstacle heights were 6, 8, 10, and 12 in.

Tests Conducted

Procedures

53. M60A1 tank. The vehicle was positioned at right angles to and at a sufficient distance from the obstacle to enable the desired speed to be reached at least 5 ft before striking the obstacle. The test engineer instructed the driver to accelerate to a preselected speed and try to hold this speed constant while crossing the obstacle. Some tests were run at as nearly the same speed as possible over the same obstacle height to determine repeatability of test results.

54. M37 truck. The starting position for each test was sufficiently far from the obstacle to permit the driver adequate distance to reach and maintain a constant vehicle speed before striking the obstacle. Several methods of maintaining constant speed while crossing the obstacle were attempted, and the technique that appeared most effective employed an engine tachometer calibrated in miles per hour. Some tests were rerun at the approximate speed of the first test to determine repeatability of test results.

Number of tests

55. The number of tests conducted over selected obstacle heights is given below:

<u>Obstacle Height</u> <u>in.</u>	<u>Number of Tests Conducted</u>	
	<u>M60A1 Tank</u>	<u>M37 Truck</u>
6	14	10
8	3	11
10	4	12

(Continued)

Obstacle Height in.	Number of Tests Conducted	
	M60A1 Tank	M37 Truck
12	11	2
16	9	*
18	<u>2</u>	<u>--</u>
Total	43	35

* The vertical acceleration was so great on the 12-in.-high obstacle that it was felt tests on higher obstacles might damage the vehicle.

Data Collected

56. For each test, instrumentation installed on the test vehicles recorded continuous measurements of time, distance traveled by the vehicle, and vertical and longitudinal accelerations at selected positions within the vehicle. Event marks on the oscillogram indicated the beginning and end of the test. Impact speed, peak vertical acceleration, and peak longitudinal acceleration were determined from the oscillogram. A summary of these data is given in tables C5 and C6 for the M60A1 tank and the M37 truck, respectively. Other data collected included notes, observations, and photographs.

Prediction Data Obtained

57. Predictions of peak vertical acceleration and peak longitudinal acceleration were made for 20 obstacle height-impact speed combinations for the M60A1 tank, and predictions of peak vertical acceleration were made for 14 obstacle height-impact speed combinations for the M37 truck, using the previously described models. The speeds selected for the M60A1 tank predictions in table C7 were selected on the basis of preliminary reduction of field test data and are generally close, although not identical, to the measured speeds for the M60A1 tests shown in table C5. The speeds for the M37 predictions in table C8 were arbitrarily selected to yield dynamic response predictions above and below the 2.5-g peak vertical acceleration tolerance limit.

PART IV: ANALYSIS OF DATA

Method of Analysis and Evaluation of Predictions

58. In this study, vehicle performance was described in terms of peak vertical acceleration-speed relations, peak longitudinal acceleration-speed relations, and speed-obstacle height relations for the 2.5- and 2.0-g levels of peak vertical acceleration and peak longitudinal acceleration, respectively. Peak vertical acceleration-speed relations and peak longitudinal acceleration-speed relations for several obstacle heights were developed from measured and predicted data. These relations express the peak vertical acceleration and peak longitudinal acceleration to be expected when a vehicle traverses an obstacle of a specific size at a given speed. From these relations, the speed-obstacle height relations that express the speed at which the vehicle can traverse a given obstacle without exceeding the 2.5-g peak vertical acceleration level and the 2.0-g peak longitudinal acceleration level were developed.

59. The prediction accuracy of the models was evaluated by (a) comparing the predicted peak vertical acceleration-speed and peak longitudinal acceleration-speed relations with the measured peak vertical acceleration-speed and peak longitudinal acceleration-speed relations and (b) comparing speeds at 2.5-g peak vertical acceleration and 2.0-g peak longitudinal acceleration levels developed from the predicted relations with the speeds at 2.5-g peak vertical acceleration and 2.0-g peak longitudinal acceleration developed from the measured data. The quality of the prediction accuracy was evaluated on the basis of the simple statistical parameters, root mean square (RMS)* and percent error.**

* RMS is a measure of the quality of a relation in terms of the RMS of the deviation

$$RMS = \sqrt{\frac{\sum(d)^2}{n}}$$

where Σ = the sum of; n = number of deviations; and d = deviation, i.e. predicted minus measured.

** Percent error = $\frac{\text{predicted} - \text{measured}}{\text{measured}} \times 100$.

60. Other conditions peculiar to a particular part of the analysis are discussed in the appropriate section.

Peak Vertical Acceleration-Obstacle Height-Speed Relations

61. As stated, vertical acceleration performance was described in terms of peak vertical acceleration-speed relations for several obstacle heights and speed-obstacle height relations for 2.5-g peak vertical acceleration level. Peak vertical acceleration-speed relations developed from measured and predicted data at the driver's seat are shown in plates C1 and C2 for the M60A1 tank and M37 truck, respectively. The curves drawn represent the lines of best visual fit. Where the location of the line was doubtful, judgment was aided by the location and curvature of lines on better defined plots. These curves are summarized for the M60A1 tank and the M37 truck in plates C3 and C4, respectively. Speed-obstacle height relations for both vehicles are given in plate C5. The speed-obstacle height relations were established from values of speed and corresponding values of obstacle height in plates C3 and C4 at which 2.5-g peak vertical acceleration occurred.

M60A1 tank

62. It can be seen in plates C1 and C3 that both measured and predicted peak vertical accelerations for the M60A1 tank at the driver's seat increased with an increase in speed. There appears to be a tendency for the curves to crest at higher speeds, suggesting that after a critical speed has been reached, a further increase in speed would not result in an increase in peak vertical acceleration. In plate C1 it can be seen that except for the 6-in.-high obstacles the predicted peak vertical acceleration was higher than that measured at low speeds, and lower than that measured at higher speeds. The reverse is indicated for the 6-in.-high obstacles. The agreement of the measured and predicted curves for the 8- and 10-in. obstacles is very good, and at the 2.5-g tolerance limit the curves for the 12-, 16-, and 18-in. obstacles seem to be reasonably close.

63. In plate C5, the speed-obstacle height curve for the M60A1

tank shows that the speed at which 2.5-g peak vertical acceleration is reached at the driver's seat decreases with an increase in obstacle height. The effect of obstacle height on 2.5-g peak vertical acceleration begins to diminish rapidly at about the 9-in. obstacle height. An examination of predicted data points shows that they are in good agreement with curves developed from the measured data.

M37 truck

64. In plates C2 and C4, both measured and predicted peak vertical accelerations for the M37 truck at the driver's seat increased with an increase in speed. At the higher speeds the rate of change in peak vertical acceleration was less than that at lower speeds. Except in a few cases at very low speeds (plate C2), there is a large difference between the measured and predicted peak vertical accelerations at the same speed, with the predicted peak vertical acceleration being lower than the measured. An explanation for this is not readily available without further study. It may be because of the difference in the physical characteristics of the vehicle and the model, e.g., spring rates, damping rates, etc., or because of the inability to accurately produce a computer simulation of the motion history of the vehicle immediately prior to and during obstacle traversal.

65. The speed-obstacle height curve for the M37 truck in plate C5 was established from the measured relations for the 6-, 8-, and 10-in.-high obstacles. (Note in plate C2 that even at low speeds the peak vertical acceleration measured over 12-in.-high obstacles greatly exceeded 2.5 g's.) The relation is similar to that discussed above for the M60A1 tank except that 2.5-g peak vertical acceleration at the driver's seat was reached at lower speeds and obstacle heights than that for the M60A1 tank. It can be seen that the predictions indicate a higher speed for crossing 8- and 10-in.-high obstacles than that shown by the relations developed from measured data. In addition, the predicted speed for the 12-in.-high obstacle was 4 mph, while the measured data indicate (see again plate C2) that the vehicle cannot cross a 12-in.-high obstacle at any speed without exceeding 2.5-g peak vertical acceleration. No predicted value is shown for 6-in.-high obstacles.

because the predictions of peak vertical acceleration at the driver's seat did not reach 2.5 g at speeds up to 20 mph. Hence, it is apparent that for all obstacle heights tested, the predicted speed at which 2.5-g peak vertical acceleration at the driver's seat would occur was greater than that indicated by the relations developed from measured data.

Prediction accuracy

66. The measured and predicted peak vertical accelerations, the deviations, and the percent error for the speeds at which comparisons were made are given in tables C7 and C8 for the M60A1 tank and the M37 truck, respectively. The measured data shown in column 4 of tables C7 and C8 were obtained from the relations established for measured data shown in fig. a, plate C3, for the M60A1 tank and in fig. a, plate C4, for the M37 truck. The predicted data given in column 3 of tables C7 and C8 are for predictions made for the speeds shown in column 2.

67. The measured and predicted peak vertical acceleration data given in tables C7 and C8 are plotted in plate C6 for both vehicles, and a summary of the RMS and average percent error for each obstacle height is given in the following tabulation:

Obstacle Height in.	M60A1 Tank		M37 Truck	
	Average		Average	
	RMS	Percent Error	RMS	Percent Error
6	0.59	81	2.06	65
8	0.10	11	1.45	28
10	0.22	41	1.17	18
12	0.43	18	4.00	68
16	0.87	22	--	--
18	0.16	6	--	--
Overall	0.51	37	1.94	39

In the tabulation above it can be seen that the overall percent error for the tracked vehicle was only slightly lower than for the wheeled vehicle, but in terms of RMS the predictions for the tracked vehicle were much better than for the wheeled vehicle. For each vehicle at several obstacle heights the percent error and RMS are sufficiently large to indicate that some refinement is needed in the mathematical

models. In fig. a, plate C6, the predictions for the M60A1 tank are generally reasonable except for a few points--the two highest accelerations for the 6- and 16-in. obstacles, and the highest acceleration for the 12-in. obstacle. In fig. b, plate C6, the predictions for the M37 truck are generally poor except for three points--the two lowest accelerations for the 10-in. obstacle and the lowest acceleration for the 8-in. obstacle.

68. A comparison of measured and predicted speeds at 2.5-g peak vertical acceleration was made by selecting the speed and obstacle heights at which 2.5-g peak vertical acceleration occurred in the figures given in plates C3 and C4. The data obtained in this manner, along with values of prediction accuracy, are given in the following tabulation.

Obstacle Height in.	M60A1 Tank				M37 Truck			
	Speed, mph, at 2.5-g PVA*		Deviation (Predicted - Measured)	Percent Error	Speed, mph, at 2.5-g PVA		Deviation (Predicted - Measured)	Percent Error
	Measured	Predicted			Measured	Predicted		
6	--	--	--	--	8.8	--	--	--
8	15.6	15.6	0.0	0	5.1	7.3	2.2	35
10	11.0	11.6	0.6	6	4.4	5.0	0.6	14
12	7.4	7.2	-0.2	3	--	4.0	--	--
16	5.3	6.1	0.8	15	--	--	--	--
18	4.9	5.1	0.2	4	--	--	--	--
Average				7	Average			25

* PVA designates peak vertical acceleration.

The speed-obstacle height relations developed from the data in the tabulation above are shown in plate C5. It can be seen that the relations are reasonably well defined and that as obstacle height increases, the speed at which the limiting acceleration value is reached decreases and that the predicted data agree reasonably well with the curves drawn for the measured data, particularly for the M60A1 tank. For a given obstacle height, the M60A1 tank can cross that obstacle at almost twice the speed that the M37 truck can cross it before 2.5-g peak vertical acceleration is reached. The tabulation above and plate C7 reveal that the accuracy of predicting speeds at 2.5-g vertical acceleration is very good for the M60A1 tank and reasonably good for the M37 truck throughout the speed range shown.

Peak Longitudinal Acceleration-Obstacle Height-Speed Relations

69. Longitudinal acceleration performance was described in terms of peak longitudinal acceleration-speed relations for several obstacle heights, and speed-obstacle height relations for 2.0-g peak longitudinal acceleration. Peak longitudinal acceleration-speed relations developed from measured and predicted data at the driver's seat are shown in plate C8 for the M60A1 tank. Since no predictions of peak longitudinal acceleration were made for the M37 truck, the peak longitudinal acceleration-speed relations from measured data only are shown in plate C9. The curves drawn represent the lines of best visual fit, and they are summarized in plates C9 and C10 for the M37 truck and the M60A1 tank, respectively. Speed-obstacle height relations for the M60A1 tank are shown in plate C11. The speed-obstacle height relation for the M60A1 tank was established from values of speed and corresponding values of obstacle height in plate C10 at which 2.0-g peak longitudinal acceleration occurred.

M60A1 tank

70. It can be seen in plates C8 and C10 that both measured and predicted peak longitudinal accelerations for the M60A1 tank at the driver's seat increased with an increase in speed. In all cases, the predicted curves indicate higher values of peak longitudinal acceleration than the measured curves. Although the scatter in data is not excessive, additional data are required to better define the relations. In table C5 it can be seen that the test data include only one measured peak longitudinal acceleration greater than 2.0 g's. However, the curves for the larger obstacles shown in plates C8 and C10 were extended to 2.0 g's.

71. The speed-obstacle height relations (plate C11) for the M60A1 tank show that the speed at which 2.0-g peak longitudinal acceleration is reached at the driver's seat decreases with an increase in obstacle height. The predicted data shown in the plot do not agree very well with the measured data.

M37 truck

72. The curves in plate C9, developed for measured data only, indicate that the peak longitudinal acceleration of the M37 truck increased with speed up to about 8 to 10 mph, and then decreased with further increase in speed. An increase in peak longitudinal acceleration with increased obstacle height is also indicated, as would be expected. While the scatter of the data points is not excessive, there is an obvious need for additional data, especially for the 12-in. obstacle height.

Prediction accuracy

73. The quality of the prediction accuracy for peak longitudinal acceleration-speed and obstacle height-speed relations for the M60A1 tank was determined in the same manner as that for the vertical acceleration relations. The measured and predicted data, deviation, and percent errors for the speeds at which comparisons were made are given in table C7. The measured data shown in column 8 of table C7 were obtained from the relations established from measured data shown in plate C10. The predicted data shown in column 7 are for predictions made for the speeds shown in column 2.

74. The measured and predicted peak longitudinal acceleration data given in table C7 for the M60A1 tank are plotted in plate C12, and a summary of the RMS and average percent error for each obstacle height is given below.

Obstacle Height in.	<u>M60A1 Tank</u>	
	<u>RMS</u>	<u>Average Percent Error</u>
6	0.26	74
8	0.33	80
10	0.22	43
12	0.56	102
16	1.07	119
18	1.05	76
Overall	0.64	82

The preceding tabulation shows that the overall prediction accuracy is not very good and no consistent pattern is evident other than that prediction accuracy generally decreased with obstacle height increase. In plate C12 the individual data points reveal perhaps more meaningful trends. Except for two points for the 6-in. obstacle height, predicted peak longitudinal accelerations are higher than the measured accelerations. Predictions for the 12-, 16-, and 18-in.-high obstacles are consistently higher than the measured data. The deviations for these obstacle heights are also much greater than for the other obstacle heights.

75. A comparison of M60A1 measured and predicted speeds at 2.0-g peak longitudinal acceleration was made by selecting the speed and obstacle height at which 2.0-g peak longitudinal acceleration occurred in plate C10. Since only two points were available for the 2.0-g level of acceleration, a comparison was also made for the 1.0-g level of peak longitudinal acceleration. The data obtained in this manner, along with values of prediction accuracy, are given below.

Obstacle Height in.	M60A1 Tank							
	Speed, mph, at 2.0-g PLA*		Deviation (Predicted - Measured)	Percent Error	Speed, mph, at 1.0-g PLA		Deviation (Predicted - Measured)	Percent Error
	Measured	Predicted			Measured	Predicted		
6	--	--	--	--	17.3	--	--	--
8	--	--	--	--	14.5	12.0	-2.5	-17
10	--	--	--	--	12.0	10.6	-1.4	-12
12	--	--	--	--	8.0	4.2	-3.8	-48
16	10.0	5.6	-4.4	-44	6.6	--	--	--
18	7.4	4.6	-2.8	-38	4.6	--	--	--
Average				-41	Average -26			

* PLA designates peak longitudinal acceleration.

The speed-obstacle height relations developed from the data given in the tabulation above for the M60A1 tank are shown in plate C11. The data from which the curve for the speed-obstacle heights at which 2.0-g peak longitudinal acceleration is reached are limited, but the curve for the 1.0-g level is well defined. Both curves show that as the obstacle height increases, the speed at which the limiting acceleration value is reached decreases. From the data above and plate C13, it can be

seen that the predicted speed at which a given level of peak longitudinal acceleration will occur for a given obstacle height is lower than the measured speed. The difference in measured and predicted values is greater for the 2.0-g level than for the 1.0-g peak longitudinal acceleration level. The prediction accuracy for the 1.0-g peak longitudinal acceleration level is acceptable for the 8- and 10-in. obstacle heights, but it is not acceptable for the 12-in. obstacle. For the 2.0-g peak longitudinal acceleration level, the prediction accuracy is not acceptable.

Notes and Observations

76. During the test program, it was observed that in all of the tests the vehicles appeared to strike the obstacles at or very near an angle of 90 deg; however, in some tests there was a change in vehicle orientation during traversal of the obstacle. Since the peak vertical acceleration generally occurs when the vehicle strikes the ground after crossing the obstacle, the magnitude of the peak vertical acceleration is influenced by the attitude and orientation of the vehicle. The M60A1, for instance, might strike the ground with both tracks simultaneously, thus deriving the maximum benefit of the suspension system; one track may strike the ground first with the vehicle in such position that the major portion of the shock is imposed on the suspension system of one track only, resulting in some roll motion; or the vehicle may strike the ground in any position between these two extremes with a possibility of a slight change in vehicle direction. The extremes are even wider for the M37 truck. A wheeled vehicle may land on all wheels simultaneously, on two wheels, or on a single wheel. Not all of these extremes were evidenced in these tests; however, there were occasions when one track or wheel appeared to make contact with the ground before the other track or wheel.

77. In the M60A1 tests, the peak longitudinal acceleration at the driver's seat occurred when the vehicle contacted the obstacle, whereas the peak longitudinal acceleration of the M37 truck generally

occurred when the front wheels struck the obstacle, although there were some occasions when the peak longitudinal acceleration occurred when the rear wheels contacted the obstacle. Since some combinations of obstacle height and speed caused the M37 truck to become airborne, i.e. lose contact with the ground, it is easy to hypothesize a condition in which the peak longitudinal acceleration for the M37 might occur when the vehicle strikes the ground after crossing the obstacle. The M60A1 tank did not become airborne during any of the tests described herein.

78. As previously stated, the drivers attempted to maintain a constant speed across the obstacle. Since this would be patently impossible if the driver waited until he felt the vehicle slowing before he applied additional power, the procedure evolved was to apply additional power as close to the moment of impact as possible. The success of this procedure, in terms of repeatability of the test results, has its limitations. Obviously, there was nothing the driver could do toward maintaining a constant speed when the M37 truck was airborne. Rather than attempting to maintain a constant speed, it is suggested that future tests be conducted with the throttle in a fixed position throughout the test.

PART V: CONCLUSIONS AND RECOMMENDATIONS

Conclusions

79. Based on the data reported herein and subject to the limits imposed by these data, the following conclusions are offered:

- a. Discrete rigid obstacles affect vehicle performance by producing adverse vertical and longitudinal motions that may endanger the driver or damage the cargo.
- b. The magnitudes of peak vertical and longitudinal accelerations are dependent primarily on speed, obstacle height, and characteristics of the vehicle suspension system.
- c. Vehicle performance in terms of peak vertical and peak longitudinal accelerations when traversing discrete, rigid obstacles can be correlated with impact speed.
- d. The speed at which the M60A1 tank may contact a rigid obstacle without exceeding the 2.5-g peak vertical acceleration tolerance limit or the 2.0-g peak longitudinal acceleration tolerance limit can be predicted by the described mathematical techniques with reasonable accuracy.
- e. The speed at which the M37 may contact a rigid obstacle without exceeding the 2.5-g peak vertical acceleration tolerance limit can be predicted by the described mathematical techniques with reasonable accuracy for 8- to 10-in.-high obstacles. Above and below this height range, however, the prediction accuracy left much to be desired.
- f. Refinement is needed in the dynamic response prediction models with more improvement required in predicting dynamic response of wheeled vehicles.

Recommendations

80. It is recommended that:

- a. Additional systematic controlled testing be done with tracked and wheeled vehicles to refine and extend the relations and revise the vehicle dynamic prediction models presented herein.
- b. Refinements be made in the dynamic response prediction models to bring the predictions, particularly those for

higher speed and acceleration levels, more clearly in line with the measured dynamic response.

- c. Investigation be continued to explore, in addition to peak acceleration, other performance parameters such as root mean square acceleration and absorbed power as tolerance descriptors.

LITERATURE CITED

1. Rowell, H. S., "Principles of Vehicle Suspension," Automotive Engineer, Vol 13, No. 175, Apr 1923, pp 118-122.
2. Guest, J. J., "The Main Free Vibrations of an Autocar," Automotive Engineer, Vol 16, No. 215, May 1926, pp 190-198.
3. Olley, M., "Independent Wheel Suspensions - Its Why and Wherefore," Society of Automotive Engineers Journal, Vol 34, No. 3, 1934, pp 73-81.
4. Schilling, R. and Fuchs, H., "Modern Passenger-Car Ride Characteristics," Transactions, American Society of Mechanical Engineers, Vol 63, 1941, pp A59-A66.
5. Jeska, R. D., "A Comparison of Real and Simulated Automobile Suspension Analysis," Society of Automotive Engineers Transactions, Vol 64, 1956, pp 273-283.
6. Bodeau, A. C., Bollinger, R., and Lipkin, L., "Passenger Car Suspension Systems," VMM-117, 1953, University of Michigan, Ann Arbor, Mich.
7. Kohr, R. H., "Analysis and Simulation of Automobile Ride," Society of Automotive Engineers Journal, Vol 68, No. 4, 1960, pp 149, 151.
8. Van Deusen, B. D., "A Study of the Vehicle Ride Dynamics Aspects of Ground Mobility; Human Response to Vehicle Vibration," Contract Report No. 3-114, Vol II, Mar 1965, U. S. Army Engineer Waterways Experiment Station, CE, Vicksburg, Miss.
9. Dieckman, D., "Einfluss Vertihaler Mechanischer Schwingungen auf den Menschen," Internat. Z. Angew Physol., 1947, p 16.
10. Janeway, R. N., "Vehicle Vibration Limits to Fit the Passenger," preliminary copy of paper presented to Society of Automotive Engineers Passenger Car and Production Meeting, Detroit, Mich., Mar 1958.
11. Von Eldik Thieme, H. C. A., "Passenger Riding Comfort Criteria and Methods of Analyzing Ride and Vibration Data," Paper No. 295A, presented at Society of Automotive Engineers Meeting, Jan 1961.
12. Van Deusen, B. D., "Computing the Ride," Detroit Engineer, Mar 1962.
13. _____, "Ride Evaluation," Automobile Engineer, Vol 53, No. 13, Dec 1963.
14. Versace, J., "Measurement of Ride Comfort," Paper No. 638A, presented at Society of Automotive Engineers Meeting, Jan 1963.
15. Bogdanoff, J. L. and Kozin, F., "Behavior of a Linear One Degree of Freedom Vehicle Moving with Constant Velocity on a Stationary Gaussian Random Track," Report No. 48, Feb 1959, Land Locomotion Research Laboratory, U. S. Army Ordnance Tank-Automotive Command, Center Line, Mich.

16. Bieniek, M. P., "Suspension Dynamics," Automobile Engineer, Vol 50, No. 4, Apr 1960, pp 143-147.
17. Van Deusen, B. D., "Systems Analysis with Analog Computer Using Stochastic Processes," Paper No. 453A, presented at Society of Automotive Engineers Meeting, Jan 1962.
18. Bussman, D. R., "Vibrations of a Multi-Wheeled Vehicle," Report No. RF-573-64-1, Aug 1964, U. S. Army Combat Development Command, Armor Agency, Fort Knox, Ky.
19. U. S. Army Engineer Waterways Experiment Station, CE, "A Computer Analysis of Vehicle Dynamics While Traversing Hard Surface Terrain Profiles," Contract Report No. 3-155, Feb 1966, Vicksburg, Miss.
20. Benn, B. O. and Keown, M. P., "An Analytical Model for Predicting Cross-Country Vehicle Performance; Appendix A: Instrumentation of Test Vehicles," Technical Report No. 3-783, Jul 1967, U. S. Army Engineer Waterways Experiment Station, CE, Vicksburg, Miss.
21. Blackmon, C. A., Stinson, B. G., and Stoll, J. K., "An Analytical Model for Predicting Cross-Country Vehicle Performance; Appendix D: Performance of Amphibious Vehicles in the Water-Land Interface (Hydrologic Geometry)," Technical Report No. 3-783, Feb 1970, U. S. Army Engineer Waterways Experiment Station, CE, Vicksburg, Miss.
22. Blackmon, C. A. and Stoll, J. K., "An Analytical Model for Predicting Cross-Country Vehicle Performance; Appendix B: Vehicle Performance in Lateral and Longitudinal Obstacles (Vegetation), Vol I: Lateral Obstacles," Technical Report No. 3-783, Dec 1968, U. S. Army Engineer Waterways Experiment Station, CE, Vicksburg, Miss.
23. Cardwell, D., "The Acceleration of Military Vehicles During Cross-Country Operations," Advances in Automobile Engineering, edited by G. H. Tidbury, Macmillan, New York, 1963, pp 3-32.
24. Cohron, G. T. and Werner, R. A., "An Exploratory Study of the Effects of Terrain Surface Obstacles on Vehicle Performance," Contract Report No. 3-120, Mar 1965, U. S. Army Engineer Waterways Experiment Station, CE, Vicksburg, Miss.
25. Lessem, A. S., "Dynamics of Wheeled Vehicles; A Mathematical Model for the Traversal of Rigid Obstacles by a Pneumatic Tire," Technical Report M-68-1, Report 1, May 1968, U. S. Army Engineer Waterways Experiment Station, CE, Vicksburg, Miss.
26. Switzer, G. G., "Dynamics of Wheeled Vehicles; A Statistical Analysis of Obstacle-Vehicle-Speed Systems," Technical Report M-68-1, Report 4 (in preparation), U. S. Army Engineer Waterways Experiment Station, CE, Vicksburg, Miss.

Table C1

Vehicle Characteristics Used in Predicting M60A1 Dynamic Response

 Distance from road wheel to body center of gravity:

Road wheel l_1	76 in.
Road wheel l_2	44 in.
Road wheel l_3	12 in.
Road wheel l_4	24 in.
Road wheel l_5	56 in.
Road wheel l_6	88 in.
Body pitch inertia	581,700 in.-lb/sec ² *
Sprung weight	54,500 lb*
Vertical distance S from each bogie center to body center of gravity in no-load condition	46 in.
Effective unsprung weight for each bogie, lower track assembly	1420 lb

* The values for the body pitch inertia and sprung weight represent but one-half of the true value in order to fit the two-dimensional model which represents one-half of the vehicle that is assumed to be split down its longitudinal axis.

Table C2

Vehicle Characteristics Used in the Dynamic
Response Predictions for the M37 Truck

Vertical distance from wheel hub center to body center of gravity:	
Road wheel l_1	20.95 in.
Road wheel l_2	21.50 in.
Road wheel l_3	21.00 in.
Road wheel l_4	21.95 in.
Undeformed wheel radius.	17.0 in.
Total weight (loaded)	7550 lb
Sprung weight	6212 lb
Unsprung weight	1338 lb
Front axle.	722 lb
Rear axle	616 lb
Sprung* pitch moment of inertia about center of gravity	50,892 lb-sec ² /in.
Sprung roll moment of inertia about center of gravity	11,425 lb-sec ² /in.
Front axle roll moment of inertia	1256 lb-sec ² /in.
Rear axle roll moment of inertia.	955 lb-sec ² /in.
Wheel travel from static to bump stop:	
Front	4 in.
Rear.	8.5 in.
Tire (9.00-16, 8-PR, 45 psi) damping rate	9.56 lb-sec/in.

Note: One-half of these values was used in the two-dimensional model under the assumption that the vehicle is symmetrical.

* Sprung mass, $M = \frac{6212}{386} = 16.1 \text{ lb-sec}^2/\text{in.}$

Front axle unsprung mass, $M_1 = \frac{722}{386} = 1.87 \text{ lb-sec}^2/\text{in.}$

Rear axle unsprung mass, $M_2 = \frac{616}{386} = 1.60 \text{ lb-sec}^2/\text{in.}$

Table C3

Summary of Vehicle Characteristics and
Performance Data for M60A1 Tank

Cross-country gross weight, fully equipped plus payload and personnel	
Track weight, lb	
Left	54,500
Right.	54,500
Total gross weight, lb	109,000
Payload, lb.	6,000 plus crew
Dimensions	
Overall length, in. (hull only).	273.5
Height of leading edge, in.	45.0
Width, in.	143.0
Horizontal distance from leading edge (omitting gun) to center line of front sprocket of vehicle, in.	21.77
Vehicle approach angle, deg	90
Vehicle departure angle, deg	90
Ground clearance of hull between tracks, in.	18
Force leading edge can withstand, lb	Not limited
Winch capacity, lb	None
Water performance characteristics	
Fording depth	
Normal fording (no kit), in.	48
Fording with kit, in.	69
Fording with snorkel kit, in.	162
Water speed, mph	2
Volume of water displaced, cu ft	910.4
Engine	
Make	Continental
Model.	AVDS-1790-2A
Fuel type.	Diesel
Brake horsepower	642
Maximum torque, lb-ft.	1720
RPM at maximum torque.	1800
Transmission	
Make	Allison
Model.	CD-850-6A
Gear ratios	
1st gear	3.497:1

(Continued)

Table C3 (Concluded)

2nd gear	1.256:1
Torque convertor ratio (maximum)	3.43:1 (computed)
Final drive	
Type	Single stage speed reduced
Ratio	5.08:1
Pitch diameter of sprocket, in.	24.504
Track data	
Length of track in contact with ground, in.	166.7
Width of track, in.	28.0
Grouser height, in.	1.5
Total number of bogies in contact with ground.	12
Area of one track shoe, sq in.	194.3
No. of tracks	2
Steering data	
Turning radius at a forward speed determined from point at center of outside track, ft	
Pivot	9.6
Normal	35.0
Horizontal distance from leading edge of vehicle to midpoint of track in contact with the ground, in. . .	135.41
Width of track, in.	28.0
Center of gravity location	
Horizontal distance from front sprocket, in.	73.45
Vertical distance above bottom of track, in.	54.5
Maximum performance data	
Maximum speed, mph	
Forward.	30.0
Reverse.	Not applicable
Gradeability, %	60
Bridging, in.	102
Side-slope holding capacity, %	36
Maximum vertical height vehicle will climb, in.	36

Table C4
Summary of Vehicle Characteristics and
Performance Data for the M37 Truck

Cross-country gross weight, fully equipped plus payload and personnel	
Axle loads (front to rear), lb	
No. 1	3,600
No. 2	3,600
Total gross weight, lb	7,200
Payload, lb (cross country)	1,500
Dimensions, in.	
Overall length (including winch if available)	189.4
Wheelbase	112
Height of leading edge	26
Width	72.8
Distance between wheel center lines	62
Distance between axles	112
Vehicle approach angle, deg	38
Vehicle departure angle, deg	32
Undercarriage clearance, in.	
Axle	11
Interior	16
Force leading edge can withstand, lb	10,000
Winch capacity, lb	7,500
Water performance characteristics	
Fording depth, in.	
Normal	30
With fording kit	79
Water speed, mph	2
Engine	
Make	Dodge
Model	T-245
Fuel type	Gasoline
Brake horsepower	77
Maximum torque, lb-ft	188
Engine RPM at maximum torque	1,200
Engine RPM at brake horsepower	3,200

(Continued)

Table C4 (Concluded)

Transmission

Type or model	T-245-3955
Ratios	
1st	6.40:1
2d	3.09:1
3d	1.69:1
4th	1.00:1

Transfer case

Model	Timken
Ratios	
High.	1.00:1
Low	1.96:1

Axles

Model	T-245
Ratio	5.83:1

Tire data

Type.	Mud and snow
Size.	9.00x16
Ply	8
Tread design.	NDMS
Unloaded diameter (including tread), in.	25
Unloaded width, in.	10.2
Tread depth, in.	1
No. of tires.	4
No. of wheels	4
Cross-country inflation pressure, psi	14
Highway inflation pressure, psi	40

Steering data

Turning radius (curb to curb), ft	25
Time required to steer from straight ahead to full lock turn, sec	3
Distance from front wheel steering (hub) pivot to front of vehicle, in.	35.62
Distance from front wheel steering (hub) pivot to outside of vehicle, in.	10.0

Center of gravity location, in.

Horizontal distance from front axle	63
Vertical distance above ground at full load static position	34

Table C5

Summary of Measured Data and Test Results for
M60A1 Tank Tests

Test No.	Field Identification No.	Obstacle Height in.	Impact Speed mph	Peak Vertical Acceleration g's	Peak Longitudinal Acceleration g's
1	1-1	6	3.75	0.42	0.24
2	1-2	6	4.87	0.42	0.21
3	1-3	6	3.52	0.42	0.12
4	2-1	6	6.20	0.48	0.27
5	2-2	6	5.88	0.54	0.42
6	2-3	6	5.81	0.54	0.36
7	3-1	6	10.51	0.48	0.36
8	3-2	6	10.27	0.48	0.33
9	3-3	6	10.05	0.54	0.39
10	4-1	6	16.50	0.73	0.89
11	4-2	6	17.17	0.54	0.89
12	4-3	6	17.47	0.54	0.89
13	5-2	6	18.15	0.67	1.13
14	5-3	6	18.15	0.48	1.12
15	15-1	8	6.15	0.50	0.47
16	15-2	8	11.25	1.56	0.38
17	15-3	8	17.62	2.75	1.47
18	16-1	10	6.07	0.62	0.38
19	16-2	10	10.65	2.44	0.94
20	16-3	10	17.17	3.12	1.44
21	16-4	10	17.27	2.56	1.26
22	6-1	12	4.42	0.96	0.36
23	6-2	12	5.02	1.39	0.89
24	6-3	12	4.87	1.82	0.36
25	7-1	12	6.45	1.88	0.60
26	7-2	12	5.85	1.51	0.36
27	7-3	12	6.07	1.82	0.30
28	9-1	12	8.44	4.24	1.49
29	9-2	12	8.60	3.64	1.19
30	9-3	12	8.60	3.82	1.25
31	8-1	12	10.17	2.72	1.88
32	8-2	12	10.52	3.76	1.40
33	10-1	16	5.40	2.56	0.73
34	10-2	16	4.50	1.44	1.03
35	10-3	16	4.42	1.56	1.76
36	11-1	16	6.37	3.75	0.91
37	11-2	16	6.91	3.44	1.18
38	11-3	16	6.52	4.25	1.03
39	12-1	16	8.71	3.75	2.29
40	12-2	16	7.65	3.75	1.32
41	12-3	16	8.77	3.12	1.41
42	13-2	18	5.40	2.87	1.18
43	13-3	18	4.92	2.50	1.20

Table C6

Summary of Measured Data for M37 Truck Tests

Test No.	Field Identification No.	Obstacle Height in.	Impact Speed mph	Peak Vertical Acceleration g's	Peak Longitudinal Acceleration g's
44	F68-0024	6	4.0	1.48	0.74
45	F68-0025	6	3.5	1.43	0.76
46	F68-0026	6	6.4	1.48	0.82
47	F68-0027	6	8.9	2.57	NA
48	F68-0028	6	11.8	3.40	0.80
49	F68-0029	6	11.6	3.22	0.76
50	F68-0030	6	15.1	3.66	0.79
51	F68-0031	6	14.5	3.40	0.82
52	F68-0032	6	15.3	3.85	0.70
53	F68-0033	6	14.8	3.64	0.81
54	F68-0103	8	2.8	1.64	0.85
55	F68-0104	8	3.0	1.63	0.96
56	F68-0105	8	8.1	4.38	1.57
57	F68-0106	8	5.4	2.43	1.50
58	F68-0107	8	10.8	5.78	1.48
59	F68-0109	8	13.3	6.59	1.45
60	F68-0110	8	13.3	6.20	1.50
61	F68-0111	8	19.1	7.99	1.19
62	F68-0112	8	9.3	3.44	1.48
63	F68-0113	8	19.0	8.73	1.25
64	F68-0114	8	19.6	8.72	1.40
65	F68-0034	10	2.9	1.68	1.07
66	F68-0035	10	3.0	1.77	1.05
67	F68-0036	10	2.3	1.59	1.11
68	F68-0037	10	6.2	4.56	1.64
69	F68-0038	10	10.3	6.47	1.56
70	F68-0039	10	6.9	4.58	1.64
71	F68-0040	10	10.5	7.45	1.84
72	F68-0041	10	10.6	5.85	1.71
73	F68-0042	10	15.2	7.30	1.42
74	F68-0043	10	15.8	9.00	1.76
75	F68-0044	10	15.5	8.39	1.41
76	F68-0045	10	11.5	7.67	1.69
77	F68-0046	12	3.3	6.29	1.70
78	F68-0047	12	3.4	6.43	1.30

Table C7

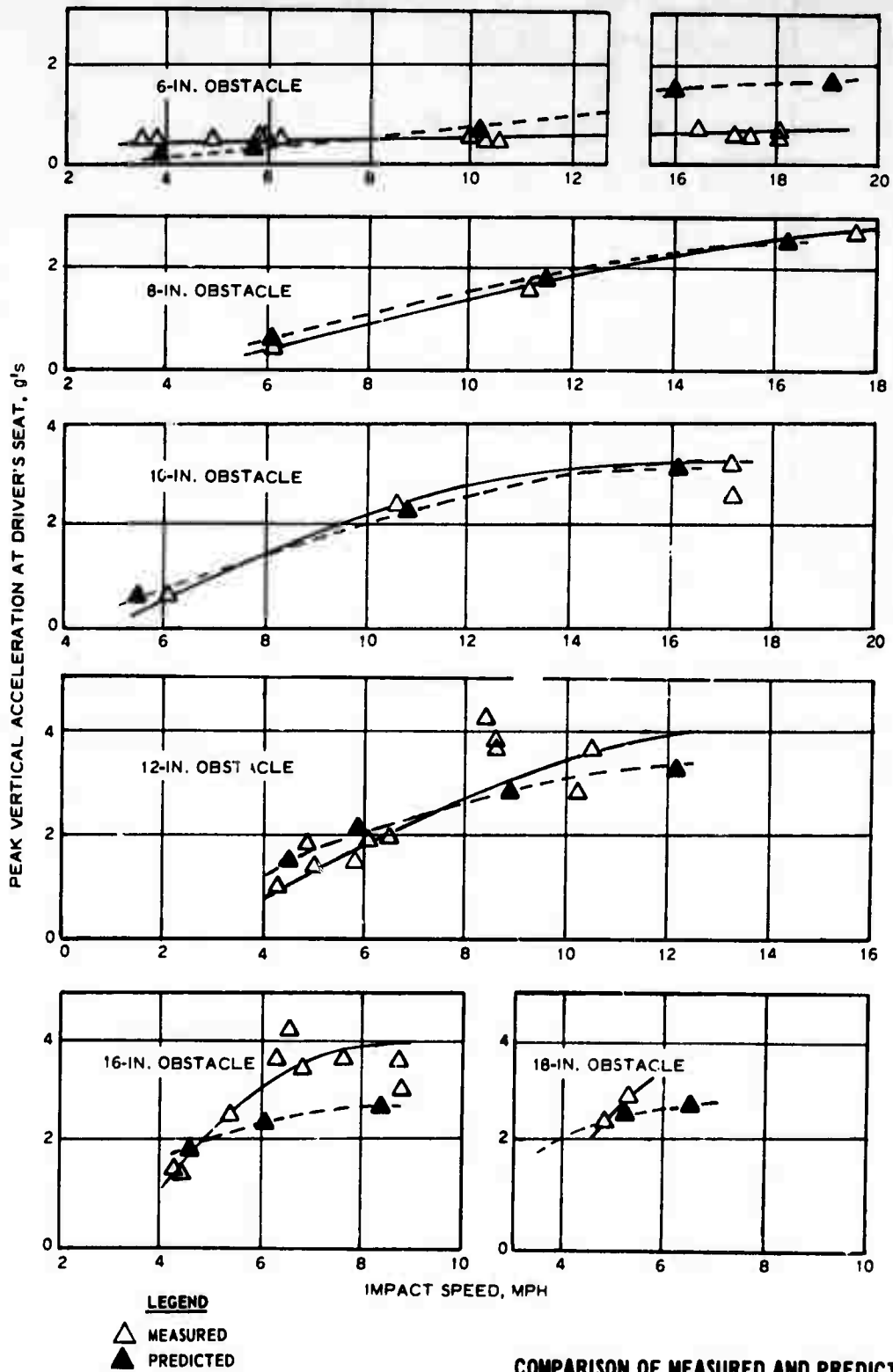
Summary of Predicted Data and Comparison of Prediction Accuracy for M60A1 Tank

Obstacle Height in.	Impact Speed mph	Driver's Seat				Driver's Seat			
		Peak Vertical Acceleration		Peak Longitudinal Acceleration		Peak Vertical Acceleration		Peak Longitudinal Acceleration	
		Predicted g's	Measured g's	Deviation g's	Percent Error	Predicted g's	Measured g's	Deviation g's	Percent Error
6	3.90	0.20	0.40	-0.20	-50	0.41	0.20	0.21	105
6	5.70	0.26	0.41	-0.15	-37	0.52	0.22	0.30	136
6	10.15	0.63	0.44	0.19	43	0.72	0.36	0.36	100
6	15.97	1.48	0.61	0.87	143	0.83	0.78	0.05	6
6	19.17	1.64	0.70	0.94	134	0.90	1.15	-0.25	-22
8	6.12	0.65	0.50	0.15	30	0.63	0.23	0.40	174
8	11.56	1.83	1.81	0.02	-1	0.99	0.60	0.39	65
8	16.32	2.53	2.60	-0.07	-3	1.24	1.24	0.00	0
10	5.44	0.66	0.30	0.36	120	0.61	0.30	0.31	103
10	10.88	2.30	2.40	-0.10	-4	1.00	0.88	0.12	14
10	16.09	3.19	3.20	-0.01	0	1.62	1.46	0.16	11
12	4.45	1.44	1.05	0.39	37	1.08	0.33	0.75	227
12	5.89	2.10	1.92	0.18	9	1.31	0.50	0.81	162
12	8.84	2.82	3.10	-0.28	-9	1.39	1.26	0.13	10
12	12.24	3.30	4.00	-0.70	-18	1.85	1.70	0.15	9
16	4.64	1.98	1.78	0.20	11	1.69	0.65	1.04	160
16	6.12	2.49	3.12	-0.63	-20	2.10	0.88	1.22	139
16	8.38	2.69	4.05	-1.36	-34	2.52	1.60	0.92	58
18	5.27	2.66	2.82	-0.16	-6	2.22	1.22	1.00	82
18	6.48	2.75	--	--	--	2.64	1.54	1.10	71

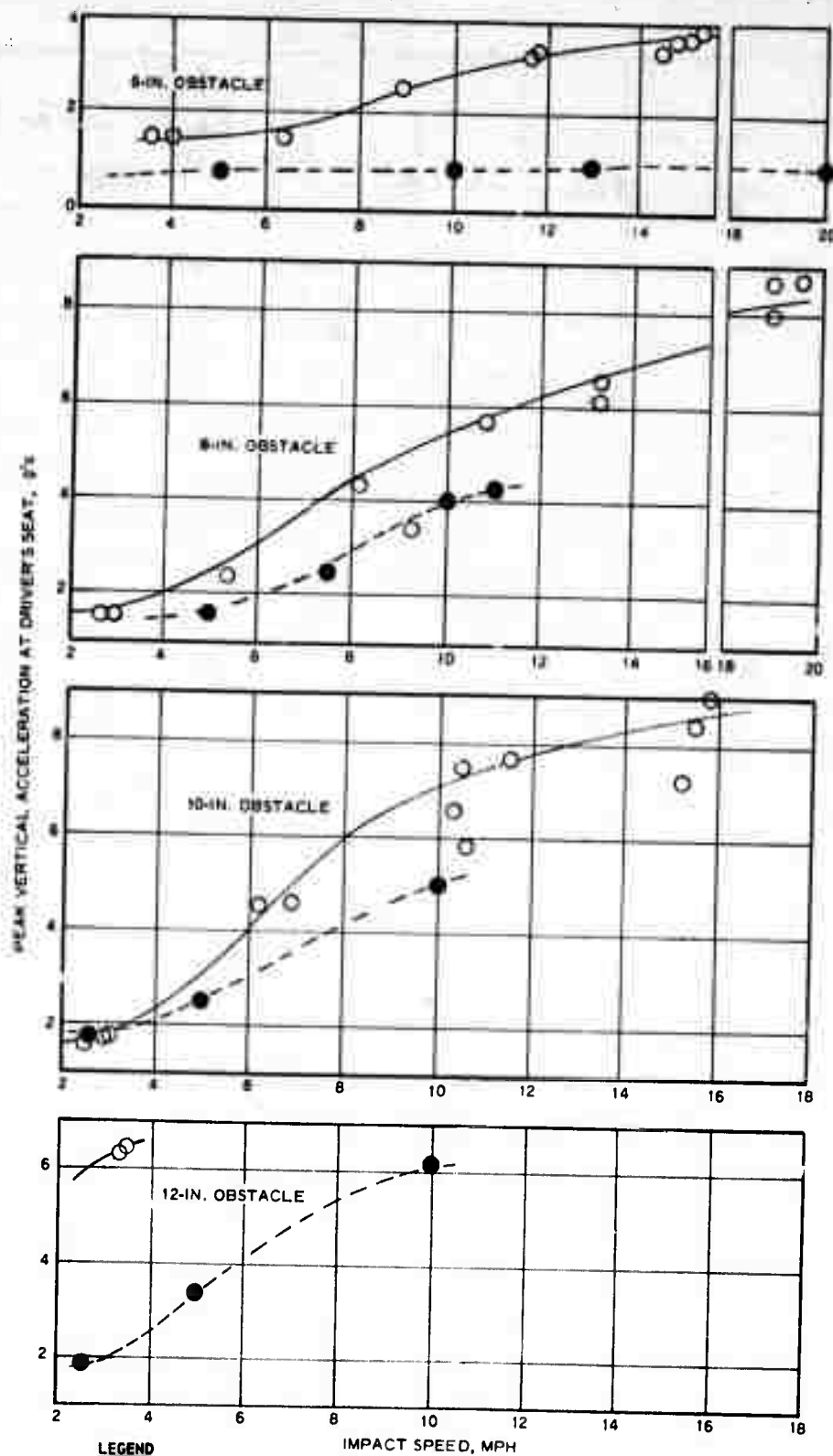
Table C8

Summary of Predicted Data and Comparison of Prediction
Accuracy for M37 Truck

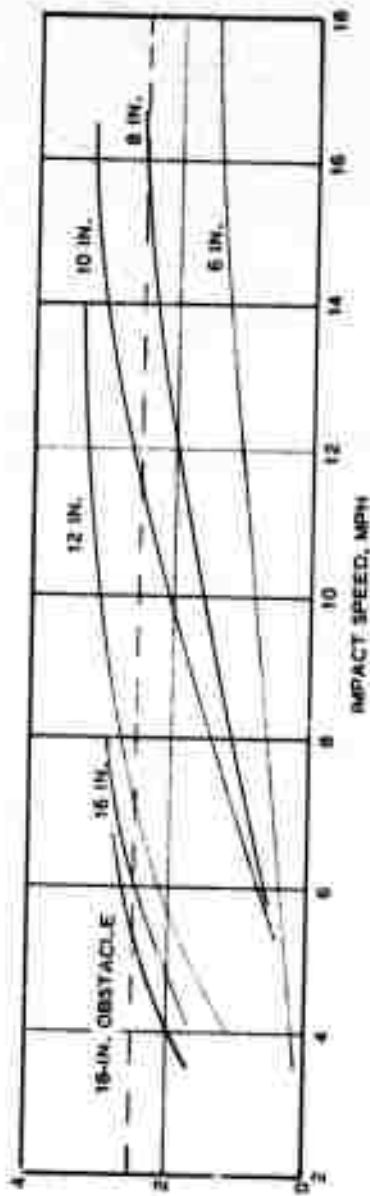
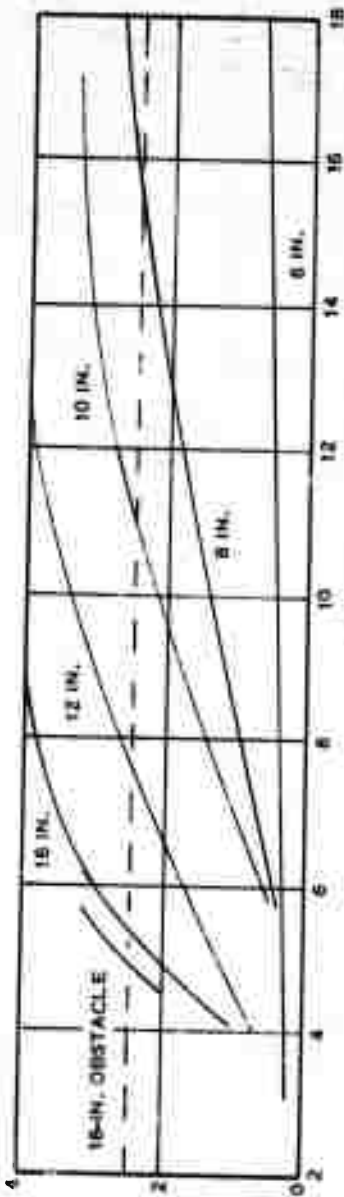
Obstacle Height in.	Impact Speed mph	Driver's Seat Peak Vertical Acceleration			
		Predicted g's	Measured g's	Deviation g's	Percent Error
6	5.0	0.70	1.40	-0.70	-50
6	10.0	0.85	2.98	-2.13	-71
6	13.0	0.94	3.72	-2.78	-75
6	20.0	0.85	--	--	--
8	5.0	1.41	1.64	-0.23	-14
8	7.5	2.43	4.10	-1.67	-41
8	10.0	4.00	5.70	-1.70	-30
8	11.0	4.29	5.92	-1.63	-28
10	2.5	1.78	1.60	0.18	11
10	5.0	2.52	2.94	-0.42	-14
10	10.0	5.03	7.00	-1.97	-28
12	2.5	1.90	5.90	-4.00	-68
12	5.0	3.40	--	--	--
12	10.0	6.09	--	--	--



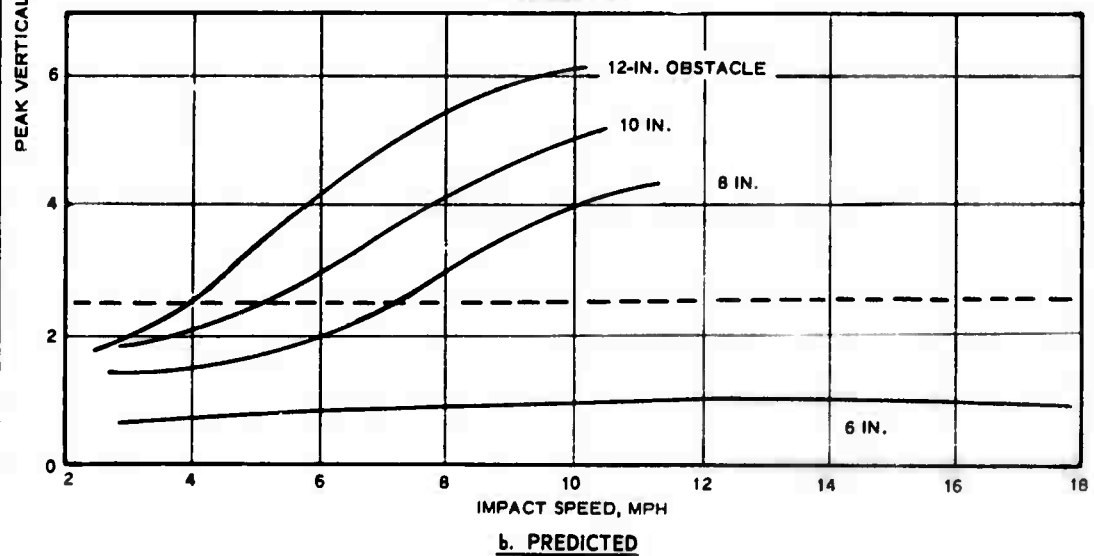
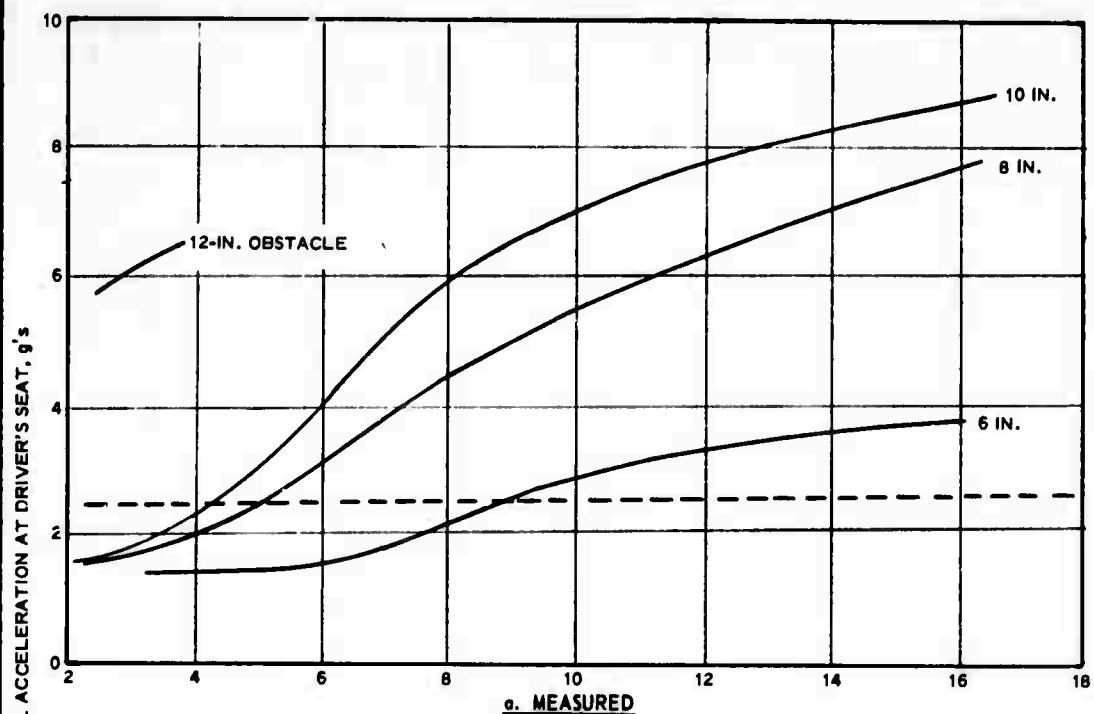
COMPARISON OF MEASURED AND PREDICTED
PEAK VERTICAL ACCELERATIONS AT
DRIVER'S SEAT, M60A1 TANK



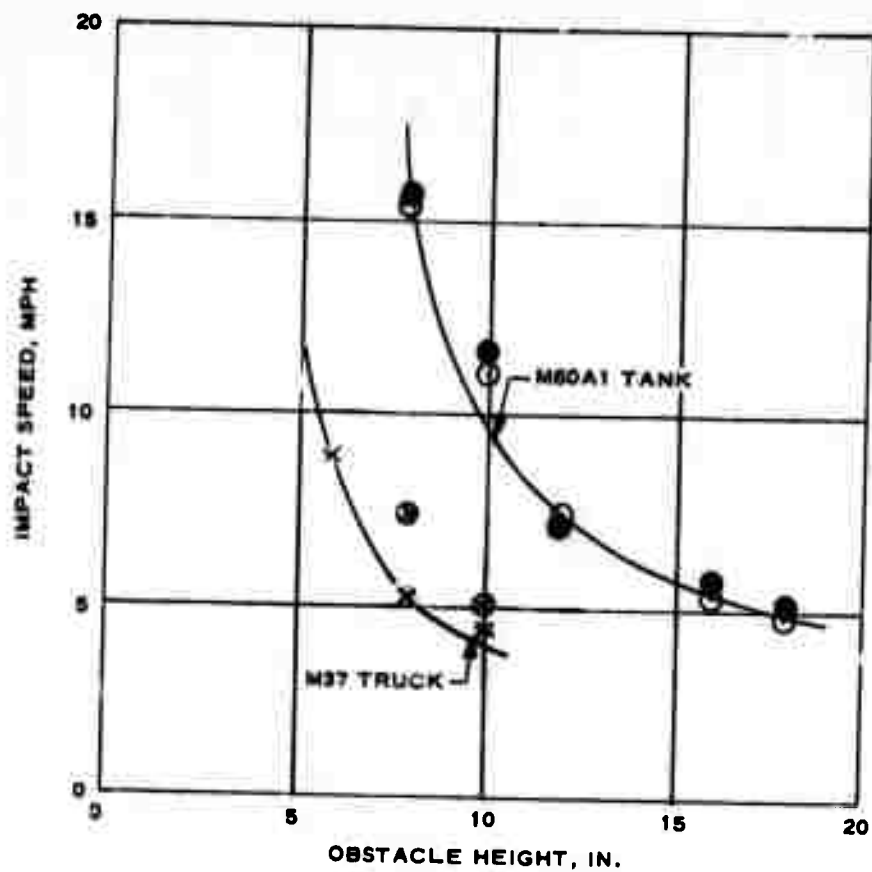
COMPARISON OF MEASURED AND PREDICTED PEAK VERTICAL ACCELERATIONS AT DRIVER'S SEAT, M37 TRUCK



SUMMARY OF MEASURED AND PREDICTED SPEED-OBSTACLE HEIGHT-PEAK VERTICAL ACCELERATION RELATIONS, M60A1 TANK



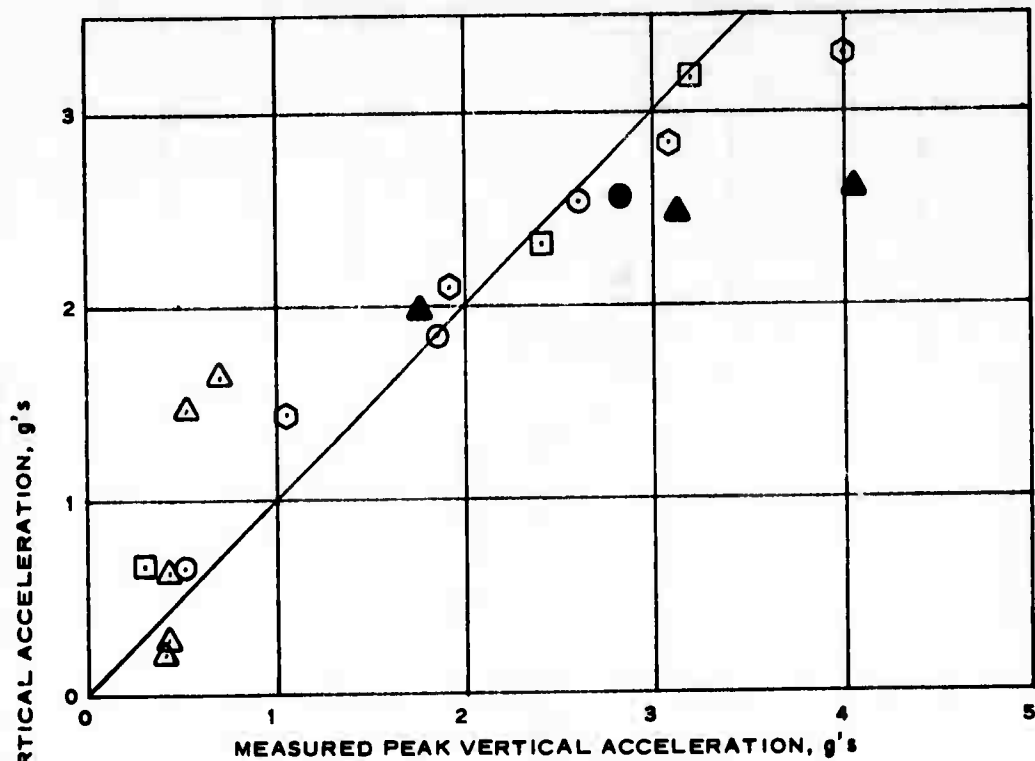
SUMMARY OF MEASURED AND PREDICTED SPEED-OBSTACLE HEIGHT-PEAK VERTICAL ACCELERATION RELATIONS, M37 TRUCK



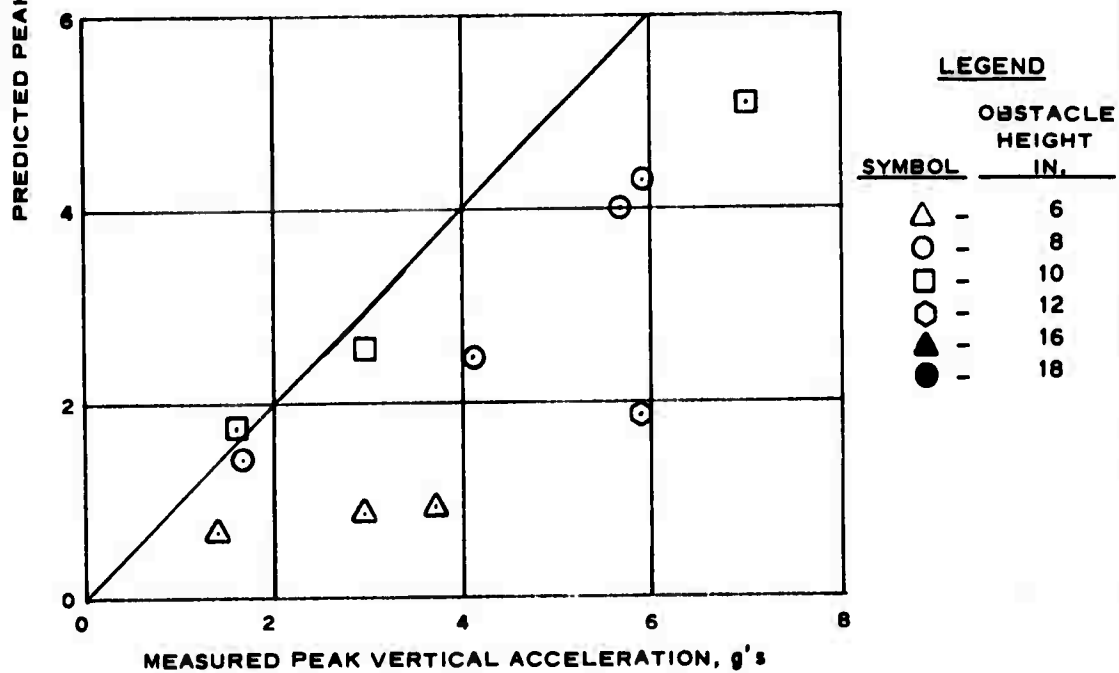
LEGEND

- - MEASURED, M60A1 TANK
- - PREDICTED, M60A1 TANK
- X - MEASURED, M37 TRUCK
- ⊗ - PREDICTED, M37 TRUCK

SPEED-OBSTACLE HEIGHT RELATIONS AT 2.5-g PEAK VERTICAL ACCELERATION



a. M60A1 TANK

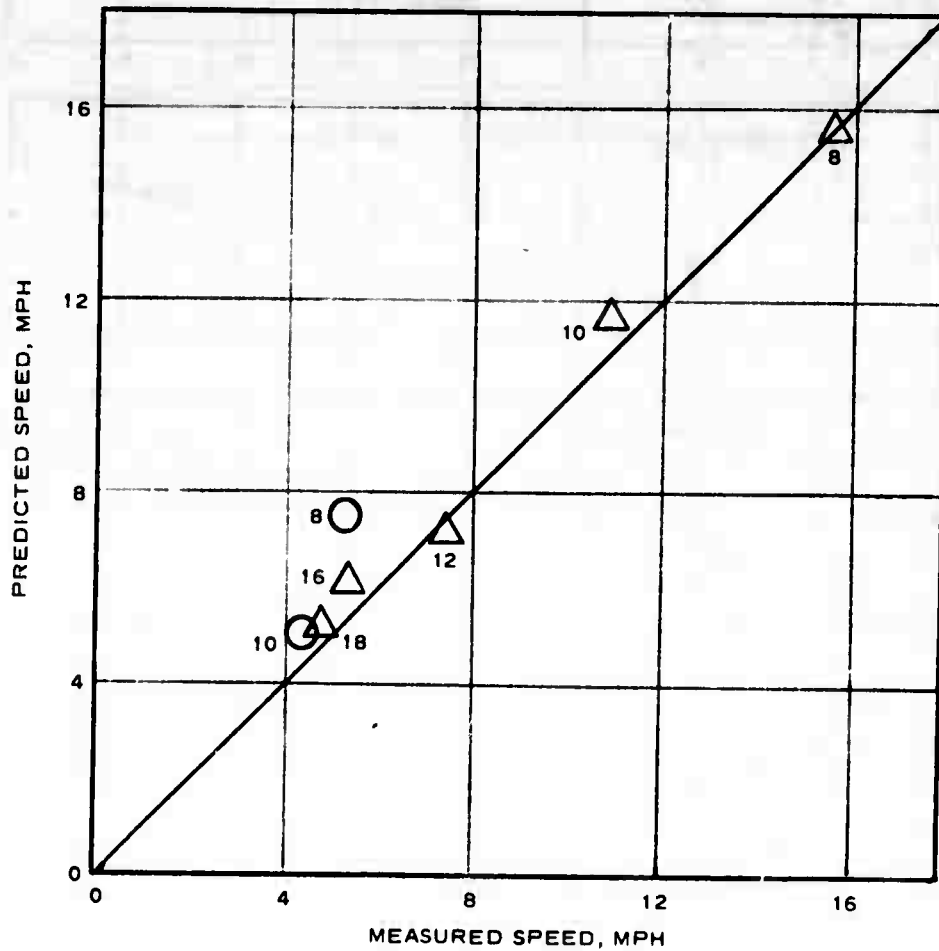


LEGEND

SYMBOL	OBSTACLE HEIGHT IN.
△	6
○	8
□	10
◊	12
▲	16
●	18

b. M37 TRUCK

COMPARISON OF MEASURED AND
PREDICTED PEAK VERTICAL
ACCELERATIONS

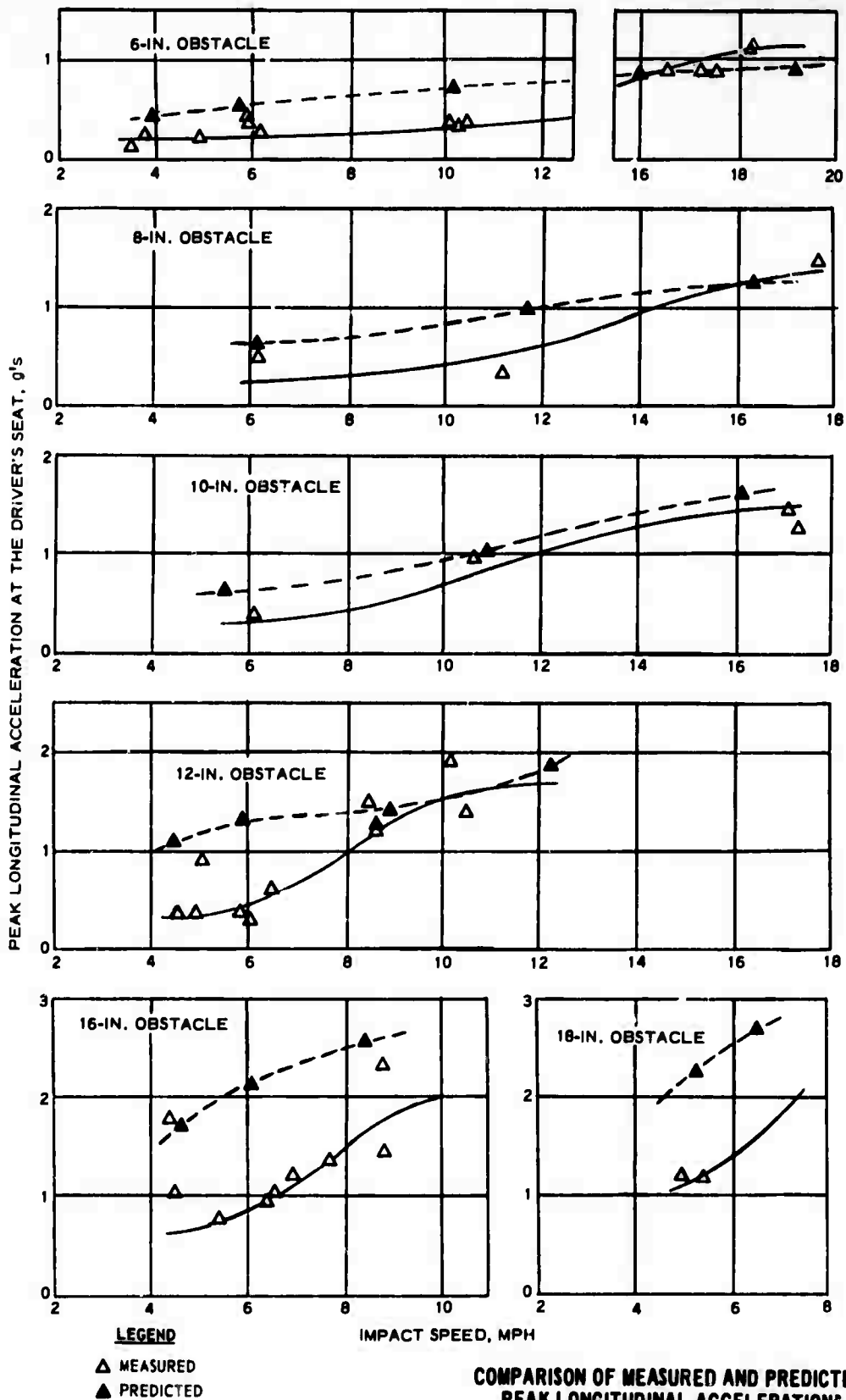


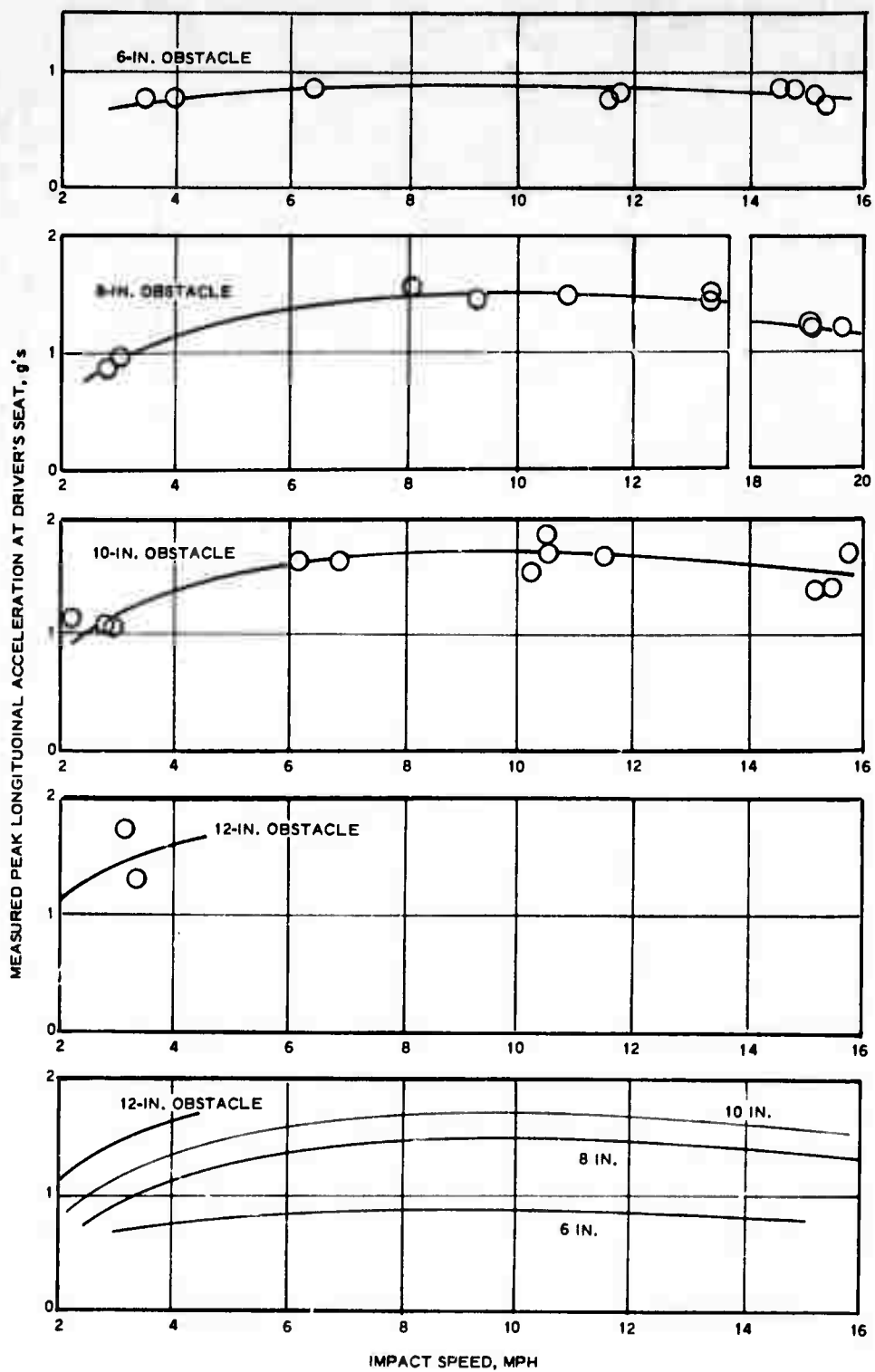
NOTE: NUMBERS NEAR PLOTTED POINTS INDICATE OBSTACLE HEIGHT IN INCHES.

LEGEND

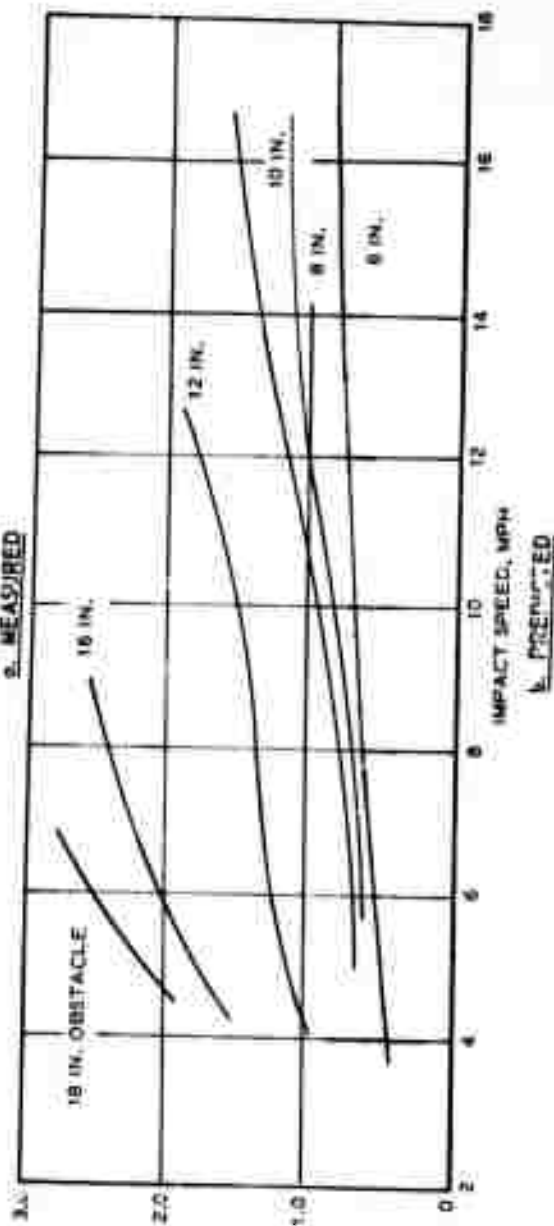
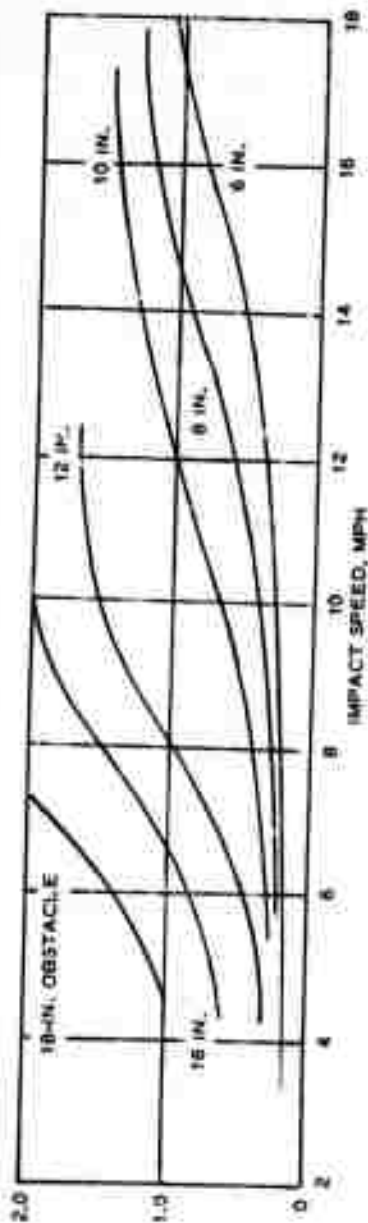
- △ M60A1 TANK
- M37 TRUCK

COMPARISON OF MEASURED AND PREDICTED SPEEDS AT WHICH PEAK VERTICAL ACCELERATION EQUALS 2.5 g's



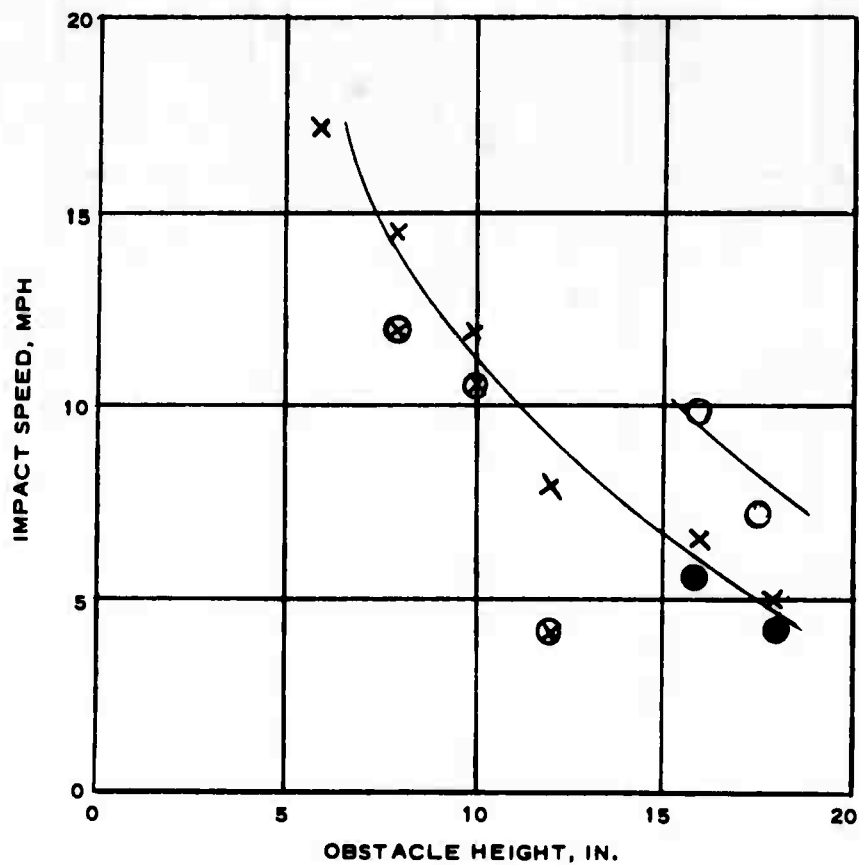


SPEED-OBSTACLE HEIGHT-PEAK LONGITUDINAL
ACCELERATION RELATIONS, M37 TRUCK



PEAK LONGITUDINAL ACCELERATION AT DRIVER'S SEAT, g's

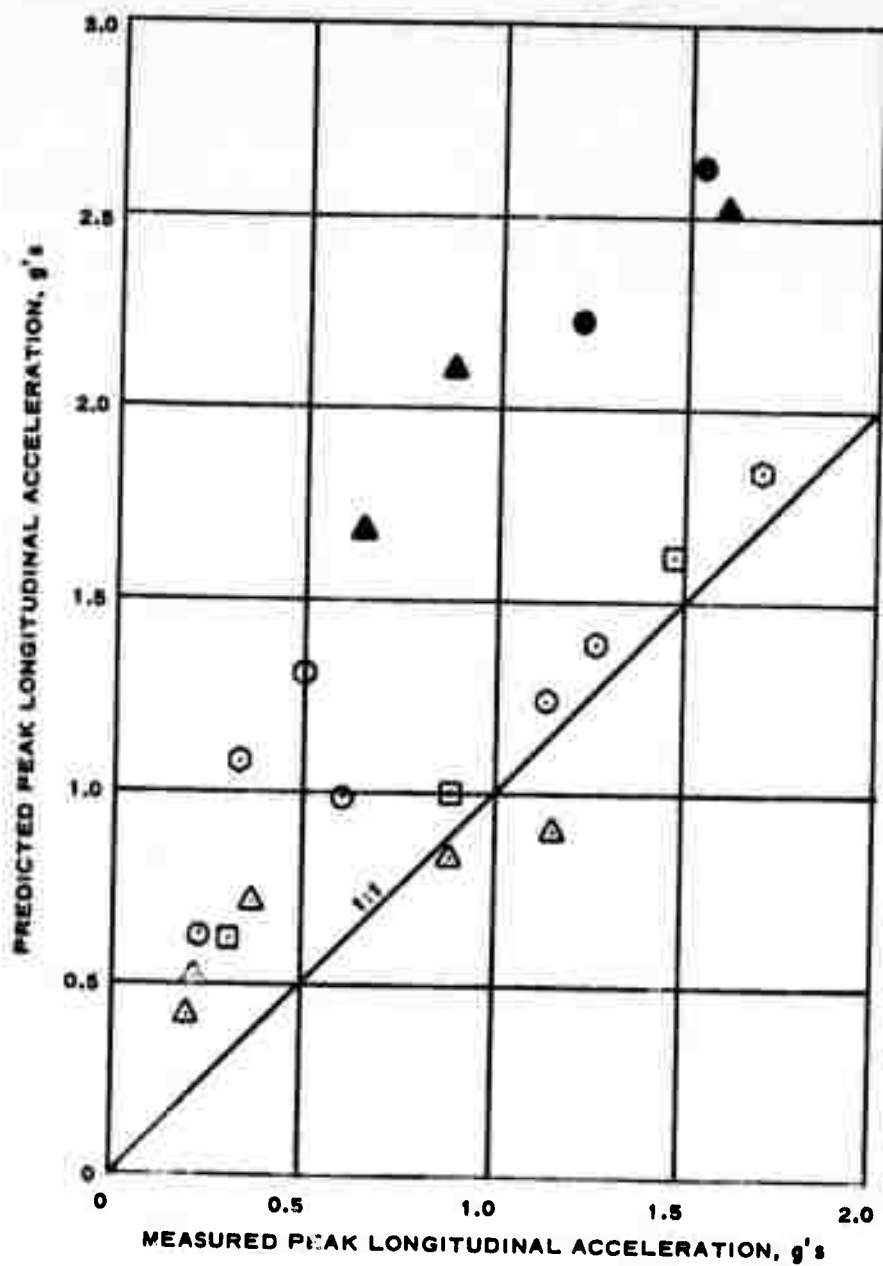
SUMMARY OF MEASURED AND PREDICTED SPEED-OBSTACLE HEIGHT-PEAK LONGITUDINAL ACCELERATION RELATIONS, M60A1 TANK



LEGEND

- - MEASURED, 2.0 g
- - PREDICTED, 2.0 g
- × - MEASURED, 1.0 g
- ⊗ - PREDICTED, 1.0 g

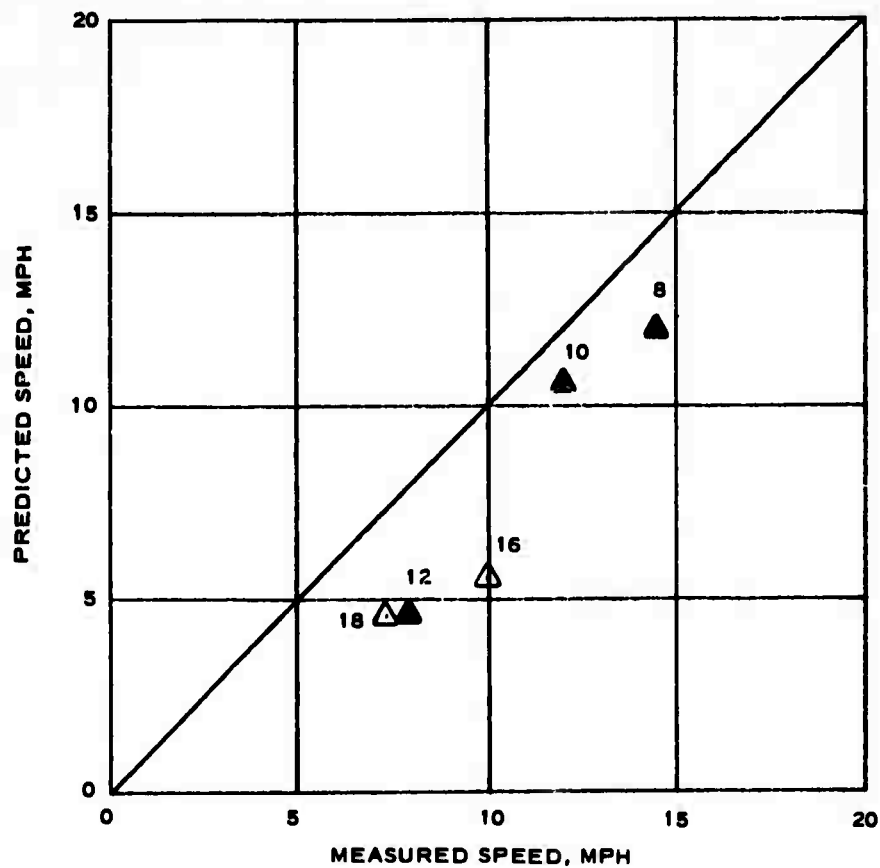
**SPEED-OBSTACLE HEIGHT RELATIONS
FOR M60A1 TANK AT 1.0-g AND 2.0-g
PEAK LONGITUDINAL ACCELERATIONS**



LEGEND

- △ - 6 IN.
- - 8 IN.
- - 10 IN.
- ◇ - 12 IN.
- ▲ - 16 IN.
- - 18 IN.

COMPARISON OF MEASURED AND
PREDICTED PEAK LONGITUDINAL
ACCELERATIONS, M60A1 TANK



NOTE: NUMBERS NEAR PLOTTED POINTS
INDICATE OBSTACLE HEIGHTS IN
INCHES.

LEGEND

△ - 2.0 g

▲ - 1.0 g

COMPARISON OF MEASURED AND PREDICTED
SPEEDS AT WHICH LONGITUDINAL ACCELER-
ATION EQUALS 1.0 AND 2.0 g's

COMPUTER PROGRAM FOR SIMULATING DYNAMIC RESPONSE OF M60A1 TANK, AND
DICTIONARY OF PROGRAM VARIABLES

Program

TANK

```

1 SLIB, DIFFEQ
2 SLIB, ALGEBR
3 STTY, 120
4 SRPC
5 SNDM
6 SSAV
100 COMMON FORCD1, FORCD2, FORCD3, FORCD4, FORCD5, FORCD6
110 COMMON FORCW1, FORCW2, FORCW3, FORCW4, FORCW5, FORCW6
120 COMMON FORCH1, FORCH2, FORCH3, FORCH4, FORCH5, FORCH6
130 COMMON FORCK1, FORCK2, FORCK3, FORCK4, FORCK5, FORCK6
140 COMMON FORCT1, FORCT2, FORCT3, FORCT4, FORCT5
150 COMMON SPDEF1, SPDEF2, SPDEF3, SPDEF4, SPDEF5, SPDEF6
160 COMMON DSPDF1, DSPDF2, DSPDF3, DSPDF4, DSPDF5, DSPDF6
170 COMMON VAR1, VAR2, VAR3, VAR4, VAR5, VAR6, VAR7, VAR8, VAR9, VAR10,
180 VAR11, VAR12, VAR13, VAR14, VAR15, VAR16, VAR17, VAR18, VAR19
190 COMMON DRV1, ZETA1, HORZ1, ETA1, AXL11, AXL21, AXL31, AXL41, AXL51, AXL61
200 COMMON DRV2, ZETA2, HORZ2, ETA2, AXL12, AXL22, AXL32, AXL42, AXL52, AXL62
210 COMMON DDRV2, DZETA2, DHORZ2, DETA2, DAXL12, DAXL22, DAXL32, DAXL42,
220 DAXL52, DAXL62
230 COMMON H, NSTEPS, HORMOM
240 COMMON THRESH(72), GAMMA(72), SIGMA(72), SEGDEF(72), Y(86)
250 COMMON TH(4)
260 DIMENSION FORCW(6), FORCK(6), SPDEF(6), DSPDF(6)
270 DIMENSION FORCH(6), FORCD(6)
280 DIMENSION DISPL(10), VELCTY(10), ACCISS(10), ACCGS(10)
290 DIMENSION ACCMAX(10), ACCMIN(10), SACCSEQ(10), RMSACC(10)
300 DIMENSION FID(12), VARID(10)
310 EQUIVALENCE (FORCH1, FORCH(1)), (FORCD1, FORCD(1))
320 EQUIVALENCE (FORCW1, FORCW(1)), (FORCK1, FORCK(1))
330 EQUIVALENCE (SPDEF1, SPDEF(1)), (DSPDF1, DSPDF(1))
340 EQUIVALENCE (DRV1, DISPL(1)), (DRV2, VELCTY(1))
350 EQUIVALENCE (DDR2, ACCISS(1))
360 DATA IBELL/458752/
370 DATA VARIU/SHV, DRV, SHV, C-G, SHH, C-G, SHPITCH, SHAXLE1, SHAXLE2,
380 SHAXLE3, SHAXLE4, SHAXLE5, SHAXLE6/
390 PRINT, "MURPHY'S M-60 TANK MODEL"
400 PRINT,
410C-----DATA INITIALIZATION-----
420 CALL OPENF(1, "THRESH")
430 READ(1, ) (THRESH(I), I=1, 72)
440 CALL CLOSEF(1)
450 CALL OPENF(1, "GAMMA")
460 READ(1, ) (GAMMA(I), I=1, 72)
470 CALL CLOSEF(1)
480 CALL OPENF(1, "SIGMA")
490 READ(1, ) (SIGMA(I), I=1, 72)
500 CALL CLOSEF(1)
510 TH(1)=13.
520 TH(2)=10.
530 TH(3)=8.

```

(1 of 15 sheets)

TANK CONTINUED

```

540      TH(4) = 3.
550      DO 10 I=1,6
560        FORCW(I)=0.
570        FORCK(I)=0.
580        SPDEF(I)=0.
590      10 DSPDF(I)=0.
600      DO 20 I=1,10
610        DI SPL(I)=0.
620        VELCTY(I)=0.
630        ACCISS(I)=0.
640        ACCGS(I)=0.
650        RMSACC(I)=0.
660        ACCMAX(I)=0.
670        ACCMIN(I)=0.
680      20 SACCSEQ(I)=0.
690      DO 30 I=1,36
700      30 Y(I)=0.
710      ZETA1 = -5.79
720      HORZ1=0.
730      ETA1 = -.0089
740      AXL0=13.
750      AXL11 = -.966
760      AXL21 = -.970
770      AXL31 = -.942
780      AXL41 = -.913
790      AXL51 = -.884
800      AXL61 = -.856
810      TP=0.
820      TIP=.5
830      T=0.
840      DELTAL=33./14.
850      NPL=4
860      NSTOP=0
870      JJ=1
880      H=.001
890C-----DATA READ IN-----
900      PRINT,"GIVE THE FOLLOWING INFORMATION"
910      PRINT,
920      PRINT,"NAME OF PROFILE INPUT FILE"
930      READ 1,FNAME
940      PRINT,"TANK VELOCITY IN M.P.H."
950      READ,XMPH
960      PRINT,"PRINTOUT TIME INTERVAL"
970      READ,TIP
980      PRINT,"NAME OF OUTPUT DATA FILE"
990      READ 1,FNAME2
1000     PRINT,"*****END OF INPUT DATA*****"
1010     VEL=XMPH*17.6
1020     DELTAT=DELTAL/VEL
1030     NSTEPS=DELTAT/H

```

(2 of 15 sheets)

TANK CONTINUED

```

1040      H=DEL TAT/NSTEPS
1050      PRINT 2,XMPH,VEL,DEL TAL,DEL TAT,NSTEPS,H
1060      WRITE(2,11)
1070      CALL OPENF(1,FINAME)
1080      READ(1,1)FID
1090      PRINT,
1100      PRINT,"INPUT PROFILE IS:"
1110      PRINT 1,FID
1120      PRINT 3
1130      WRITE(2,12) FID,FINAME
1140      WRITE(2,13)XMPH,VEL,DEL TAL,DEL TAT,NSTEPS,H
1150      WRITE(2,14)VARID
1160      GO TO 190
1170 150 IF(JJ-2)50,40,50
1180 50 READ(1,15)YINPUT
1190      CALL EOFTST(1,JJ)
1200      GO TO (60,40)JJ
1210 40 NSTOP=NSTOP+1
1220 60 I=85
1230 70 Y(I+1)=Y(I)
1240      I=I-1
1250      IF(I)70,80,70
1260 80 Y(I)=YINPUT
1270      CALL DIFFEQ
1280      NPL=NPL+1
1290      T=T+DEL TAT
1300      DO 90 I=1,10
1310 90 ACCGS(I)=ACCI SS(I)/386.
1320      ACCGS(4)=ACCI SS(4)
1330      DO 100 I=1,10
1340      ACCMAX(I)=AMAX1(ACCMAX(I),ACCGS(I))
1350      ACCMIN(I)=AMIN1(ACCMIN(I),ACCGS(I))
1360      SACC SQ(I)=SACC SQ(I)+ACCGS(I)*ACCGS(I)
1370 100 RMSACC(I)=SQRT((SACC SQ(I)+DEL TAT)/T)
1380 190 IF(T-TP)110,120,120
1390 120 TP=TP+TIP
1400      PRINT 4,T,Y(I),(VARID(I),DISPL(I),VELCTY(I),ACCGS(I),
1410&      RMSACC(I),I=1,10)
1420 110 WRITE(2,16)T,Y(I),DISPL,VELCTY,ACCGS,RMSACC
1430      IF(NPL-11)140,130,140
1440 130 WRITE(2,14)VARID
1450      NPL=0
1460 140 IF (NSTOP-86) 150,160,150
1470 160 WRITE(2,5)(VARID(I),ACCMAX(I),ACCMIN(I),I=1,10)
1480      PRINT 5,(VARID(I),ACCMAX(I),ACCMIN(I),I=1,10)
1490      IF(FNAME2-64)NOFILE)170,190,170
1500 170 CALL CLOSEF(2,FNAME2,2)
1510      PRINT 6,FNAME2
1520 180 PRINT 7,(IBELL,I=1,40)
1530      CALL EXIT

```

TANK CONTINUED

```

1540 1 FORMAT(12A6)
1550 2 FORMAT(///,"VELOCITY=",F5.2," MPH (" ,F6.1," IPS )",/,
1560& "DELTA-L=",F5.3,3X,"DELTA-T=",F6.4,/,
1570& "NSTEPS=",I4,4X,"H=",F7.6)
1580 3 FORMAT(/////2X,4H TIME,3X,4HY(1),12X,5HDISPL,5X,5HVELOC,
1590& 5X,5HACCEL,4X,6HRMSACC,/)
1600 4 FORMAT(F8.4,F7.2,2X,A5,4G10.3,/,9(17X,A5,4G10.3,/)
1610 5 FORMAT(37HPEAK ACCELERATIONS MAXIMUM MINIMUM,/,
1620& 10(10X,A5,2X,2F10.3,/)
1630 6 FORMAT(38HCALL 2530 TO OBTAIN A LISTING OF FILE:,X,A6)
1640 7 FORMAT(40A1)
1650 11 FORMAT(//,37X,45(1H*),/,37X,1H*,43X,1H*,/,37X,
1660& 45H* MURPHY'S M-60 TANK PROGRAM OUTPUT FILE *,/,
1670& 37X,1H*,43X,1H*,/,37X,45(1H*),/)
1680 12 FORMAT(16HINPUT PROFILE IS,X,12A6,X,11H(FILE NAME ,A6,1H),/)
1690 13 FORMAT(9HVELOCITY=F5.2,17H MILES PER HOUR (F6.1,
1700& 19H INCHES PER SECOND)4X,8HDELTA-L=F5.3,7H INCHES4X,
1710& 8HDELTA-T=F10.8,8H SECONDS//,
1720& 35HNUMBER OF STEPS IN RKG INTEGRATION=I4,4X,
1730& 12HSTEP SIZE H=F10.8)
1740 14 FORMAT(//,2X,4H TIME3X,4HY(1)12X,10(A5,3X),/)
1750 15 FORMAT(E20.10)
1760 16 FORMAT(F8.4,F5.1,2X,6HDISPL.2X,10F8.3,/,15X,8HVELOCITY,
1770& 10F8.3,/,15X,6HACCEL.2X,10F8.3,/,15X,8HRMS.ACC.10F8.3,/)
1780 END
2000 SUBROUTINE DIFFEQ
2010 RH=1./H
2020 INDEX=0.
2030 1 INDEX=INDEX+1
2040 VAR1=ZETA1
2050 VAR2=ZETA2
2060 VAR3=HORZ1
2070 VAR4=HORZ2
2080 VAR5=ETA1
2090 VAR6=ETA2
2100 VAR19 = AXL0
2110 VAR7=AXL11
2120 VAR8=AXL12
2130 VAR9=AXL21
2140 VAR10=AXL22
2150 VAR11=AXL31
2160 VAR12=AXL32
2170 VAR13=AXL41
2180 VAR14=AXL42
2190 VAR15=AXL51
2200 VAR16=AXL52
2210 VAR17=AXL61
2220 VAR18=AXL62
2230 PZETA2=ZETA2
2240 PHORZ2=HORZ2

```

TANK CONTINUED

2250 PETA2=ETA2
 2260 PAXL12=AXL12
 2270 PAXL22=AXL22
 2280 PAXL32=AXL32
 2290 PAXL42=AXL42
 2300 PAXL52=AXL52
 2310 PAXL62=AXL62
 2320 CALL ALGEBR
 2330 CALL EQVSC(FK12, FK14, FK16, FK18, FK110, FK112, FK114, FK116, FK118)
 2340 FK11=H*VAR2
 2350 FK13=H*VAR4
 2360 FK15=H*VAR6
 2370 FK17=H*VAR8
 2380 FK19=H*VAR10
 2390 FK111=H*VAR12
 2400 FK113=H*VAR14
 2410 FK115=H*VAR16
 2420 FK117=H*VAR18
 2430 VAR1=ZETA1+FK11*.5
 2440 VAR2=ZETA2+FK12*.5
 2450 VAR3=HORZ1+FK13*.5
 2460 VAR4=HORZ2+FK14*.5
 2470 VAR5=ETA1+FK15*.5
 2480 VAR6=ETA2+FK16*.5
 2490 VAR7=AXL11+FK17*.5
 2500 VAR8=AXL12+FK18*.5
 2510 VAR9=AXL21+FK19*.5
 2520 VAR10=AXL22+FK110*.5
 2530 VAR11=AXL31+FK111*.5
 2540 VAR12=AXL32+FK112*.5
 2550 VAR13=AXL41+FK113*.5
 2560 VAR14=AXL42+FK114*.5
 2570 VAR15=AXL51+FK115*.5
 2580 VAR16=AXL52+FK116*.5
 2590 VAR17=AXL61+FK117*.5
 2600 VAR18=AXL62+FK118*.5
 2610 CALL ALGEBR
 2620 CALL EQVSC(FK22, FK24, FK26, FK28, FK210, FK212, FK214, FK216, FK218)
 2630 FK21=H*VAR2
 2640 FK23=H*VAR4
 2650 FK25=H*VAR6
 2660 FK27=H*VAR8
 2670 FK29=H*VAR10
 2680 FK211=H*VAR12
 2690 FK213=H*VAR14
 2700 FK215=H*VAR16
 2710 FK217=H*VAR18
 2720 VAR1=ZETA1+.29289322*FK21+.20710673*FK11
 2730 VAR2=ZETA2+.29289322*FK22+.20710673*FK12
 2740 VAR3=HORZ1+.29289322*FK23+.20710673*FK13

TANK CONTINUED

2750 VAR4=HORZ2+.29289322*FK24+.20710678*FK14
 2760 VAR5=ETA1+.29289322*FK25+.20710678*FK15
 2770 VAR6=ETA2+.29289322*FK26+.20710678*FK16
 2780 VAR7=AXL11+.29289322*FK27+.20710678*FK17
 2790 VAR8=AXL12+.29289322*FK28+.20710678*FK18
 2800 VAR9=AXL21+.29289322*FK29+.20710678*FK19
 2810 VAR10=AXL22+.29289322*FK210+.20710678*FK110
 2820 VAR11=AXL31+.29289322*FK211+.20710678*FK111
 2830 VAR12=AXL32+.29289322*FK212+.20710678*FK112
 2840 VAR13=AXL41+.29289322*FK213+.20710678*FK113
 2850 VAR14=AXL42+.29289322*FK214+.20710678*FK114
 2860 VAR15=AXL51+.29289322*FK215+.20710678*FK115
 2870 VAR16=AXL52+.29289322*FK216+.20710678*FK116
 2880 VAR17=AXL61+.29289322*FK217+.20710678*FK117
 2890 VAR18=AXL62+.29289322*FK218+.20710678*FK118
 2900 CALL ALGEBR
 2910 CALL EQNS(FK32, FK34, FK36, FK38, FK310, FK312, FK314, FK316, FK318)
 2920 FK31=H*VAR2
 2930 FK33=H*VAR4
 2940 FK35=H*VAR6
 2950 FK37=H*VAR8
 2960 FK39=H*VAR10
 2970 FK311=H*VAR12
 2980 FK313=H*VAR14
 2990 FK315=H*VAR16
 3000 FK317=H*VAR18
 3010 VAR1=ZETA1-.70710678*FK21+1.70710678*FK31
 3020 VAR2=ZETA2-.70710678*FK22+1.70710678*FK32
 3030 VAR3=HORZ1-.70710678*FK23+1.70710678*FK33
 3040 VAR4=HORZ2-.70710678*FK24+1.70710678*FK34
 3050 VAR5=ETA1-.70710678*FK25+1.70710678*FK35
 3060 VAR6=ETA2-.70710678*FK26+1.70710678*FK36
 3070 VAR7=AXL11-.70710678*FK27+1.70710678*FK37
 3080 VAR8=AXL12-.70710678*FK28+1.70710678*FK38
 3090 VAR9=AXL21-.70710678*FK29+1.70710678*FK39
 3100 VAR10=AXL22-.70710678*FK210+1.70710678*FK310
 3110 VAR11=AXL31-.70710678*FK211+1.70710678*FK311
 3120 VAR12=AXL32-.70710678*FK212+1.70710678*FK312
 3130 VAR13=AXL41-.70710678*FK213+1.70710678*FK313
 3140 VAR14=AXL42-.70710678*FK214+1.70710678*FK314
 3150 VAR15=AXL51-.70710678*FK215+1.70710678*FK315
 3160 VAR16=AXL52-.70710678*FK216+1.70710678*FK316
 3170 VAR17=AXL61-.70710678*FK217+1.70710678*FK317
 3180 VAR18=AXL62-.70710678*FK218+1.70710678*FK318
 3190 CALL ALGEBR
 3200 CALL EQNS(FK42, FK44, FK46, FK48, FK410, FK412, FK414, FK416, FK418)
 3210 FK41=H*VAR2
 3220 FK43=H*VAR4
 3230 FK45=H*VAR6
 3240 FK47=H*VAR8

TANK CONTINUED

3250 FK 49=H*VAR10
 3260 FK 411=H*VAR12
 3270 FK 413=H*VAR14
 3280 FK 415=H*VAR16
 3290 FK 417=H*VAR18
 3300 ZETA1=ZETA1+.166667*FK11+.09763107*FK21+.56903559*FK31
 3310& +.166667*FK41
 3320 ZETA2=ZETA2+.166667*FK12+.09763107*FK22+.56903559*FK32
 3330& +.166667*FK42
 3340 HORZ1=HORZ1+.166667*FK13+.09763107*FK23+.56903559*FK33
 3350& +.166667*FK43
 3360 HORZ2=HORZ2+.166667*FK14+.09763107*FK24+.56903559*FK34
 3370& +.166667*FK44
 3380 ETA1=ETA1+.166667*FK15+.09763107*FK25+.56903559*FK35
 3390& +.166667*FK45
 3400 ETA2=ETA2+.166667*FK16+.09763107*FK26+.56903559*FK36
 3410& +.166667*FK46
 3420 AXL11=AXL11+.166667*FK17+.09763107*FK27+.56903559*FK37
 3430& +.166667*FK47
 3440 AXL12=AXL12+.166667*FK18+.09763107*FK28+.56903559*FK38
 3450& +.166667*FK48
 3460 AXL21=AXL21+.166667*FK19+.09763107*FK29+.56903559*FK39
 3470& +.166667*FK49
 3480 AXL22=AXL22+.166667*FK110+.09763107*FK210+.56903559*FK310
 3490& +.166667*FK410
 3500 AXL31=AXL31+.166667*FK111+.09763107*FK211+.56903559*FK311
 3510& +.166667*FK411
 3520 AXL32=AXL32+.166667*FK112+.09763107*FK212+.56903559*FK312
 3530& +.166667*FK412
 3540 AXL41=AXL41+.166667*FK113+.09763107*FK213+.56903559*FK313
 3550& +.166667*FK413
 3560 AXL42=AXL42+.166667*FK114+.09763107*FK214+.56903559*FK314
 3570& +.166667*FK414
 3580 AXL51=AXL51+.166667*FK115+.09763107*FK215+.56903559*FK315
 3590& +.166667*FK415
 3600 AXL52=AXL52+.166667*FK116+.09763107*FK216+.56903559*FK316
 3610& +.166667*FK416
 3620 AXL61=AXL61+.166667*FK117+.09763107*FK217+.56903559*FK317
 3630& +.166667*FK417
 3640 AXL62=AXL62+.166667*FK118+.09763107*FK218+.56903559*FK318
 3650& +.166667*FK418
 3660 DZETA2=(ZETA2-PZETA2)*RH
 3670 DHORZ2=(HORZ2-PHORZ2)*RH
 3680 DETA2=(ETA2-PETA2)*RH
 3690 DAXL12=(AXL12-PAXL12)*RH
 3700 DAXL22=(AXL22-PAXL22)*RH
 3710 DAXL32=(AXL32-PAXL32)*RH
 3720 DAXL42=(AXL42-PAXL42)*RH
 3730 DAXL52=(AXL52-PAXL52)*RH
 3740 DAXL62=(AXL62-PAXL62)*RH

TANK CONTINUED

```

3750 DRV1 = ZETA1 + 25 * ETA1
3760 DRV2 = ZETA2 + 25 * ETA2
3770 DDRV2 = DZETA2 + 25 * DETA2
3780 IF (INDEX-NSTEPS) 1, 2, 2
3790 2 RETURN
3800 END
3810 SUBROUTINE EQNS(FK2, FK4, FK6, FK8, FK10, FK12, FK14, FK16, FK18)
3820C
3830C-----VERTICLE C-G EQUATION-----
3840 FK2=H*((-FORCK1-FORCK2-FORCK3-FORCK4-FORCK5-FORCK6
3850& -FORCD1-FORCD2-FORCD3-FORCD4-FORCD5-FORCD6)*.008-386.)
3860C
3870C-----HORIZONTAL C-G EQUATION-----
3880 FK4=H*(FORCH1+FORCH2+FORCH3+FORCH4+FORCH5+FORCH6)*.008
3890C
3900C-----MOMENT AT C-G EQUATION-----
3910 FK6=H*(-77.*FORCK1-44.*FORCK2-11.*FORCK3+22.*FORCK4
3920& +55.*FORCK5+88.*FORCK6-77.*FORCD1-44.*FORCD2-11.*FORCD3
3930& +22.*FORCD4+55.*FORCD5+88.*FORCD6-HORMOM)/581700.
3940C
3950C-----BOGIE EQUATIONS (6)-----
3960 FK8=H*(FORCK1+FORCD1-FORCT1-FORT11+FORCW1-1420.)*.2717
3970 FK10=H*(FORCK2+FORCD2-FORCT1+FORCT2+FORCW2-1420.)*.2717
3980 FK12=H*(FORCK3+FORCD3-FORCT2+FORCT3+FORCW3-1420.)*.2717
3990 FK14=H*(FORCK4+FORCD4-FORCT3+FORCT4+FORCW4-1420.)*.2717
4000 FK16=H*(FORCK5+FORCD5-FORCT4+FORCT5+FORCW5-1420.)*.2717
4010 FK18=H*(FORCK6+FORCD6-FORCT5+FORCW6-1420.)*.2717
4020 RETURN
4030 END
5000 SUBROUTINE ALGEBR
5010 DO 95 I = 1, 6
5020 FORCW(I) = 0.
5030 95 FORCH(I) = 0.
5040 VAR19=0.
5050 DO 20 I=1, 4
5060 IF(Y(I)-TH(I))20, 20, 30
5070 30 VTH=Y(I)-TH(I)
5080 VAR19=AMAX1(VAR19, VTH)
5090 20 CONTINUE
5100 DO 100 I=1, 12
5110 SEGDEF(I)=Y(I+4)-VAR7-THRESH(I)
5120 IF(SEGDEF(I))50, 60, 60
5130 50 SEGDEF(I)=0.
5140 60 FORCW1=FORCW1+SEGDEF(I)*GAMMA(I)
5150 100 FORCH1=FORCH1+SEGDEF(I)*SIGMA(I)
5160 DO 200 I=13, 24
5170 SEGDEF(I)=Y(I+6)-VAR9-THRESH(I)
5180 IF(SEGDEF(I))150, 160, 160
5190 150 SEGDEF(I)=0.
5200 160 FORCW2=FORCW2+SEGDEF(I)*GAMMA(I)

```

(8 of 15 sheets)

TANK CONTINUED

```

5210 200 FORCH2=FORCH2+SEGDEF(I)*SIGMA(I)
5220 DO 300 I=25,36
5230 SEGDEF(I)=Y(I+8)-VAR11-THRESH(I)
5240 IF( SEGDEF(I)) 250,260,260
5250 250 SEGDEF(I)=0.
5260 260 FORCW3=FORCW3+SEGDEF(I)*GAMMA(I)
5270 300 FORCH3=FORCH3+SEGDEF(I)*SIGMA(I)
5280 DO 400 I=37,48
5290 SEGDEF(I)=Y(I+10)-VAR13-THRESH(I)
5300 IF( SEGDEF(I)) 350,360,360
5310 350 SEGDEF(I)=0.
5320 360 FORCW4=FORCW4+SEGDEF(I)*GAMMA(I)
5330 400 FORCH4=FORCH4+SEGDEF(I)*SIGMA(I)
5340 DO 500 I=49,60
5350 SEGDEF(I)=Y(I+12)-VAR15-THRESH(I)
5360 IF( SEGDEF(I)) 450,460,460
5370 450 SEGDEF(I)=0.
5380 460 FORCW5=FORCW5+SEGDEF(I)*GAMMA(I)
5390 500 FORCH5=FORCH5+SEGDEF(I)*SIGMA(I)
5400 DO 600 I=61,72
5410 SEGDEF(I)=Y(I+14)-VAR17-THRESH(I)
5420 IF( SEGDEF(I)) 550,560,560
5430 550 SEGDEF(I)=0.
5440 560 FORCW6=FORCW6+SEGDEF(I)*GAMMA(I)
5450 600 FORCH6=FORCH6+SEGDEF(I)*SIGMA(I)
5460 SPDEF1=VAR1+77.*VAR5-VAR7
5470 DSPDF1=VAR2+77.*VAR6-VAR8
5480 SPDEF2=VAR1+44.*VAR5-VAR9
5490 DSPDF2=VAR2+44.*VAR6-VAR10
5500 SPDEF3=VAR1+11.*VAR5-VAR11
5510 DSPDF3=VAR2+11.*VAR6-VAR12
5520 SPDEF4=VAR1-22.*VAR5-VAR13
5530 DSPDF4=VAR2-22.*VAR6-VAR14
5540 SPDEF5=VAR1-55.*VAR5-VAR15
5550 DSPDF5=VAR2-55.*VAR6-VAR16
5560 SPDEF6=VAR1-88.*VAR5-VAR17
5570 DSPDF6=VAR2-88.*VAR6-VAR18
5580 DO 700 I=1,6
5590 IF( SPDEF(I)-.402) 710,710,720
5600 720 SPDEF(I)=.402
5610 DSPDF(I)=0.
5620 710 IF( SPDEF(I)+12.) 730,740,740
5630 730 FORCK(I)=29998.*SPDEF(I)+339972.
5640 GO TO 700
5650 740 FORCK(I)=1667.*SPDEF(I)
5660 700 CONTINUE
5670 DO 800 I=1,6
5680 IF(ABS(DSPDF(I))-1.) 810,820,820
5690 810 FORCD(I)=2750.*DSPDF(I)
5700 GO TO 800

```

TANK

```

5710 820 FORCD(I)=SIGN(2750., DSPDF(I))
5720 800 CONTINUE
5730     IF(VAR7-VAR19)950,950,960
5740 950 FORT11=600.*(VAR7-VAR19)
5750     GO TO 970
5760 960 FORT11=0.
5770 970 FORCT1 = 375. * (VAR9-VAR7)
5780     FORCT2 = 375. * (VAR11-VAR9)
5790     FORCT3 = 375. * (VAR13-VAR11)
5800     FORCT4 = 375. * (VAR15-VAR13)
5810     FORCT5 = 375. * (VAR17-VAR15)
5820     HORMOM=0.
5830     HORMOM=FORCH1*( 46.+SPDEF1+77.*VAR5)
5840     HORMOM=HORMOM+FORCH2*( 46.+SPDEF2+44.*VAR5)
5850     HORMOM=HORMOM+FORCH3*( 46.+SPDEF3+11.*VAR5)
5860     HORMOM=HORMOM+FORCH4*( 46.+SPDEF4-22.*VAR5)
5870     HORMOM=HORMOM+FORCH5*( 46.+SPDEF5-55.*VAR5)
5880     HORMOM=HORMOM+FORCH6*( 46.+SPDEF6-88.*VAR5)
5890     RETURN
5900     END

```

THRESH

100 7.4, 5., 3., 1.8, .6, .05,
 110 .05, .6, 1.8, 3., 5., 7.4,
 120 7.4, 5., 3., 1.8, .6, .05,
 130 .05, .6, 1.8, 3., 5., 7.4,
 140 7.4, 5., 3., 1.8, .6, .05,
 150 .05, .6, 1.8, 3., 5., 7.4,
 160 7.4, 5., 3., 1.8, .6, .05,
 170 .05, .6, 1.8, 3., 5., 7.4,
 180 7.4, 5., 3., 1.8, .6, .05,
 190 .05, .6, 1.8, 3., 5., 7.4,
 200 7.4, 5., 3., 1.8, .6, .05,
 210 .05, .6, 1.8, 3., 5., 7.4



GAMMA

100 2296, 2828, 3276, 3624, 3864, 3984,
 110 3984, 3864, 3624, 3276, 2828, 2296,
 120 2296, 2828, 3276, 3624, 3864, 3984,
 130 3984, 3864, 3624, 3276, 2828, 2296,
 140 2296, 2828, 3276, 3624, 3864, 3984,
 150 3984, 3864, 3624, 3276, 2828, 2296,
 160 2296, 2828, 3276, 3624, 3864, 3984,
 170 3984, 3864, 3624, 3276, 2828, 2296,
 180 2296, 2828, 3276, 3624, 3864, 3984,
 190 3984, 3864, 3624, 3276, 2828, 2296,
 200 2296, 2828, 3276, 3624, 3864, 3984,
 210 3984, 3864, 3624, 3276, 2828, 2296

SIGMA

```

100 7119,6150,4987,3687,2250,757,
110 -757,-2250,-3687,-4987,-6150,-7119,
120 7119,6150,4987,3687,2250,757,
130 -757,-2250,-3687,-4987,-6150,-7119,
140 7119,6150,4987,3687,2250,757,
150 -757,-2250,-3687,-4987,-6150,-7119,
160 7119,6150,4987,3687,2250,757,
170 -757,-2250,-3687,-4987,-6150,-7119,
180 7119,6150,4987,3687,2250,757,
190 -757,-2250,-3687,-4987,-6150,-7119,
200 7119,6150,4987,3687,2250,757,
210 -757,-2250,-3687,-4987,-6150,-7119

```

FIMAKE

```

1$NDM
100 THIS PROGRAM IS USED TO MAKE OBSTACLE DATA FILES TO BE INPUT TO
110 THE VEHICLE DYNAMICS PROGRAM.
120 DIMENSIONX(1000),FILEID(12)
130 PRINT, FILE NAME
140 READ1,FINAME
150 PRINT, FILE IDENTIFICATION"
160 READ1,FILEID
170 PRINT, NO. OF POINTS"
180 READ, N
190 PRINT2, N
200 READ, (X(I), I=1, N)
210 WRITE(1,1)FILEID
220 WRITE(1,3)(X(I), I=1, N)
230 PRINT, TYPE NO. OF TRAILING ZEROES"
240 READ, M
250 Y=0
260 WRITE(1,3)(Y, I=1, M)
270 N=N+M
280 PRINT4, N, FINAME
290 CALLCLOSEF(1, FINAME, 2)
300 CALLEXIT
310 1FORMAT(12A6)
320 2FORMAT(5HTYPE, 14, 12H DATA POINTS)
330 3FORMAT(E20.10)
340 4FORMAT("THERE ARE", , 13, "POINTS IN FILE ", A6)
350 END

```

Dictionary of Variables

Variable	Description
FORCK(I)	FORCE OF ITH SUSPENSION SPRING
FORCW(I)	RESULTANT VERTICAL FORCE OF SPRING SEGMENTS OF ITH BOGIE
FORCH(I)	RESULTANT HORIZONTAL FORCE OF SPRING SEGMENTS OF ITH BOGIE
FORCD(I)	FORCE OF ITH SUSPENSION DAMPER
SPDEF(I)	DEFLECTION OF ITH SUSPENSION SPRING
DSPDF(I)	VELOCITY OF ITH BOGIE DAMPER (DERIVATIVE OF SPDEF(I))
FORCT(I)	TRACK TENSION FORCE BETWEEN BOGIE(I) AND BOGIE(I+1)
FORT11	TRACK TENSION FORCE OF FEELER SPRING
VAR1-VAR19	PAST VALUES OF ALL VARIABLES IN RUNGE KUTTA SOLUTION
DRV1	VERTICAL DISPLACEMENT OF DRIVER
DRV2	VERTICAL VELOCITY OF DRIVER
DDRV2	VERTICAL ACCELERATION OF DRIVER
ZETA1	VERTICAL DISPLACEMENT OF CG
ZETA2	VERTICAL VELOCITY OF CG
DZETA2	VERTICAL ACCELERATION OF CG
HORZ1	HORIZONTAL DISPLACEMENT OF CG
HORZ2	HORIZONTAL VELOCITY OF CG
DHORZ2	HORIZONTAL ACCELERATION OF CG
ETA1	PITCH DISPLACEMENT ABOUT CG
ETA2	PITCH VELOCITY ABOUT CG
DETA2	PITCH ACCELERATION ABOUT CG
AXL(I)1	VERTICAL DISPLACEMENT OF ITH BOGIE
AXL(I)2	VERTICAL VELOCITY OF ITH BOGIE
DAXL(I)2	VERTICAL ACCELERATION OF ITH BOGIE
H	RUNGE KUTTA TIME STEP
RH	RECIPROCAL OF H
NSTEPS	NUMBER OF STEPS IN RUNGE KUTTA SOLUTION
HORMOM	MOMENT OF HORIZONTAL FORCES ABOUT CG
THRESH(I)	THRESHOLD HEIGHTS OF ITH SPRING SEGMENT
GAMMA(I)	$k_v \cos i$
SIGMA(I)	$k_h \sin i$
SEGDEF(I)	DEFLECTION OF SEGMENT SPRING(I)

Variable	Description
Y(I)	INPUT PROFILE
TH(I)	FEELEER THRESHOLD HEIGHTS
DISPL(I)	OUTPUT DISPLACEMENTS (EQUIVALENCED TO DRV1)
VELCTY(I)	OUTPUT VELOCITIES (EQUIVALENCED TO DRV2)
ACCISS(I)	OUTPUT ACCELERATIONS IN IN./SEC ² (EQUIVALENCED TO DRV2)
ACCGS(I)	OUTPUT ACCELERATIONS IN g's (ACCISS(I)/386)
ACCMAX(I)	MAXIMUM ACCELERATION
ACCMIN(I)	MINIMUM ACCELERATION
SACCSQ(I)	SUM OF THE ACCELERATIONS SQUARED
RMSACC(I)	RMS ACCELERATION
VARID(I)	BCD VARIABLE IDENTIFICATION
FID	BCD INPUT FILE IDENTIFICATION
IBELL	BCD CHARACTER TO RING TELETYPE BELL
TP	CONTROLS TELETYPE PRINTOUT
TIP	PRINTOUT TIME INTERVAL ON TELETYPE
T	REAL TIME
NPL	CONTROLS FILE PAGING
NSTOP	CONTROLS STOPPING OF PROGRAM
JJ	END OF INPUT FILE INDICATOR
XMPII	TANK SPEED IN MPII
VEL	TANK SPEED IN IPS
DELTAT	REAL TIME INCREMENT
DELTAL	QUANTA OF LENGTH BETWEEN INPUT PROFILE POINTS
FINAME	NAME OF INPUT PROFILE FILE
FNAME2	NAME OF OUTPUT FILE
FK's	TEMPORARY DEPENDENT VARIABLES IN RUNGE KUTTA
YINPUT	PROFILE INPUT POINT (FROM FILE)
INDEX	INDEX COUNTER FOR RK

NOTE: Many of the variables stored in array's are assigned individual names as well as subscripts by use of the "EQUIVALENCE" statement. This allows for the use of either individual names or subscripts in the program whichever is more convenient.

EXAMPLE:

```
COMMON VNAME1, VNAME2, VNAME3  
DIMENSION VNAME(3)  
EQUIVALENCE (VNAME1, VNAME(1))
```

RESULT:

```
VNAME1 = VNAME(1)  
VNAME2 = VNAME(2)  
VNAME3 = VNAME(3)
```

The following variables are used in this manner:

FORCH, FORCD, FORCW, FORCK, SPDEF, DSPDF, DISPL, VELCTY, AND ACCISS.

COMPUTER PROGRAM FOR SIMULATING DYNAMIC RESPONSE OF M37 TRUCK, AND
 DICTIONARY of PROGRAM VARIABLES

TRUCK

Program

```

1$LIB,DIFFEQ
2$LIB,ALGEBR
3$RPC
4$NDM
5$TTY,120
100  COMMON NSTEPS,DELTAT,A,B,MASS,MASS1,MASS2,CPOS1,CPOS2,CNEG1,CNEG2
110  COMMON C11,C21,INRTIA,FORCW1,FORCW2,SPDEF1,SPDEF2,DSPDF1,DSPDF2
120  COMMON FORCK1,FORCK2,VAR1,VAR2,VAR3,VAR4,VAR5,VAR6,VAR7,VAR8
130  COMMON ZETA1,ZETA2,DZETA2,ETA1,ETA2,DETA2,NU1,NU2,DMU2
140  COMMON MU1,MU2,DMU2
150  COMMON THRESH(20),GAMMA(20),SEGDEF(20),Y(47)
160  REAL NU1,NU2,MU1,MU2,MASS,MASS1,MASS2,INRTIA
165  IBELL=458752
170  PRINT 1
180  1 FORMAT(18X,33(1H*),/,18X,1H*,31X,1H*,/,
190& 18X,33H* MURPHY'S M-37 BACK-UP MODEL *,/,
200& 18X,1H*,31X,1H*,/,18X,33(1H*),///)
210C-----DATA INITIALIZATION-----
220  A=64.8
230  B=47.2
240  INRTIA=25446.
250  MASS=8.05
260  MASS1=.94
270  MASS2=.8
280  CPOS1=11.8
290  CNEG1=23.8
300  CPOS2=10.2
310  CNEG2=44.
320  THRESH(1)=7.02
330  THRESH(2)=4.5
340  THRESH(3)=2.34
350  THRESH(4)=.81
360  THRESH(5)=.09
370  THRESH(6)=.09
380  THRESH(7)=.81
390  THRESH(8)=2.34
400  THRESH(9)=4.5
410  THRESH(10)=7.02
420  THRESH(11)=7.02
430  THRESH(12)=4.5
440  THRESH(13)=2.34
450  THRESH(14)=.81
460  THRESH(15)=.09
470  THRESH(16)=.09
480  THRESH(17)=.81
490  THRESH(18)=2.34
500  THRESH(19)=4.5
510  THRESH(20)=7.02
520  GAMMA(1)=411.75
530  GAMMA(2)=506.25
    
```

TRUCK CONTINUED

```

540     GAMMA(3)=587.25
550     GAMMA(4)=648.
560     GAMMA(5)=668.25
570     GAMMA(6)=668.25
580     GAMMA(7)=648.
590     GAMMA(8)=587.25
600     GAMMA(9)=506.25
610     GAMMA(10)=411.75
620     GAMMA(11)=411.25
630     GAMMA(12)=506.25
640     GAMMA(13)=587.25
650     GAMMA(14)=648.
660     GAMMA(15)=668.25
670     GAMMA(16)=668.25
680     GAMMA(17)=648.
690     GAMMA(18)=587.25
700     GAMMA(19)=506.25
710     GAMMA(20)=411.25
720     ZETA1=-5.189
730     ZETA2=0.
740     ETA1=.028
750     ETA2=0.
760     NU1=-1.08
770     NU2=0.
780     MU1=-1.245
790     MU2=0.
800     NSP=0
810     POINT1=0.
820     POINT2=0.
830     SDZ2SQ=0.
840     T=0.
850     NSTOP=0
860     NPL=12
870     JJ=1
880     DO 10 I=1,47
890     10 Y(I)=0.
900C-----DATA READ IN-----
910     PRINT, "*****TYPE IN THE DATA FOR THE FOLLOWING"
920     PRINT,
930     PRINT, "EXTERNAL INPUT DATA"
940     PRINT,
950     PRINT, "NAME OF PROFILE INPUT FILE"
960     READ 2, FINAME
970     2 FORMAT(A6)
980     PRINT, "DATA VARIABLES"
990     PRINT,
1000    PRINT, "TRUCK VELOCITY IN INCHES PER SECOND (REAL)"
1010    READ, VEL
1020    PRINT, "PROGRAM VARIABLES"
1030    PRINT,

```

(2 of 9 sheets)

TRUCK CONTINUED

```

1040 PRINT,"NUMBER OF SPACES BETWEEN PROFILE POINTS (INTEGER)"
1050 READ,NSPACE
1060 PRINT,"NUMBER OF STEPS IN RKG (INTEGER)"
1070 READ,NSTEPS
1080 PRINT,"EXTERNAL OUTPUT DATA"
1090 PRINT
1100 PRINT,"NAME OF OUTPUT DATA FILE"
1110 READ 2,FNAME2
1120 PRINT
1130 PRINT,"*****END OF DATA INPUT*****"
1140 PRINT 3
1150 XMPH=VEL/17.6
1160 3 FORMAT(//////,"T",10X,"Y(1)",7X,"AZETA2",5X,
1170& ARMS,/)
1180 WRITE(2;6)
1190 6 FORMAT(//,37X,45(1H*),/,37X,1H*,43X,1H*,/,37X,
1200& 45H* MURPHY'S M-37 TRUCK PROGRAM OUTPUT FILE *,/,
1210& 37X,1H*,43X,1H*,/,37X,45(1H*),//)
1220 WRITE(2;11)XMPH,NSTEPS
1230 WRITE(2;9)
1240 11 FORMAT(/,9HVELOCITY=,F6.2,15H MILES PER HOUR,50X,
1250& 35HNUMBER OF STEPS IN RKG INTEGRATION=,I4)
1260 9 FORMAT(//,13X,9(1H-),12HDISPLACEMENT,8(1H-),3X,10(1H-),
1270& 8HVELOCITY,11(1H-),3X,9(1H-),12HACCELERATION,
1280& 8(1H-),2X,7HC-G RMS,/,X,4HTIME,2X,4HY(1),X,
1290& 3(2X,3HC-G,4X,5HPITCH,3X,5HFR-AX,3X,5HRE-AX,2X),
1300& X,5HACCEL,/)
1310 DELTAT=3.07/VEL
1320 CALL OPENF(1,FNAME)
1330 4 FORMAT(E20.10)
1340 50 POINT1=POINT2
1350 IF(JJ-2)55,40,55
1360 55 READ(1,4)POINT2
1370 CALL EOFTST(1,JJ)
1380 GO TO(60,40)JJ
1390 40 POINT2=POINT1
1400 NSTOP=NSTOP+1
1410 NSPACE=1
1420 60 PSTEP=(POINT2-POINT1)/NSPACE
1430 NSP=0
1440 100 I=46
1450 70 Y(I+1)=Y(I)
1460 I=I-1
1470 IF(I)70,75,70
1480 75 Y(I)=POINT1
1490 POINT1=POINT1+PSTEP
1500 NSP=NSP+1
1510 CALL DIFFEQ
1520 SDZ 2SQ=SDZ 2SQ+DZETA 2*DZETA 2
1530 RMSDZ 2=SQRT((SDZ 2SQ*DELTAT)/T)

```

TRUCK CONTINUED

```

1540 5 FORMAT(6(X,G10.4))
1550 NPL=NPL+1
1560 AZETA2=DZETA2/386.
1570 ANU2=DMU2/386.
1580 AMU2=DMU2/386.
1590 RMSAZ2=RMSDZ2/386.
1600 WRITE(2;7)T,POINT1,ZETA1,ETA1,MU1,MU1,ZETA2,ETA2,MU2,NU2,
16104 AZETA2,DETA2,AMU2,ANU2,RMSAZ2
1620 7 FORMAT(F6.1,F5.1,13F8.3)
1630 IF(NPL-54)120,110,120
1640 110 WRITE(2;9)
1650 PRINT 5,T,Y(1),AZETA2,RMSAZ2
1660 NPL=0
1670 120 IF(NSTOP-47)80,90,80
1680 80 T=T+DELTAT
1690 IF(NSP-NSPACE)100,50,100
1700 90 CALL CLOSEF(2,FNAME2,2)
1702 PRINT 12,(IBELL,I=1,40)
1704 12 FORMAT(40A1)
1710 PRINT 8,FNAME2
1720 8 FORMAT(///,"DETAILED OUTPUT IS IN FILE",X,A6,/)
1730 CALL EXIT
1740 END

```

DIFFEQ

```

100  SUBROUTINE DIFFEQ
110  REAL NU1,NU2,MU1,MU2,MASS,MASS1,MASS2,INRTIA
120  H=DELTA T /NSTEPS
130  RH=1./H
140  INDEX=0
150 100 INDEX=INDEX+1
160  VAR1=ZETA 1
170  VAR2=ZETA 2
180  VAR3=ETA 1
190  VAR4=ETA 2
200  VAR5=NU 1
210  VAR6=NU 2
220  VAR7=MU 1
230  VAR8=MU 2
240  PZETA 2=ZETA 2
250  PETA 2=ETA 2
260  PNU 2=NU 2
270  PMU 2=MU 2
280  CALL ALGEBR
290  FK 11=H*VAR 2
300  FK 12=H*(1/MASS)*(FORCK 1+C 11*DSPDF 1+FORCK 2+C 21*DSPDF 2-MASS*386.0)
310  FK 13=H*VAR 4
320  FK 14=H*(1/INRTIA)*(A*FORCK 1+A*C 11*DSPDF 1-B*FORCK 2-B*C 21*DSPDF 2)
330  FK 15=H*VAR 6
340  FK 16=H*(1/MASS 1)*(-FORCK 1-C 11*DSPDF 1+FORCW 1-MASS 1*386.0)
350  FK 17=H*VAR 8
360  FK 18=H*(1/MASS 2)*(-FORCK 2-C 21*DSPDF 2+FORCW 2-MASS 2*386.0)
370  VAR 1=ZETA 1+FK 11*.5
380  VAR 2=ZETA 2+FK 12*.5
390  VAR 3=ETA 1+FK 13*.5
400  VAR 4=ETA 2+FK 14*.5
410  VAR 5=NU 1+FK 15*.5
420  VAR 6=NU 2+FK 16*.5
430  VAR 7=MU 1+FK 17*.5
440  VAR 8=MU 2+FK 18*.5
450  CALL ALGEBR
460  FK 21=H*VAR 2
470  FK 22=H*(1/MASS)*(FORCK 1+C 11*DSPDF 1+FORCK 2+C 21*DSPDF 2-MASS*386.0)
480  FK 23=H*VAR 4
490  FK 24=H*(1/INRTIA)*(A*FORCK 1+A*C 11*DSPDF 1-B*FORCK 2-B*C 21*DSPDF 2)
500  FK 25=H*VAR 6
510  FK 26=H*(1/MASS 1)*(-FORCK 1-C 11*DSPDF 1+FORCW 1-MASS 1*386.0)
520  FK 27=H*VAR 8
530  FK 28=H*(1/MASS 2)*(-FORCK 2-C 21*DSPDF 2+FORCW 2-MASS 2*386.0)
540  VAR 1=ZETA 1+.29289322*FK 21+.20710678*FK 11
550  VAR 2=ZETA 2+.29289322*FK 22+.20710678*FK 12
560  VAR 3=ETA 1+.29289322*FK 23+.20710678*FK 13
570  VAR 4=ETA 2+.29289322*FK 24+.20710678*FK 14
580  VAR 5=NU 1+.29289322*FK 25+.20710678*FK 15
590  VAR 6=NU 2+.29289322*FK 26+.20710678*FK 16

```

DIFFEQ CONTINUED

```

600    VAR 7=MU1+.29289322*FK 27+.20710678*FK 17
610    VAR 8=MU 2+.29289322*FK 28+.20710678*FK 18
620    CALL ALGEBR
630    FK 31=H*VAR 2
640    FK 32=H*(1/MASS)*(FORCK 1+C 11*DSPDF 1+FORCK 2+C 21*DSPDF 2-MASS*386.0)
650      FK 33=H*VAR 4
660    FK 34=H*(1/INRTIA)*(A*FORCK 1+A*C 11*DSPDF 1-B*FORCK 2-B*C 21*DSPDF 2)
670      FK 35=H*VAR 6
680    FK 36=H*(1/MASS 1)*(-FORCK 1-C 11*DSPDF 1+FORCW 1-MASS 1*386.0)
690    FK 37=H*VAR 8
700    FK 38=H*(1/MASS 2)*(-FORCK 2-C 21*DSPDF 2+FORCW 2-MASS 2*386.0)
710    VAR 1=ZETA 1-.70710678*FK 21+.70710678*FK 31
720    VAR 2=ZETA 2-.70710678*FK 22+.70710678*FK 32
730    VAR 3=ETA 1-.70710678*FK 23+.70710678*FK 33
740    VAR 4=ETA 2-.70710678*FK 24+.70710678*FK 34
750    VAR 5=NU 1-.70710678*FK 25+.70710678*FK 35
760    VAR 6=NU 2-.70710678*FK 26+.70710678*FK 36
770    VAR 7=MU 1-.70710678*FK 27+.70710678*FK 37
780    VAR 8=MU 2-.70710678*FK 28+.70710678*FK 38
790    CALL ALGEBR
800    FK 41=H*VAR 2
810    FK 42=H*(1/MASS)*(FORCK 1+C 11*DSPDF 1+FORCK 2+C 21*DSPDF 2-MASS*386.0)
820      FK 43=H*VAR 4
830    FK 44=H*(1/INRTIA)*(A*FORCK 1+A*C 11*DSPDF 1-B*FORCK 2-B*C 21*DSPDF 2)
840      FK 45=H*VAR 6
850    FK 46=H*(1/MASS 1)*(-FORCK 1-C 11*DSPDF 1+FORCW 1-MASS 1*386.0)
860    FK 47=H*VAR 8
870    FK 48=H*(1/MASS 2)*(-FORCK 2-C 21*DSPDF 2+FORCW 2-MASS 2*386.0)
880    ZETA 1=ZETA 1+FK 11*.166667+.09763107*FK 21+.56903559*FK 31+FK 41*.1666
890      ZETA 2=ZETA 2+FK 12*.166667+.09763107*FK 22+.56903559*FK 32+FK 42*.16
900      ETA 1=ETA 1+FK 13*.166667+.09763107*FK 23+.56903559*FK 33+FK 43*.1666
910      ETA 2=ETA 2+FK 14*.166667+.09763107*FK 24+.56903559*FK 34+FK 44*.1666
920      NU 1=NU 1+FK 15*.166667+.09763107*FK 25+.56903559*FK 35+FK 45*.166667
930      NU 2=NU 2+FK 16*.166667+.09763107*FK 26+.56903559*FK 36+FK 46*.166667
940      MU 1=MU 1+FK 17*.166667+.09763107*FK 27+.56903559*FK 37+FK 47*.166667
950      MU 2=MU 2+FK 18*.166667+.09763107*FK 28+.56903559*FK 38+FK 48*.166667
960      DZETA 2=(ZETA 2-PZETA 2)*RH
970      DETA 2=(ETA 2-PETA 2)*RH
980      DNU 2=(NU 2-PNU 2)*RH
990      DMU 2=(MU 2-PMU 2)*RH
1000    IF (INDEX-NSTEPS) 100,200,200
1010 200 RETURN
1020    END

```

ALGEBR

```

100 SUBROUTINE ALGEBR
110 REAL NU1,NU2,MU1,MU2,MASS,MASS1,MASS2,INRTIA
120 DO 100 I=1,10
130 SEGDEF(I)=Y(I)-VAR5-THRESH(I)
140 IF(SEGDEF(I))50,100,100
150 50 SEGDEF(I)=0.
160 100 CONTINUE
170 DO 200 I=11,20
180 SEGDEF(I)=Y(I+26)-VAR7-THRESH(I)
190 IF(SEGDEF(I))150,200,200
200 150 SEGDEF(I)=0.
210 200 CONTINUE
220 FORCW1=0.
230 FORCW2=0.
240 DO 300 I=1,10
250 FORCW1=FORCW1+GAMMA(I)*SEGDEF(I)
260 300 CONTINUE
270 DO 400 I=11,20
280 FORCW2=FORCW2+GAMMA(I)*SEGDEF(I)
290 400 CONTINUE
300 SPDEF1=VAR5-VAR1-A*SIN(VAR3)
310 SPDEF2=VAR7-VAR1+B*SIN(VAR3)
320 DSPDF1=VAR6-VAR2-A*VAR4*COS(VAR3)
330 DSPDF2=VAR8-VAR2+B*VAR4*COS(VAR3)
340 FORCK1=19.54*(SPDEF1**3)-192.42*SPDEF1*SPDEF1+913.55*SPDEF1
350 FORCK2=1.39*(SPDEF2**3)-1.24*SPDEF2*SPDEF2+307.72*SPDEF2
360 IF(DSPDF1)600,500,500
370 500 C11=CPOS1
380 GO TO 700
390 600 C11=CNEG1
400 700 IF(DSPDF2)800,900,900
410 900 C21=CPOS2
420 RETURN
430 800 C21=CNEG2
440 RETURN
450 END

```

Dictionary of Variables

<u>Variable</u>	<u>Description</u>
NSTEPS	NUMBER OF STEPS IN RUNGE KUTTA SOLUTION
DELTAT	REAL TIME INCREMENT
A	DISTANCE FROM FRONT AXLE TO CG
B	DISTANCE FROM REAR AXLE TO CG
MASS	MASS OF VEHICLE
MASS1	MASS OF FRONT AXLE
MASS2	MASS OF REAR AXLE
CPOSI	DAMPING COEFFICIENT FOR POSITIVE MOTION OF FRONT AXLE
CPOS2	DAMPING COEFFICIENT FOR POSITIVE MOTION OF REAR AXLE
CNEGI	DAMPING COEFFICIENT FOR NEGATIVE MOTION OF FRONT AXLE
CNEG2	DAMPING COEFFICIENT FOR NEGATIVE MOTION OF REAR AXLE
NSPACE	NO. OF INTERPOLATION POINTS BETWEEN PROFILE POINTS
VEL	VELOCITY
ZETAI	VERTICAL DISPLACEMENT OF CG
ZETA2	VERTICAL VELOCITY OF CG
DZETA2	VERTICAL ACCELERATION OF CG
AZETA2	VERTICAL ACCELERATION IN G'S OF CG
ETAI	PITCH DISPLACEMENT ABOUT CG
ETA2	PITCH VELOCITY ABOUT CG
DETA2	PITCH ACCELERATION ABOUT CG
NUI	VERTICAL DISPLACEMENT OF FRONT AXLE
NU2	VERTICAL VELOCITY OF FRONT AXLE
DNUI	VERTICAL ACCELERATION OF FRONT AXLE
ANUI	VERTICAL ACCELERATION IN G'S OF FRONT AXLE
MUI	VERTICAL DISPLACEMENT OF REAR AXLE
MU2	VERTICAL VELOCITY OF REAR AXLE
DMU2	VERTICAL ACCELERATION OF REAR AXLE
AMU2	VERTICAL ACCELERATION IN G'S OF REAR AXLE
Y	PROFILE SHIFT REGISTER

<u>Variable</u>	<u>Description</u>
POINTI	PAST PROFILE POINT
POINT2	PRESENT PROFILE POINT
PSTEP	PROFILE INTERPOLATION INCREMENT $=[(\text{POINT2} - \text{POINTI})/\text{NSPACE}]$
SD72SQ	SUM OF THE SQUARES OF DZETA2
RMSDZ2	RMS OF DZETA2 [RMS (in./sec ²)] RMSAZ2 RMS (g) OF CG
FINAME	NAME OF PROFILE FILE
FNAME	NAME OF OUTPUT FILE
NSP	PRESENT STEP IN PROFILE INTERPOLATION
JJ	END OF PROFILE FILE INDICATOR
NSTOP	STEP COUNTER FOR T AFTER LAST POINT IS READ FROM PROFILE FILE*
I	NO SPECIAL SIGNIFICANCE USED FOR ALL "DDloop" COUNTS

* PROGRAM STOPS AFTER LAST PROFILE POINT IS READ AND SHIFTED THROUGH Y.